INVESTIGATION OF LONG PERIOD FIBER GRATINGS FOR DEVELOPMENT OF PACKAGED SENSOR DEVICES FOR NUCLEAR, MEDICAL AND INDUSTRIAL APPLICATIONS

By

SANJAY KHER

(Enrolment No: PHYS 03200804006)

Raja Ramanna Centre for Advanced Technology

Indore 452 013, INDIA

A thesis submitted to the

Board of Studies in Physical Sciences

In partial fulfillment of requirements

For the Degree of

DOCTOR OF PHILOSOPHY

of

HOMI BHABHA NATIONAL INSTITUTE

April, 2014

Homi Bhabha National Institute

RECOMMENDATIONS OF THE VIVA VOCE BOARD

As members of the Viva Voce Board, we certify that we have read the dissertation prepared by Shri Sanjay Kher entitled "Investigation of long period fiber gratings for development of packaged sensor devices for nuclear, medical and industrial applications" and recommend that it may be accepted as fulfilling the dissertation requirement for the Degree of Doctor of Philosophy.

____ **Date:**

Chairman: Prof. L. M. Kukreja

____ **Date:**

Guide / Convener: Prof. S. M. Oak

____ **Date:**

Member 1: Prof. P. A. Naik

____ **Date:**

Member 2: Prof. N. K. Sahoo

____ **Date:**

External Examiner: Prof. M. R. Shenoy

Final approval and acceptance of this dissertation is contingent upon the candidate's submission of the final copies of the dissertation to HBNI.

I hereby certify that I have read this dissertation prepared under my direction and recommend that it may be accepted as fulfilling the dissertation requirement.

Date: 10. 4. 2015
Place: Indore

Guide: Prof. S. M. Oak

STATEMENT BY AUTHOR

This dissertation has been submitted in partial fulfillment of requirements for an advanced degree at Homi Bhabha National Institute (HBNI) and is deposited in the Library to be made available to borrowers under rules of the HBNI.

Brief quotations from this dissertation are allowable without special permission, provided that accurate acknowledgement of source is made. Requests for permission for extended quotation from or reproduction of this manuscript in whole or in part may be granted by the Competent Authority of HBNI when in his or her judgment the proposed use of the material is in the interests of scholarship. In all other instances, however, permission must be obtained from the author.

DECLARATION

I, hereby declare that the investigation presented in the thesis has been carried out by me. The work is original and has not been submitted earlier as a whole or in part for a degree / diploma at this or any other Institution / University.

Sanjay Kher

List of Publications arising from the thesis

A. Total number of Publications in Refereed International / National Journals: 08

B. Total number of Publications in International / National Conferences: 06

A. Refereed International / National Journals

1. **Sanjay Kher**, Smita Chaubey, S. M. Oak, A. Gusarov, "Measurement of gamma-radiation induced refractive index changes in B/Ge doped fiber using LPGs," IEEE-Photonics Technology Letters, Vol. 25, issue 21, Nov. 1, 2013, pp. 2070-2073.

2. **Sanjay Kher**, Smita Chaubey, Jai Kishore, S. M. Oak., "Detection of fuel adulteration with high sensitivity using turnaround point long period fiber gratings in B/Ge doped fiber" IEEE Sensors Journal, Vol. 13, No. 11, pp. 4482 (2013).

3. **Sanjay Kher**, Smita Chaubey, Raman Kashyap, S. M. Oak, "Turnaround-Point long period fiber gratings (TAP-LPFG) as high radiation dose sensors", IEEE-Photonics Tech. Letters, Vol. 24, issue 9, pp. 742-744 (2012).

4. **Kher Sanjay**, Chaubey S., Oak S. M**.,** "Long period fiber grating based nuclear radiation sensors for high level dose applications", J**.** Instrumentation Science & Technology, Taylor & Francis Online, 30 Nov. 2012. D**OI:** 10.1080/10739149. 2012. 747099.

5. S. Chaubey, **Sanjay Kher**, S. M. Oak, "Radiation and taper tuning of long period grating for high sensitivity strain measurement", IEEE proceedings of WFOPC, 2011, July 2011, ISSN: 1927-5056, pp 1-4, Dec. 2011.

6. **Sanjay Kher**, S. Chaubey, Manoj Kumar Saxena, S. M. Oak "Specialty fiber gratings for refractive index sensing and Photonic switching" , International J. of Applied Engineering and Tech., Vol. 1(1), Oct.-Dec. 2011.

7. **Sanjay Kher**, Smita Chaubey, Jai Kishore, SDVSJ Raju, S. M. Oak, "Fiber Optic temperature-insensitive, strain sensor for nuclear applications", Int. J. of Applied Engineering and Tech., ISSN 2277-212X, Vol. 1(1), pp. 61-67, Oct. –Dec. 2011.

8. **Sanjay Kher,** Manoj Saxena, Smita Chaube, S. M. Oak, "Transverse micro-structuring of photonic crystal fibers for industrial sensors and side viewing probes for optical coherence tomography applications", Sensors & Transducers Journal, Vol. 116, issue 5, May 2010, pp. 112-121.

B. International/ National Conferences

1. **Sanjay Kher**, Smita Chaube, S. M. Oak, Tapered long period fiber gratings (TLPFG): Characteristics and novel applications, P-88 (Poster), DAE-BRNS symposium on Atomic, Molecular and Optical Physics, Feb. 22-25, 2011, Karnataka University, Dharwad.

2. Smita Chaube, **Sanjay Kher**, S. M. Oak, Tailoring long period fiber gratings for achievement of turnaround point: A technique for development of improved sensors and tunable filters, P-85 (Poster), DAE-BRNS symposium on Atomic, Molecular and Optical Physics, Feb. 22-25, 2011, Karnataka University, Dharwad.

3. Invited and delivered a talk on "Novel Turnaround point (TAP) long period fiber gratings: Application for high sensitivity strain and temperature sensors" at 7th Workshop on Fiber Optics and passive components (WFOPC2011) at Montreal, Canada on July 15, 2011.

4.Smita Chaube, **Sanjay Kher**, S. M. Oak, Radiation and taper tuning of long period fiber gratings for high sensitivity strain measurement, P-43 (poster) at International conference on Fiber Optics and Passive Components (WFOPC2011), July 13-15, Montreal, Canada.

5. Invited and delivered a talk on “Novel optical fiber sensors for nuclear radiation monitoring and Radiotherapy”, OSI Symposium on Frontiers in Optics and Photonics, organized at IIT, Delhi during Dec. 3-5, 2011.

6. **Sanjay Kher**, Smita Chaubey, S. M. Oak, “Long period Fiber gratings for GAST: Gamma dose, strain and temperature”, presented a paper during International conference on Fiber Optics and Photonics held at IIT Madras, Chennai during Dec. 9-12, 2012.

DEDICATIONS

I dedicate this thesis to my parents and family.

Sanjay Kher

ACKNOWLEDGEMENTS

This thesis is a result of about five years of hard work, and throughout this period I received a lot of support and encouragement from numerous sources. First and formost, I am greatly indebted to my supervisor Dr. S. M. Oak, who has been instrumental in the successful completion of this thesis. This thesis would not have been possible without his active support and keen interest. My deep regards are due for Dr. L. M. Kukreja who motivated me to work hard and do the best possible.

I would like to thank all members of fiber sensors lab and Solid State laser Division, RRCAT, Indore who provided their full cooperation during my research work. I wish to thank Prof. B. P. Pal, Prof. Arun Kumar and Prof. Thyagarajan of IIT, Delhi for their keen interest in sensor development and encouragement whenever I interacted with them. I wish to thank Dr. D. D. Bhawalkar and Dr. P. K. Gupta who provided valuable comments and numerous suggestions. I extend my appreciation to my colleagues Shri Manoj Kumar Saxena and Mrs. Smita Chaubey for their help in drawing difficult figures and diagrams.

I wish to express my sincere thanks to Dr. P. D. Gupta, Director, RRCAT for permitting me to pursue my Ph.D. and his keen interest in my research work. I wish to thank Dr. P. A. Naik, Dr. S. C. Mehendale and Dr. N. K. Sahoo, BARC, Mumbai for providing valuable suggestions. Finally, I owe a lot to my family for allowing me to spend long hours in preparing this thesis.

Sanjay Kher

CONTENTS

SYNOPSIS

The development of fiber gratings had a significant impact on research and development in telecommunications and fiber optic sensing. Optical fiber gratings are intrinsic devices that allow control over the properties of light propagating within the fiber and also have the ability to efficiently convert energy from one spatial mode to another. In sensing applications, the conventional long period fiber gratings (LPFGs) have limited wavelength sensitivity for temperature, strain and surrounding refractive index due to tight mode field confinement of lower order cladding modes. Numerous studies such as tapering, micro-structuring, chirping and tilting have been conducted to enhance the sensitivity of grating based sensors.

In this thesis, we have carried out the detailed investigation to study the effect of higher order mode coupling and operation near turnaround point (TAP) to enhance the sensitivity of these gratings. The gratings have been modeled, designed and fabricated. These specialty gratings (TAP-LPFGs) offer new physical insight into LPFG behavior and represent a useful design for ultra-sensitive operation. The sensitivity of these devices for various parameters such as temperature, strain and external medium refractive index has been studied. Gamma radiation sensitivity has not been reported yet for any type of fiber gratings above a dose of 150 kGy. We have conduced in-situ studies for high level dose up to 1.5 MGy. We show that novel fiber composition and grating writing techniques can indeed be used to develop radiation dose sensors for high dose level measurements around locations such as near nuclear reactors and for ITER applications. Based on extensive studies, we have designed and packaged high level integrated radiation dose sensors with a dynamic range of 1 kGy to 1 MGy.

The organization of the thesis is as follows:

Chapter1 will briefly review the operating principles of fiber gratings and different techniques for writing gratings in optical fibers. Fiber gratings consist of a periodic perturbation of the properties, generally the refractive index of the core, and fall into two general classifications based on the period of the grating. Short period gratings, or fiber Bragg gratings (FBGs), have a submicron period and act to couple light from the forward propagating mode of the fiber to backward, counter-propagating mode of the fiber.

The long period grating (LPFG) has a period typically in the range of 100 µm - 1 mm. The LPFG promotes coupling between the forward propagating core mode and co-propagating cladding modes. This process results in a series of attenuation bands centered at distinct wavelengths in the transmission spectrum of fiber wherein each band corresponds to a different cladding mode. A UV laser based exposure method, CO_2 laser based scanning method and Arc induced writing method are the most common methods of writing these gratings. The gratings have been modeled to calculate the relationship between $\lambda_{res.}$ and period Λ for wavelength range of 0.9-1.7 µm for first 15 cladding modes. Accordingly, a set of LPFGs with periods covering small, medium and large periods aimed to generate resonances between 950-1700 nm have been inscribed in hydrogen free B-Ge doped fibers and standard communication fibers using CO_2 laser based method and arc excitation technique. They will be described along-with the limitations of each method.

A detailed investigation was carried out into the sensitivity of LPFG as a function of temperature, strain, surrounding refractive index and gamma dose, with particular attention to higher order cladding modes and possibilities for ultra-sensitive sensors. These studies have resulted in development of specialty Turnaround point gratings (TAP-LPFG) which exhibit potentially advantageous properties such as dual resonance feature which has been exploited to realize highly sensitive devices. It has been demonstrated that these specialty gratings can detect presence of as small as 1 % adulteration of kerosene in petrol and hence offer opportunities for development of portable fuel adulteration sensors.

Nuclear Radiation effects on multimode fibers and single mode fibers have been studied. A detailed investigation on the effect of high level gamma dose (up to 1.5 MGy) on parameters of LPFGs has been carried out. These studies have proved that fiber gratings in Boron doped fibers are strong candidates for high level gamma dose sensing applications. A novel approach has been proposed to measure gamma induced refractive index changes in single mode optical fibers. These will be described in detail.

Chapter 2 will cover the sensing characteristics of fiber gratings. It will cover our parametric studies on long period gratings in commercially available fibers and the need for specialty gratings. Some of the salient features compared to fiber Bragg gratings will be described.

The characteristics of long-period fiber gratings are affected by external perturbations such as strain, temperature, dose etc. The effect is primarily due to differential change induced in the effective indices of two coupled modes. Their attractiveness stems from relatively large grating period, ease of fabrication and high sensitivity of the optical properties to grating parameters compared with Bragg gratings. We have carried out experimental studies using a set of LPFGs with small, medium and large periods and measured the sensitivities of these gratings in various commercially available fibers including photonic crystal fibers. In order to protect the fiber gratings from moisture related degradation effects, the gratings have been metal coated and characterized. Studies have been performed to measure stability of these gratings at high temperature exceeding 300 °C. Such gratings will be useful for measurement of strain at high temperature for fast breeder test reactor (FBTR) applications. These will be described in detail.

Chapter 3 will cover the investigations related to development of specialty gratings for sensitivity enhancement. The conventional LPFGs have limited wavelength sensitivity of temperature, strain and surrounding refractive index due to tight mode field confinement of lower order cladding modes. In order to enhance the sensitivity of these gratings, we have carried out the detailed investigation to study the effect of higher order mode coupling and operation near turnaround point (TAP). Their novel applications will be covered in this chapter. In order to develop high sensitivity gratings in commercially available single mode fibers, it was realized that higher order cladding mode coupling and Turnaround mode operation will be desirable. Simulation studies have been done to calculate the relationship between resonant wavelengths and grating period for coupling of higher order cladding modes in standard Germanosilicate (smf-28) and B/Ge doped photosensitive fiber. This resulted in prediction of grating periods for TAP gratings. These gratings were fabricated and their characteristic features such as dual resonant peaks were observed. This chapter will cover simulation, design, development and characteristics of these gratings.

Chapter 4 will cover some new applications of fiber gratings and fiber based sensors for transportation fuel blending/ fuel adulteration. Use of ethanol as a bio-fuel require its purity better than 93 % with water impurity as low as possible. Adulteration of kerosene in petrol leads to air pollution and consequent ill effects on public health. As on today, there is no standard universal technique for quantitative measurement of this adulteration. It has been demonstrated that TAP-LPFGs can provide very high sensitivity of 0.96 nm/ % change of kerosene in petrol up-to 10 % of adulteration. They can also detect the presence of water in ethanol with a resolution of 1%. These techniques offer opportunities for development of portable fuel adulteration sensors. These will be described in detail.

Chapter 5 will cover the studies related to the effects of gamma radiation on fiber grating parameters and development of high level dose sensors. Interaction of ionizing radiation with optical fibers and gratings leads to several physical processes that can be used for radiation dosimetry. Increase of attenuation, luminescence and radiation induced index change have been used to design dose sensors for dose ranges up to 100 kGy. The attenuation based sensors based on specialty doped fibers reach saturation level above 10 kGy. The effect of resonance wavelength shift in fiber gratings occurs due to radiation induced index changes in the optical fiber. However, Most Bragg grating based sensors, reported till date, are either less sensitive or reach saturation level near 50-150 kGy depending on composition and grating writing techniques. This chapter will cover the effects of gamma dose measurements on long period fiber gratings. It will be shown how the fiber composition and grating writing techniques were optimised to develop high level gamma dose sensors up to a dose of 1.5 MGy. Fully packaged devices have been designed and fabricated for dose sensing applications in the range of 1 kGy to 1 MGy. They are under field trials in Indus-1 and beam lines of Indus-2 Synchrotron Source. The research resulted in our hypothesis of gamma induced refractive index change due to polarizabilty changes in B/Ge codoped fiber. We have proposed a novel approach to measure gamma induced refractive index changes using LPFGs. These issues will be addressed to conclude the report.

Chapter 6 presents summary and scope for future work. It will summarize the outcome of the work carried out in the thesis. Some aspects of significance of the work and scope for future work will also be discussed.

LIST OF FIGURES

CHAPTER 1

CHAPTER 2

CHAPTER 4

CHAPTER 6

There is no figure in this chapter.

LIST OF TABLES

CHAPTER 6

There is no Table in this chapter.

LIST OF ACRONYMS

DWS	Dip Wavelength Shift
ESM-PCF	Endlessly Single Mode-PCF
FBG	Fiber Bragg Grating
ITER	International Thermonuclear Experimental Reactor
LPFG	Long Period Fiber Grating
MFD	Mode Field Diameter
NA	Numerical Aperture
OSA	Optical Spectrum Analyzer
OSL	Optically Stimulated Luminescence
PHWR	Pressurized Heavy Water Reactor
PMC	Phase Matching Curve
PCF	Photonic Crystal Fiber
PBF	Photonic Band-gap guiding Fiber
RIU	Refractive Index Unit
RI	Refractive Index
RIA	Radiation Induced Attenuation
SRI	Surrounding-medium refractive index

Smf-28	Standard single mode fiber of Corning Inc. (USA)
SPCVD	Surface Assisted Chemical Vapor Deposition
TAP-LPFG	Turn-Around-Point LPFG
WDM	Wavelength Division Multiplexing

CHAPTER 1

INTRODUCTION AND REVIEW

1.1 Introduction

Optical fiber sensors are a novel and ideal approach for performing chemical and biological measurements in a wide range of applications. Small size, EMI/RFI immunity, corrosion resistance, fast response, long lead length capability and embeddability make fiber optic sensors an attractive alternative to many competitive sensors. Fiber sensors till date resulted in relatively few commercial successes, market penetration is not remarkable and the technology remains at prototype stage. The reason for this is clear: many fiber optic sensors were developed to displace conventional electro-mechanical sensor systems which are well established, have proven reliability and available at reasonable cost. In applications where fiber sensors offer new capabilities such as distributed sensing and wavelength encoded operation, fiber sensors appear to have a distinct edge over their conventional counterparts. The development of fiber gratings has made a significant impact on research and development in telecommunications and fiber optic sensing. Fiber gratings are intrinsic devices that allow control over properties of light propagating within the fiber. The impressive environmental capabilities of such grating based devices are facilitating their acceptance in a myriad of industrial, commercial and nuclear reactor sensing applications **[1-4].**

In this chapter, I am presenting summaries of general techniques for fiber sensing applications and most important results acquired during the past years through studies on optical fibers and fiber gratings.

1.2 Review of fiber gratings

Fiber gratings consist of a periodic perturbation of the properties of the optical fiber, generally the refractive index of the core. They fall into following two general categories dictated by the period of the grating: fiber Bragg gratings and long period gratings.

1.2.1 Fiber Bragg gratings

Fiber Bragg gratings (FBGs) (also known as Short-period fiber gratings) have a sub-micron period and act to couple light from forward-propagating mode of the optical fiber to backward, counter propagating mode. When a germanium doped silica core fiber is exposed to ultraviolet radiation (with wavelength ~240 nm), the refractive index of the Ge doped region increases due to phenomenon of photosensitivity which was discovered by Hill in 1974 [**2**]. Due to submicron period required to satisfy the Bragg condition, FBGs are formed by exposing a photosensitive fiber to interference pattern formed between two UV beams resulting in the formation of periodic refractive index variation in the core (Fig. 1.1).

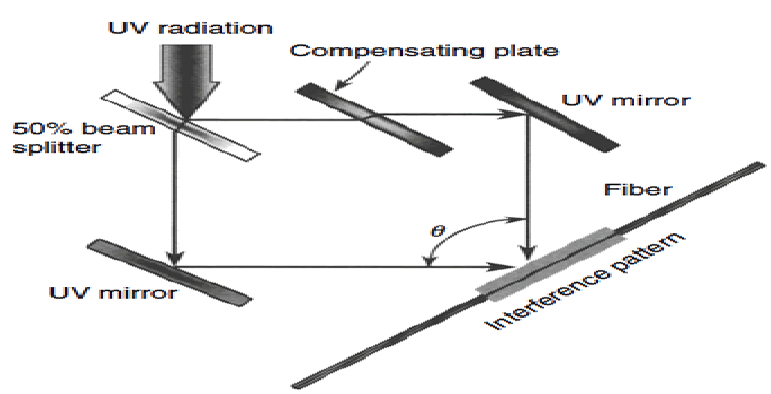

Fig. 1.1. Typical set-up for writing fiber Bragg gratings [**1**]

The coupling occurs at a specific wavelength, defined by Bragg condition for the fiber grating. The Bragg wavelength, or resonance condition of a grating, is given by the following expression **[2, 3]**

$$\lambda_B = 2\Lambda n_{eff} \tag{1.1}$$

where Λ is the period of the refractive index modulation and n_{eff} is the effective index of the propagating mode. Here, n_{eff} depends not only on the wavelength but also (for multimode waveguides) on the mode in which the light propagates. For this reason, it is also called modal index. The grating works as a narrow band reflection filter **[3]** and as a narrow-band channel-dropping filter when operated in transmission as shown in Fig. 1.2.

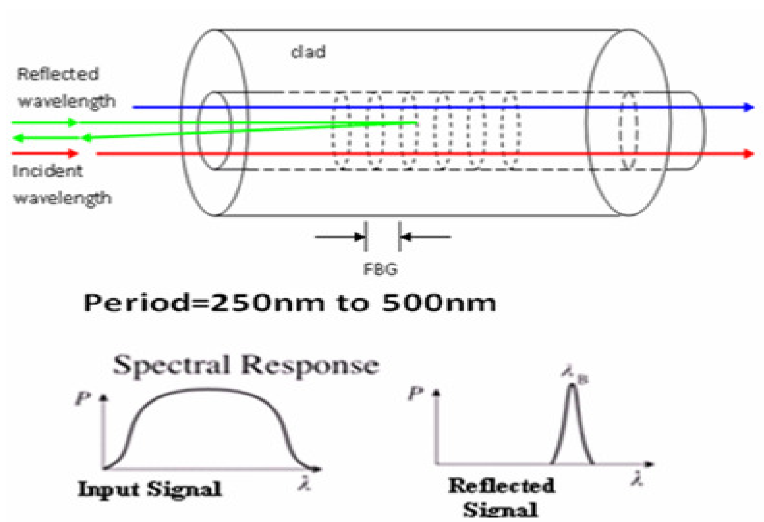

Fig. 1.2. Working principle of FBG

The wavelength spacing between the first minima (nulls), or the bandwidth ($\Delta\lambda$), is (in the strong grating limit) given by,

$$\Delta\lambda = \left[\frac{2\delta n_0 \eta}{\pi}\right]\lambda_B \tag{1.2}$$

where δn_0 is the variation in the refractive index or modulation depth, and η is the fraction of power in the core. The peak reflection ($P_B(\lambda_B)$) is approximately given as [**1**]

$$P_B\left(\lambda_B\right) \approx \tanh^2\left[\frac{N\eta(V)\delta n_0}{n}\right] \tag{1.3}$$

where N is the number of periodic variations. For a silica fiber, $n_{eff} \approx 1.46$. For a periodic structure to be reflecting at $\lambda = 1550$, it is found using Eq. (1.1) that the required grating period is 0.531 µm. Using Equations (1.2) & (1.3), the corresponding peak reflectivity and bandwidth for a 2 mm long grating (having index modulation of 4×10^{-4}) are found to be about 85 % and 1 nm, respectively.

1.2.2 Mechanism of index modulation in FBGs

When UV light radiates an optical fiber, the refractive index of the fiber is changed permanently; the effect is termed photosensitivity. At first, the observation of photo-induced refractivity in fibers was only a scientific curiosity, but over time it has become the basis for a technology that has a broad and pivotal role in optical communication and sensor systems. The photosensitivity of optical fibers has been correlated with concentration of GeO defects in the core. The presence of defects indicated by absorption at 240 nm, observed by Dong et al. **[5]** was attributed to reduced Germania state, Ge(II). The number density of defects generally increases as a function of Ge concentration and is also dependent upon preform processing, core composition and fiber drawing conditions.

The magnitude of the refractive index change (index modulation) obtained depends on several factors such as irradiation conditions (wavelength, intensity, and total dosage), the composition of glass forming the fiber core and any processing prior to irradiation. Hot hydrogenation at 650 °C or cold hydrogenation at high pressure (800 bars) is performed to increase the photosensitivity of the fiber. The hydrogen reacts with Ge ions to form GeH which change the band structure in the UV region. These changes in turn influence the local refractive index as per Kramers-Kronig model. The induced changes are reported to be large enough and are of the order of 2.8×10^{-3} [**5**].

The growth rate and maximum index change are of interest if strong gratings are to be fabricated in a short time. The incorporation of 0.1 % of nitrogen in Ge doped silica fiber by surface assisted chemical vapor deposition process (SPCVD) has been shown to have a high photosensitivity. Since addition of Ge increases the core index while Boron doping reduces the index, Boron doping is generally used to dope high level of Germania in the fiber core while maintaining the low index difference between core and cladding. This process results in high photosensitivity with identical index profile with standard single mode fibers. A point worth noting with B/Ge doped fibers is the increased stress, and consequently, increased birefringence. The preforms are difficult to handle due to high stress. However, the three real advantages with these fibers are:

(a) shortened grating writing time,

(b) the large UV induced index change (about 10^{-3}), and

(c) compatibility with standard communication fibers.

The measurement of the shift in the Bragg wavelength is a reasonable indicator for UV induced index change for a fiber well below the start of saturation effects. With saturation, the bandwidth of the grating increases and as a result, it becomes difficult to measure the wavelength accurately. Therefore, the index change should be calculated from bandwidth, reflectivity and wavelength shift.

1.2.3 Classification of FBGs

The Bragg gratings are classified based on index modulation and designed as per the desirable properties as shown in Fig. 1.3. The refractive index profile of a grating may be modified to add features, such as a linear variation in the grating period, called a chirp. The reflected wavelength changes with the grating period and broadens the reflected spectrum. A grating possessing a chirp has the property of adding dispersion, namely, different wavelengths reflected from the grating will be subject to different delays. In standard FBGs, the grading or variation of the refractive index is along the length of the fiber (the optical axis), and is typically uniform across the width of the fiber. In a tilted FBG (TFBG), the variation of the refractive index is at an angle to the optical axis. The angle of tilt in a TFBG has an effect on the reflected wavelength, and bandwidth.

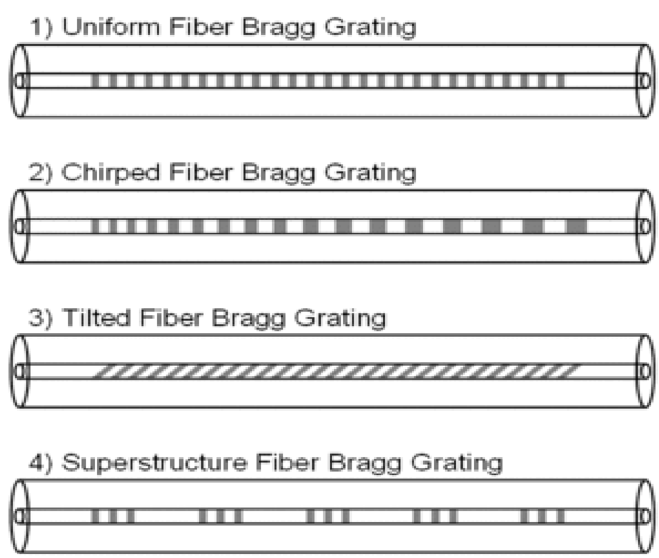

Fig. 1.3. Grating classification based on index modulation

Super structure FBG (SSFBG) generally refers to a FBG whose RI profile is not uniform in amplitude and / or phase along its length. Periodically modulated exposure makes super structure FBG function as long period grating and so introduces broadband loss peaks in transmission spectra.

1.2.4 Types of FBGs based on writing conditions

Three distinct regimes of FBGs have been identified, each appearing under different exposure conditions. The gratings formed under continuous light or weak multiple pulses (below 30 mJ) and exhibiting a nearly ideal transmission spectrum are designed as type I. Regenerated gratings after erasure of a type I grating in hydrogenated germanosilicate fibers are known as type IA. These are the gratings that are reborn at high temperature after erasure of type I gratings and usually require presence of Hydrogen. A large increase of Bragg wavelength (red shift) was observed during its formation. Recent work has shown that these gratings are extremely attractive for ultrahigh temperature applications **[6].**

Type IIA are gratings that form due to decrease of index of silica and are also labeled type In (type I grating with negative index change). Damage written gratings inscribed by multiphoton excitation with higher intensity lasers that exceed the damage threshold of the glass. Lasers employed are usually pulsed in order to reach these intensities. They include recent developments in multiphoton excitation using femto second pulses where the short timescales (commensurate on a timescale similar to local relaxation times) offer unprecedented spatial localization of the induced change. The amorphous network of the glass is usually transformed via a different ionization and melting pathway to give either higher index changes or create, through micro-explosions, voids surrounded by more dense glass.

It has been shown that it was possible to inscribe gratings of ~100% (>99.8%) reflectance with a single UV pulse in fibers on the draw tower [**97**]. The resulting gratings were shown to be stable at temperatures as high as 800 °C (up to 1,000 °C in some cases, and higher with femtosecond laser inscription). The gratings were inscribed using a single 40 mJ pulse from an excimer laser at 248 nm. It was further shown that a sharp threshold was evident at ~30 mJ; above this level the index modulation increased by more than two orders of magnitude, whereas below 30 mJ the index modulation grew linearly with pulse energy [**96, 97**]. For ease of identification, and in recognition of the distinct differences in thermal stability, they labeled gratings fabricated below the threshold as type I gratings and above the threshold as type II gratings [**96**]. Microscopic examination of these gratings showed a periodic damage track at the grating's site within the fiber, hence type II gratings are also known as damage gratings.

Typically, gratings in B/Ge doped fiber decay more rapidly than low Ge doped (5 mol %) fibers when annealed at 400 °C for 30 minutes. If annealed, Boron doped fibers have additional losses in the 1550 nm window which are not desirable for communication applications.

1.2.5 Applications of Bragg gratings

Fiber Bragg gratings are the candidates for number of applications in space-borne systems and nuclear reactor sites not only due to their optical functionality but also because of the fact that they have small dimensions, low mass and are immune to electromagnetic interference. The Bragg wavelength is governed by the period of the FBG and the effective index of the propagating mode. Therefore, any change in either of these parameters, induced by a change in temperature, pressure or strain changes the wavelength and forms the basis of sensing schemes.

Because of the extremely small bandwidth of the reflected spectrum, FBGs are extensively used as sensors. For telecommunication satellites, the multiplexing based on FBGs allow a significant reduction in complexity of on-board electronic systems. The strain sensors integrated into fuel tanks and reactor vessels are useful for health monitoring of large structures [**1, 3**]. These applications require high stability of their properties, especially in nuclear radiation environment. Sensor applications of FBGs can be summarized as follows:

(a) FBG as temperature sensor:

The use of FBGs as a temperature sensor is based on detection of the Bragg peak shifts with a temperature change. The sensitivity of Bragg wavelength to temperature arises from the change in period associated with the thermal expansion of the fiber, coupled with a change in the refractive index arising from the thermo-optic effect. This shift is well approximated by a linear expression [**4**]:

$$\frac{\Delta\lambda_B}{\Delta T} = (\alpha + \beta) . \lambda_B \qquad (1.4)$$

where, α is the coefficient of thermal expansion of the fiber and β is the fiber refractive index variation with temperature, respectively. The practical values of these constants for typical silica fiber are:

$$\alpha = 0.55\times10^{-6}/\ °C,$$

$$\text{and, } \beta = 6.67\times 10^{-6}/\ °C$$

The information about temperature changes is wavelength encoded and is essentially independent of radiation induced transmission losses.

(b) FBG as strain sensor:

The strain sensitivity arises due to both properties; the physical elongation of the optical fiber (corresponding change in the grating pitch) and the change in the refractive index of the fiber due to strain-optic effect. This strain induced shift can be written as [**7**]

$$\Delta\lambda_B = (1 - p_e)\ \lambda_B \varepsilon \tag{1.5}$$

where, ε is the applied strain and p_e is an effective photo-elastic coefficient term given by

$$p_e = \frac{n^2}{2}\left[p_{12} - \nu\ (p_{11} - p_{12})\right] \tag{1.6}$$

where, p_{ij} are the Pockels coefficients of the strain optic tensor and ν is the Poisson ratio. Typically, FBG sensors have sensitivities to temperature and strain which are of the order of 13 pm/ K^{-1} and 1 pm $\mu\varepsilon^{-1}$ respectively **[7].** There is a limited scope for enhancing the sensitivity using FBGs. A wavelength resolution of 10 pm is required to resolve a temperature change of about 1 Degree C and 10 με. The use of UV exposure and hydrogen treatment for writing FBGs has implications for thermal stability of such gratings and limits their usage below 300 °C. Some industrial, nuclear and aerospace applications require sensors to operate at elevated temperatures for extended periods of time. Various writing techniques and new fiber compositions are under development for stabilizing FBGs up-to 900 °C for emerging applications such as oil well monitoring and strain measurement at high temperature in Fast Breeder Reactors (FBTRs) **[8].**

(c) Distributed sensors

One of the main advantages of the FBG sensors is the fact that several gratings can be written on a single fiber. Each grating can be designed with a different period and therefore a specific wavelength at which peak reflectivity occurs. If such a distributed sensor is embedded in concrete structure of the bridge, one can measure the strain corresponding to the particular region. This type of design offers distributed strain sensing capabilities and are extensively used in modern bridges [**9].**

(d) Nuclear Radiation effects on fiber optic components and FBGs

Optical fibers and fiber optic devices such as WDM components, surface emitting laser diodes are subject to many investigations with respect to the influence of nuclear radiation. Also, various fiber optic sensors which are serious candidates for integration in nuclear environments require proper characterization due to presence of ionizing radiation fields. The resulting system malfunction might have dramatic consequences on safety and cost. The unit of radiation dose used throughout the thesis is Gy ("Gray"), where 1 Gy corresponds to an absorbed energy of 1 Joule per kilogram of the material. Temperature sensors based on Fabry-Perot cavity, fluorescence sensors and fiber gratings have been studied for possible performance degradation due to gamma and neutron effects **[10]**.

For a pressurized heavy water reactor (PHWR), the typical operation dose over a period of 40 years is 500 kGy while the accidental condition dose is 1.5 MGy. For spent fuel manipulation, fuel handling and inspection the total dose is expected to be [**8, 10**] 1-10 MGy. Obviously, the presence of such high level radiation calls for using remote controlled devices and sensors. Generally, pure silica fibers or fibers with very low Ge doping show the lowest radiation-induced losses. The radiation induced loss measured at 850 nm for a pure silica core MM fiber at a total dose of 1.5 MGy and dose rate of 2 kGy/h would be around 2.5 dB in a 100 meter length. Fabry-Perot type sensors and fluorescence temperature sensors are strongly affected below kGy level. Little information is available about the radiation response of optical fiber couplers. For broadband couplers, an increased loss at 1310/ 1550 nm and decreased isolation at levels not detrimental to its performance have been reported. The narrowband WDM couplers exhibit a drift of the wavelength isolation channels of approximately 0.5 pm/ kGy [**8, 10**].

For Bragg gratings, the changes of grating strength, width of the peak and shift of the Bragg wavelength depend upon the chemical composition of the fiber and writing conditions **[11]**. For example, the amplitude and the width of the Bragg peak changed during gamma irradiation in hydrogen loaded Ge-doped fibers and N-doped fibers while it did not change for gratings written in unloaded Ge-doped fibers. The radiation induced shift of Bragg peak gets more saturated at higher level for FBGs written in hydrogen loaded fibers as compared to unloaded high Ge-doped fibers **[12]**.

The radiation response of FBGs also strongly depends upon the type/regime of gratings such as type I, type IIa etc. Both blue and red (shorter and longer) wavelength shifts have been reported in type I FBGs while the exact physical mechanisms are yet to be identified. One of the possible mechanisms is the creation and existence of two different types of defects: One type is responsible for refractive index increase while the other type of defects results in decrease of refractive index **[13].** Changes of grating strength during irradiation are attributed to different kinetics in radiation-induced changes of refractive index at maxima and minima of UV fringe pattern. The higher gamma radiation sensitivity of FBGs in hydrogen loaded fibers is thought to be due to radiolytic ruptures of OH-bonds. It has been observed that temperature sensitivity of most FBGs remain unaffected due to high level of gamma radiation. Various pre-and post-fabrication treatments were applied with the aim to improve the radiation tolerance of the FBGs.

(e) Radiation dose measurements using Fiber sensors and FBGs

Optical fiber offers a unique capability for remote monitoring of radiation in difficult-to- access or hazardous locations **[12].** Fiber Optic radiation monitors are under evaluation for dose monitoring applications due to certain advantages compared to conventional radiation monitors. Real-time monitoring of local dose deposition, distributed hot-spots dose monitoring along single fiber using OTDR techniques are some of the key features of fiber optic sensors. Radiation induced optical attenuation, scintillation and luminescence measurements such as optically stimulated luminescence (OSL) have been used to measure radiation dose in real time. An ideal fiber optic dosimeter should not only exhibit a high radiation sensitivity, but also weak annealing effects. Most commercially available fibers do not meet these requirements. Therefore, specialty fibers with specific dopants are developed to obtain weakly recovering fibers [**8, 11**].

In the low dose regime up-to 1 kGy, it has been shown that Phosphorous core doped fibers with dopants like Ge, show linear attenuation with no annealing even after several months when interrogated at 1.5 micron wavelength range [**8**]. However, for such fibers attenuation increase with dose is reduced above dose values greater than about 1 kGy and reaches saturation above 50 kGy in the whole wavelength range of 670-1550 nm. A fiber coupled optically stimulated luminescence crystal samples of SrS:Ce:Sm and/or CsI (Tl) works as a useful dosimeter in 10 μGy to 100 Gy range.

New materials, crystal scintillators and techniques are being developed for high level dose monitoring applications in critical diagnostic system for international thermonuclear experimental reactor (ITER). The expected dose rate at the ITER first wall will be about 2-10^3 Gy/s and the total dose during plasma burn inside the vacuum vessel is expected to be 1 GGy. As a result of this intense radiation which severely degrades most insulators, proactive radiation monitoring will be essential to reduce the risk of catastrophic failure of vital components and equipment.

Plastic dosimeters based on PMMA fibers are under intense investigation where the ratio of the attenuation at two carefully chosen wavelengths is used to derive the dose information up-to 30 kGy. The dose information is derived form radiation induced coloration of certain dyed and colorless PMMA fibers. The first wavelength is chosen that is affected by gamma radiation but exhibits a minimal fading. The second wavelength should be chosen which is least affected by gamma. Presently they show a threshold in terms of dose (100-1000 Gy), some annealing effects and fading and so can not be used as re-usable dosimeter but as a low cost single use integrating dosimeters **[14].** High doses are believed to affect the main polymer structure while the fading affect is observed due to spontaneous reforming of polymer chains that are damaged during irradiation.

It has been observed that high dose regime of 100 kGy to 10 MGy seem to be unreachable with dosimeters based on established techniques of attenuation, fluorescence, OSL etc. Therefore, radiation induced change of the refractive index has been studied for high level radiation dosimetry. The nuclear radiation sensitivity of FBGs strongly depends on the chemical composition of the fiber and the method of their fabrication. Based on various studies, some conclusions can be drawn:

(a) it is published that the hydrogen content during grating writing has a significant influence on the radiation sensitivity of FBGs **[13].**

(b) the radiation induced Bragg wavelength shift (BWS) increases from 657 to 1516 nm, despite the fact that fibers show distinctively higher radiation induced attenuation at shorter wavelengths **[15].**

(c) it has been shown that coating does not influence the radiation sensitivity of FBG.

1.2.6 Limitations of FBG sensors

Most often FBGs are written using an UV source or femtosecond laser and it is believed that these techniques can influence the fiber sensitivity to gamma radiation. For example, for type 1A gratings prolonged UV exposure results in significant increase of sensitivity to ionizing radiation but they have been studied only up-to a dose of 100 kGy **[12].** However, for type 1 and type IIA gratings very little influence of an additional UV exposure was observed **[13].** In other cases, Bragg gratings showed poor gamma radiation sensitivity with saturation for doses of 50-150 kGy or blue shifts after a certain dose **[14].** Such variability has complicated the analysis of ionizing radiation induced RI changes in optical fibers based on FBG behavior. Therefore, FBG based gamma dose sensor devices were not developed or reported in literature.

The FBG sensors suffer from limited external conditions-induced spectral shifts because of confinement of modal fields in the core and they are difficult to manufacture because of stringent stability requirements of UV laser. Due to limited sensitivity, they require spectrometers/interrogators with high resolution. These shortcomings of Bragg gratings have spurred the intensive investigation of long period fiber gratings as described in this thesis.

We have developed techniques for writing long period fiber gratings in different types of commercially available single mode fibers including photonic crystal fibers (PCFs). The effect of fiber composition and order of the cladding mode has been studied for development of high sensitivity sensors for temperature and strain measurements. Specialty gratings such as turn-around point (TAP) LPFGs have been fabricated and their use for transportation fuel adulteration has been demonstrated. In order to develop fiber gratings for high level gamma dose sensing applications, modeling and experimental studies were done. These studies have led to fully packaged devices for sensing gamma dose up to 1 MGy.

1.3 Review of long period Fiber gratings

1.3.1 Operating Principle

The invention of long period fiber gratings by Ashish Vengasarkar in 1996, introduced a very important optical device platform that presented a key functionality in optical communication systems during the evolution of WDM systems **[16, 17].** It also established the new applications of optical fiber devices in the emerging field of optical sensing. Long period gratings are periodic structures that couple co-propagating modes in optical fiber. The LPFGs provide the phase matching between the core guided mode (the fundamental LP01) and higher order modes that propagate in the cladding region. The long period fiber grating (LPFG) has a period typically in the range of 100 µm to 1 mm.The excited cladding mode attenuates in the coated fiber part after the grating, which results in the appearance of resonance loss in the transmission spectrum. This result in the transmission spectrum of the fiber containing a series of attenuation bands centered at discreet wavelengths, where each band correspond to the coupling to a different cladding mode. Fig. 4 shows the transmission characteristics of a typical LPFG.

An optical fibre has two waveguide structures, one is the high-index core surrounded by the lower-index cladding and another being the cladding surrounded by air. In an LPFG, phase matching condition between the fundamental core mode and the copropagating cladding modes is achieved at resonance wavelengths λ which is determined by following expression [16]

$$\lambda = \left[n_{co}^{eff}(\lambda) - n_{cl,i}^{eff}(\lambda) \right] \Lambda \qquad (1.7)$$

where, $n_{co}^{eff}(\lambda)$ is the effective refractive index of the propagating core mode at wavelength λ, $n_{cl,i}^{eff}(\lambda)$ is the effective refractive index of the i^{th} cladding mode at a wavelength λ and Λ is the period of the LPFG . Higher order cladding modes (5 to 10) can be coupled if the grating period is kept shorter than 250 micron for B/Ge doped single modes fibers.

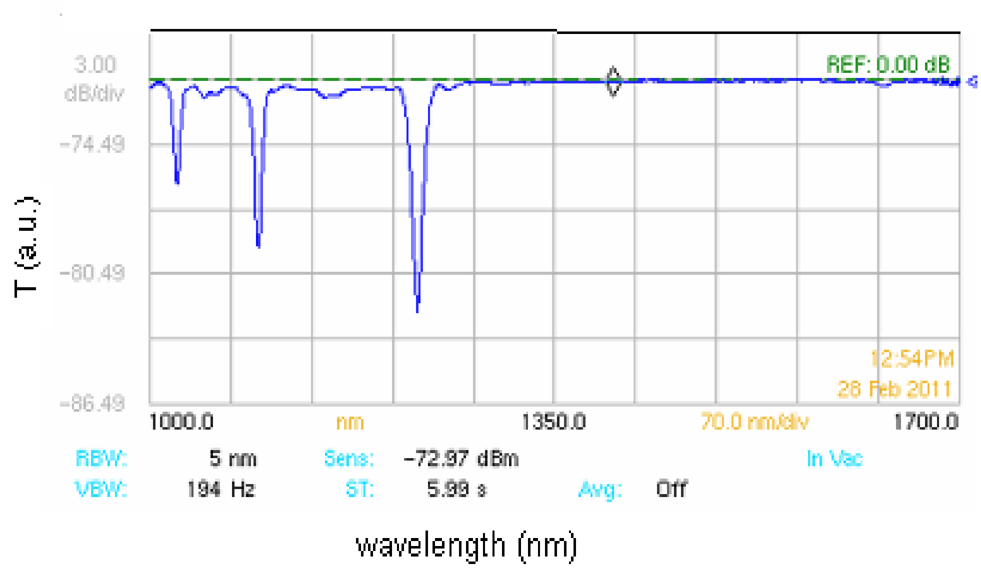

Fig. 1.4. Transmission spectrum of a typical LPFG

The smallest transmission of the attenuation bands is governed by the expression [1]

$$T_i = 1 - (\sin \kappa_i L)^2 \qquad (1.8)$$

where L is the length of the grating and κ_i is the coupling coefficient for the i^{th} cladding mode, which is determined by the overlap integral of the core and cladding mode and by the amplitude of the periodic modulation of the mode propagation constants. The 3 dB bandwidth of the resonance peak of an LPFG of length L is given by the expression [**16**]

$$\Delta\lambda_{3dB} = \frac{0.8\lambda_{res}^2}{L\left|\Delta n_g\right|} \qquad (1.9)$$

Where $\Delta n_g = n_{co}^g - n_{cl,m}^g$ is the difference in group index between core mode and the mth cladding mode. The group index of core mode is defined as $n_{co}^{eff} - \lambda\left[\frac{dn_{co}^{eff}}{d\lambda}\right]$.

1.3.2. Grating writing techniques

In contrast to Bragg grating, LPFG does not produce reflected light and can serve as spectrally selective loss element. Vengasarkar et al**. [14]** wrote the first LPFG in conventional glass fibers in 1996 using UV laser-induced index modulation. Since then, various fabrication methods, such as ultraviolet (UV) laser exposure, CO_2 laser irradiation, electric arc discharge, femtosecond laser exposure, mechanical micro bends and ion implantation have been demonstrated to write LPFGs in different types of optical fibers.

(a) CO_2 laser based technique

Davis et al**. [18]** reported the first grating written by CO_2 laser irradiation technique in a conventional glass fiber in 1998. Compared with UV-laser exposure technique, the CO_2 laser irradiation technique is much more flexible and low cost because no photosensitivity and any other pretreated processes are required to write the gratings in glass fibers. It has been shown that this technique can be controlled to generate complicated grating profiles without expensive masks. It also produces LPFGs with high temperature stability and polarization insensitivity **[19].**

Typically, in the CO_2 laser technique, the fiber is periodically moved along its axis direction via a computer controlled translation stage and CO_2 beam irradiates periodically the fiber through a shutter, controlled by the same computer. A light source and an optical spectrum analyzer are employed to monitor the evolution of the grating spectrum during laser irradiation. Recently, a novel writing method based on two dimensional scanning of CO_2 laser beam has been demonstrated [**19**]. The focused high frequency CO_2 laser pulses are scanned periodically across the fiber along X direction and then shifted by grating pitch along Y direction, i.e., the fiber axis, to create next grating period by means of 2-D optical scanners under computer control. Since no movement of fiber is required, this technique can write high quality LPFGs with zero insertion loss and accurate period as supported by the modeling studies.

Specialty gratings such as Turnaround-point LPFGs (TAP-LPFGS) have also been designed and fabricated for very high sensitivity applications using CO_2 lasers. Most studies have been focused on the resonant coupling of lower order cladding modes. However, high order cladding modes exhibit some quite different properties including dual resonance feature that can be exploited for designing very sensitive device. Fig. 5 shows the transmission spectrum of TAP-LPFG.

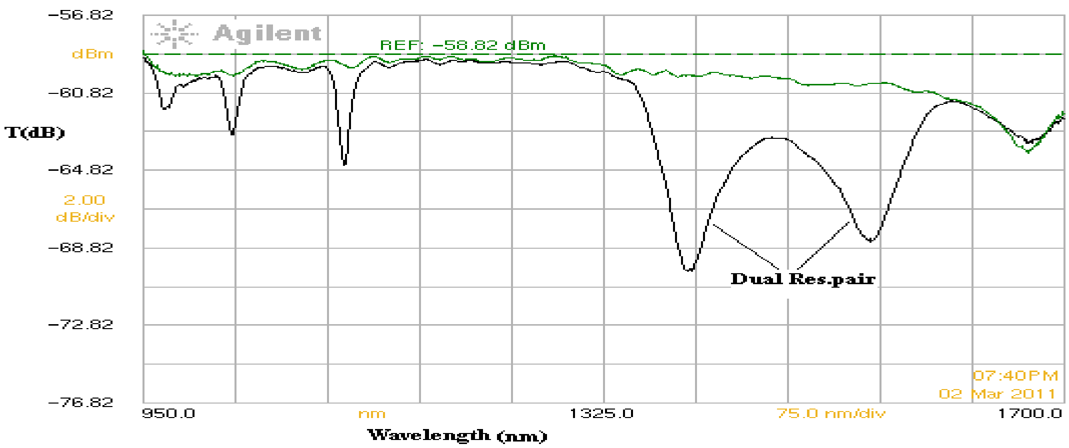

Fig. 1.5. Transmission spectrum of TAP-LPFG in B/Ge co-doped fiber

Compared with normal UV-laser technique, the CO_2 laser irradiation technique is easily used to write special gratings such as phase shifted LPFGs, chirped LPFGs, grating pairs and apodized LPFGs. Moreover, this technique could be used to write LPFGs in almost all types of fibers including pure silica PCF fibers **[20].** The most exciting development is to successfully write the first LPFG in an air-core Photonic bandgap fiber (PBF) by the use of focused CO_2 laser beam to periodically deform the air holes along the fiber axis. Such breakthrough opens the door to PCF based gratings and devices in air-core PBFs [**19**].

(b)Arc excitation method for LPFG writing

The gratings with period exceeding 300 micron have also been written using electric arc-discharge technique with point by point exposure method in various types of SM fibers. The gratings have been reported **[21]** with low insertion loss (0.2 dB) and high isolation peaks (-20 dB) in standard single-mode fiber (Corning SMF28). An electric discharge is produced with a current less than 10 mA and duration of 0.5 Sec. exposing a portion of about 150 micron fiber length. The fiber is then moved by the required grating pitch and the arc is activated again. High temperature characterizations of the fabricated gratings in the range of 300-1200 °C have been performed. Temperature annealing of such gratings at 200, 400, 600 ^{0}C shows high thermal stability compared to UV-induced gratings. This technique is also capable of writing gratings in fiber types where UV based technique shows poor performance.

1.3.3 The Mechanism of Index Modulation

The mechanism of index change is believed to be stress relaxation, physical deformation and breakage of Si-O-Ge chains depending on the composition and fiber drawing methods. Residual stress is formed in optical fibers during the drawing process, resulting from thermal stress due to difference in expansion coefficients between core and cladding and mechanical stress caused due to difference in visco-elastic properties of two regions. In B-Ge doped fibers and standard communication fibers, the stress relaxation by CO_2 laser is found to be the main mechanism of formation of grating. Residual stress relaxation usually results in a decrease in the refractive index in the fibers and the efficiency of index decrease depends strongly on the types of the fiber and drawing force during drawing process of the fiber. For example, the index change from residual stress relaxation in a B/Ge codoped fiber drawn at 0.53N, 1.38 N, 2.50 N and 3.43 N was measured to be -3.6×10^{-5}, -8×10^{-5}, -1.7×10^{-4} and $- 2\times 10^{-4}$ respectively **[22].** The glass structure change plays an important role in commercial Boron doped fibers that have small residual stresses.

A combination of up to four effects is responsible for generation of periodic modulation in arc method. The fiber diameter change (periodic tapering), induction of microbends, the dopant diffusion and change of glass properties by local cooling and heating process are believed to be the main mechanisms of mode coupling in such gratings [**21**]. Prominent changes in fiber structure were observed in high Ge doped fibers. Microscopy, Raman and luminescence spectroscopy of arc-Induced gratings in standard single mode fiber (SMF-28) reveal rearrangement of local fiber structure and a weak geometrical deformation as the main mechanism of index change [**23**].

1.3.4. Gratings in Holey fiber

Over the past decade, PCFs (Holey fiber) have attracted a great deal of interest due to their unique optical properties and a quest of fiber designs for ultrahigh bandwidth fiber communication. The gratings in these fibers are realized by periodic collapse of air holes in the index guiding PCF via heat treatment with a CO_2 laser. The resulting periodic hole size perturbation produces core-to-cladding mode conversion thus creating a novel LPFG in the PCF. In another type of PCFs, especially photonic band-gap guiding fibers (PBF), the gratings offer a number of unique features including high dispersion, low non-linearity and new possibilities for long length light-matter interactions. However, gratings in PBF have not been reported until 2008 due to difficulty of inducing index changes in air core PBF due to air core structure. Wang et al. **[19]** reported the first LPFG in air-core PBF using X-Y scanning, low average power, and highly stable CO_2 laser. It was observed that the outer rings of air-holes in the cladding were deformed with little deformation in the innermost ring of air holes and in the air core. As a result, periodic index modulations were achieved along the fiber axis due to photo elastic effect, thus creating a novel LPFG in air-core PBF.

1.4 Applications of LPFGs

Numerous LPFG-based devices have also been developed to realize their sensing and communication applications. LPFG sensors have many advantages over FBGs, such as ease of fabrication, very low back reflection, and low insertion loss and in particular, high sensitivity to temperature, strain, bending and nuclear radiation. It is known that the exact form of the spectrum and the center wavelengths of attenuation bands are sensitive to the period of the LPFG, by the order of cladding mode to which coupling takes place, the length of the LPFG, by the composition of the optical fiber and to the local environment such as temperature, strain, bend radius and the refractive index of the medium surrounding the fiber cladding. This combination of factors allows the fabrication of LPFGs that have range of responses to a particular measurement parameter; a single LPFG may have attenuation bands that have a positive sensitivity to a parameter, others that are insensitive to the parameter and others with a negative sensitivity.

1.4.1 LPFG based temperature sensors:

The origin of temperature sensitivity may be understood by expression [**23, 27**]

$$\frac{d\lambda}{dT} = \frac{d\lambda}{d(\delta n_{eff})}\left\{\frac{dn_{co}^{eff}}{dT} - \frac{dn_{cl,i}^{eff}}{dT}\right\} + \frac{\Lambda}{L}\frac{d\lambda}{d\Lambda}\frac{dL}{dT} \qquad (1.10)$$

where, λ is the central wavelength of the attenuation band, T is the temperature, n_{co}^{eff} is the effective index of the core mode, $n_{cl,i}^{eff}$ is the effective index of the i^{th} cladding mode, $\delta n_{eff} = n_{co}^{eff} - n_{cl,i}^{eff}$, L is the length of LPFG and Λ is the period of the LPFG.

The first term on the right hand side of Eq (1.10) is the material contribution, and is related to change in the differential refractive index due to thermo-optic effect. This is dependent upon the composition of the fiber and is strongly dependent upon the order of cladding mode. The second term is the waveguide contribution which results from changes in the LPFG's period due to temperature. The overall shift of a resonance dip is a function of fiber properties, the grating period and the order of cladding mode. For coupling to low order cladding modes $d\lambda / d\Lambda$ is positive, while for higher order cladding modes this term is negative. Thus, by appropriate choice of LPFG period it is possible to balance the two contributions to produce a temperature-independent attenuation band and also to produce attenuation bands with positive or negative sensitivities appropriate to specific applications. Also, the fiber composition can be tailored for core and clad thermo-optic coefficients so as to achieve required temperature sensitivity.

LPFGs fabricated in standard telecommunication optical fiber exhibit temperature sensitivities in the range of 0.03 nm/ $^{\circ}$C to 0.1 nm / $^{\circ}$C **[23].** This is an order of magnitude larger than the sensitivity of FBG fibers. Temperature compensated LPFGs have been demonstrated by coupling to higher order modes, which have lower material contribution. For example, an LPFG with a period 40 micron was found to have sensitivity of 1.8 pm C^{-1}, an order smaller than FBG **[24].** For enhancing the temperature sensitivities, a number of techniques such as specialty turnaround point (TAP) gratings, use of fibers with special dopants and use of polymer coatings of large thermo-optic coefficients have been reported **[25].** For temperature-insensitive gratings, athermal packagings, recoating the fiber with negative thermo-optic coefficient, exploitation of bend sensitivity and use of PCF fibers have been reported.

1.4.2 LPFG based strain sensors

The axial strain sensitivity of LPFG can be understood by the expression [**27**]

$$\frac{d\lambda}{d\varepsilon}=\frac{d\lambda}{d(\delta n_{eff})}\left\{\frac{dn_{co}^{eff}}{d\varepsilon}-\frac{dn_{cl,i}^{eff}}{d\varepsilon}\right\}+\Lambda\frac{d\lambda}{d\Lambda} \qquad (1.11)$$

The strain sensitivity of LPFG consists of material and waveguide effects. The material contribution results from strain-optic (change in refractive index) and Poisson effect (change in transverse dimensions), while the waveguide contribution depends on the slope of $\frac{d\lambda}{d\Lambda}$ of the characteristic curve of the resonance band. Again, the appropriate choice of grating period and fiber composition allows the generation of gratings with positive, negative or zero sensitivity to strain. An LPFG with a period of 340 micron written in Corning Flexcore fiber exhibited strain sensitivity of 0.04 pm/με which is an order of magnitude less than FBG operating at 1330 nm [**23**]. An LPFG with a period 40 micron exhibited a large strain sensitivity of – 2.2 pm/με as both contributions to strain sensitivity are negative [**23**]. Generally, each attenuation band exhibits a different, linear response to the applied strain. A CO_2 laser written, highly sensitive LPFG strain sensor (-7.6 pm/με) with low temperature sensitivity (3.9 pm/ °C was demonstrated in a large mode area PCF fiber **[19].** Also, a CO_2 written, strain insensitive (-0.192 pm/ με) LPFG for temperature sensing up to 900 °C was demonstrated in endlessly single-mode PCF **[25].** The LPFG was made by periodic stress relaxation without geometrical deformation and elongation of the fiber. Specialty gratings such as TAP-LPFGs have been designed and fabricated for intensity and wavelength encoded strain sensors. Some novel methods such as gamma ray based tuning of LPFG bands and laser based tapering of grating zones are recently under study for enhancing strain sensitivity of fiber gratings.

1.4.3 Specialty sensors

The wide range of responses make LPFG sensors particularly attractive for multi- parameter sensing that makes use of only a single sensor element [**26, 27**]. As explained earlier, the sensitivity of LPFGs to the various measurands is dependent on the composition, the period of LPFG and the order of the cladding mode to which the coupling takes place. The differential shifts in two or more resonance bands of a single LPFG may, be used to measure simultaneously and independently the temperature and strain, by virtue of the difference in their sensitivities to the measurands. The measurement of bend induced splitting of attenuation bands has allowed the simultaneous measurement of bend radius and temperature, where the wavelength separation of the split components of the band gave a measurement of bend radius, while the average wavelength was dependent on temperature.

In the application of LPFG based strain sensors, one of the main difficulties is the cross sensitivity between strain and the temperature. The common methods for cross sensitivity reduction are using temperature compensation and simultaneous strain and temperature measurement. Conventional fibers contain at least two different glasses, each with a different thermal expansion coefficient, thereby giving rise to high temperature sensitivity. PCFs are virtually insensitive to temperature because they are made of only one material (and air hole). This property can be used to obtain temperature insensitive PCF-based devices. A systematic investigation has been conducted on long period fiber gratings (LPFGs) written by CO_2 lasers and arc induced technique in different types of fibers such as conventional glass fibers and PCF fibers. Compared with UV-laser exposure technique, these techniques are much more flexible and low cost because no photosensitivity and any other pretreatment process are required to write gratings in glass fibers. Moreover, the CO_2 laser based writing process can be controlled to generate specialty gratings such as Turn-around point long period fiber gratings (TAP-LPFGs) without using any expensive mask [**28, 29**].

1.4.4 External liquid refractive index sensing

Precision refractive index sensing is of prime importance for industrial, biological and petroleum sectors. Being a fundamental quantity, its accurate determination can identify a number of substances in test liquids. The standard method of measuring liquid refractive index is Abbe refractometer which is not amenable to real time monitoring. Fiber optic sensors based on taper/etched Sections, LPFG and surface plasmon resonance (SPR) are under evaluation for high sensitive measurements. Both resonant wavelength and attenuation dip of LPFGs are sensitive to the change in ambient material index due to dependence of the phase matching condition upon the effective refractive index of the cladding modes. This feature arises as the effective indices of the cladding modes, $n^{cl,m}{}_{eff}$ and is strongly influenced by ambient refractive index. LPFGs can thus be used for biochemical sensing and fuel adulteration detection based on evanescent-wave detection principle.

The typical sensitivity of LPFG based sensor is ~700 nm/RIU where RIU stands for refractive index unit. On the other hand, for biosensors the desired RI sensitivity is at least 1000 nm/RIU. Therefore, various techniques have been demonstrated to enhance the sensitivities of LPFG based refractometers and to solve the cross sensitivity issue between temperature and RI. A CO_2 laser-induced LPFG in a microfiber drawn by taping technique has a high sensitivity of 1900 nm/RI to external refractive index **[31].** This value is 60 times larger than in-fiber Michelson interferometer made from abrupt taper of SMF and is comparable to SPR.

There have been studies to exploit the power coupling to higher order cladding modes leading to phenomenon of dual resonance which can nearly double the sensitivity. At duel resonance, the same cladding mode is excited at two distinct wavelengths, both of them shifting towards opposite direction with any change in the analyte. The LPFGs, with nanostructures coatings, operating near TAP have been demonstrated to achieve a high sensitivity [**31**]**.** By precise introduction of path difference between two identical concatenated LPFGs written by UV laser, the sensor with a record sensitivity of 2500 nm /RIU has been obtained [**32**]. In slightly modified version of duel resonance, tunable optical fiber devices for pumped microfluidics have been demonstrated based on broadband long period gratings (TAP-LPFGs)**[33, 34].**

1.4.5 Optical fiber and LPFG sensors for radiation dosimetry

(a) Low level dosimetry

Effects of nuclear radiation on sensing and data transmission components are of great interest in many applications such as homeland security, nuclear power generation and military. Many studies have been done for use of optical fibers for detection of ionizing radiation. Researchers showed that the radiations generate, at the microscopic scale, point defects in amorphous silica glass network through ionization or knock-on processes. The point defects, or color centers induce the appearance of new energy levels located inside the band gap of the dielectric. This increases the absorption called Radiation induced attenuation (RIA) at some selected wavelengths. The amplitude and time kinetics of these changes depend on the nature, concentration and stability of point defects [**35, 36**]. This in turn depends on core and cladding dopants, impurity levels and glass physical characteristics (fictive temperature, strain etc.) and on fabrication parameters (preform deposition and drawing processes) [**37**].

Losses in Ge-doped cores can be attributed to defects Ge(1), GeX and GeNBOHC. A detailed study in which the Ge, B, P contents and OH impurity were systematically varied independently of other dopants revealed that the addition of even a small amount of P to fiber core resulted in enhanced radiation sensitivity (induced attenuation) to the fiber during steady state irradiation [**36**]. The comparison between the fiber and fiber preform radiation response show that the drawing process increases the fiber sensitivity to radiation [**37**].

Induced loss in single mode fibers doped with TiO_2 in silica core matrix was studied in the dose range of 0-12 Gy at 1310 nm transmission wavelength. The high radiation sensitivity along with linear response behavior, low recovery and dose rate independence show their capability for application in fiber optic radiation dosimeter in low dose range [**38**]. Other effects such as luminescence from native defects or induced effects, population of metastable charge trapping effects exhibiting thermo luminescence or optically stimulated luminescence have been exploited to develop fiber optic dosimeters [**14**].

(b) High level dose sensors

The field of high level (MGy) gamma dose sensing using fiber gratings and radiation tolerance of optical fiber and devices is a promising grey area **[23, 24].** The attenuation band sensors based on specialty doped fibers reach saturation level above 10 kGy dose. Therefore, for high dose values of 10 kGy to 1 MGy, another radiation effect i.e. radiation induced change of refractive index can be used for radiation dosimetry. Interferometric evaluation or fiber gratings are the useful devices for such high dose range. Besides, the wavelength encoded sensors such as fiber grating sensors can solve measurement problems such as radiation induced broadband loss in optical fibers and errors due to source fluctuation etc.

Commercially available fiber optic sensors may need to be redesigned to withstand substantial radiation doses, in particular when their working principle relies on broad spectrally-encoded and intensity based measurements. The wavelength encoded sensors based on fiber gratings can operate in high radiation environment because of insensitivity to broadband radiation-induced losses. Sensitive fiber grating above a dose of 150 kGy have not been reported anywhere. As most fiber gratings including Bragg gratings are fabricated using UV based technique, the fiber gratings have been found to be insensitive to gamma due to involvement of identical physical phenomenon.

The dose studies on FBGs up-to 100 kGy have not clearly identified the influence of fiber composition and manufacturing parameters. The main reason being that FBGs are written by high intensity UV based technique which changes fiber properties to a great extent by changing population of color centers and compaction, and therefore, the gamma dose effects on such gratings could not be predicted. There exist only very few publications about irradiation tests of LPFGs. Vasilev et al. **[38]** found no clear spectral shift in gratings written by UV or CO_2 laser in Ge and N doped fibers up-to a dose of about 70 kGy. Rego et al. **[39]** could not find any radiation induced spectral changes up-to a dose of 500 kGy in LPFGs written by arc discharge technique in pure silica core fibers. Recently, Henning Henschel et al**. [40]** have shown high sensitivity in Chiral LPFGs written in some fibers supplied by Nufern, USA. However, the manufacturer did not disclose the composition of the fiber and it was not possible to know the cladding mode order of the gratings. There are no commercial devices for dose measurements based on LPFGs till today.

(c) Mechanism of gamma-induced refractive index changes

For sensors in nuclear and space applications, it would be necessary to know the radiation induced increase in refractive index of silica doped with a variety of frequently used elements in differing concentration. Among the applications are intra-reactor sensors, fiber gyroscopes and diagnostic systems for thermonuclear reactors. There is also keen interest to study the kinetics of radiation induced refractive index (RI) changes in doped fibers due to evidence of a link between gamma radiation and UV induced effects.

The measurement of RI profile of standard optical fibers exposed to gamma radiation using micro-interferometric tomography was reported in **[41].** For SMF-28 fiber, the core RI changes were 10^{-3} at 5 MGy. For high Ge doped fibers, Vasilev et al. **[38],** using two LPFGs in an interferometric configuration, estimated the index change of the order of 2.8×10^{-5} for ~100 kGy dose. From measurements of a channel peak wavelength shift of a wavelength division multiplexing (WDM) coupler induced by gamma radiation, a value of 6×10^{-3} was found for Ge-doped fibers exposed to a dose of 13 MGy **[42].** Using FBGs, Gusarov et al. **[12, 13]** found a RI change of about 10^{-4} at 1.6 MGy dose in hydrogen loaded telecom grade fiber. However, gamma induced changes in FBGs have a complex dependence on several parameters such as composition, UV dose, writing conditions and fiber drawing parameters. Therefore, the Gamma induced resonance wavelength shifts of LPFGs could provide an alternate way for investigation of RI changes in some fibers. RI measurements using LPFGs have not yet been reported by any group except by the author of this thesis **[43, 44].**

CHAPTER 2

OPERATING PRINCIPLE, DESIGN, MODELING AND FABRICATION OF LONG PERIOD FIBER GRATINGS

2.1 Introduction

Optical fibers have the ability to efficiently convert energy from one spatial mode to another, which make them potential candidate for devices such as wavelength filters, sensors and dispersion compensators. They have revolutionized medicine as they can be introduced into the body to remotely sense, image and treat the patients. The fiber phase grating has developed into a critical component in fiber-optic communication and sensor systems. Advantages of fiber gratings over competing technologies include all fiber geometry, low insertion loss, high return loss, and potentially low cost. But the most distinguishing feature of fiber gratings is the flexibility they offer for achieving desired spectral characteristics. Numerous physical parameters can be varied, including: induced index change, length, period chirp, fringe tilt, and whether the grating supports counterpropagating or copropagating coupling at a desired wavelength. By varying these parameters, gratings can be made with normalized bandwidths ($\Delta\lambda/\lambda$) between 0.1 and 10^{-4}, extremely sharp spectral features, and tailorable dispersive characteristics.

The part of the results reported in this chapter has been published in the following paper: Sanjay Kher, Smita Chaubey, Jai Kishore, SDVSJ Raju, S. M. Oak, "Fiber Optic temperature-insensitive, strain sensor for nuclear applications", Int. J. of Applied Engineering and Tech., ISSN 2277-212X, Vol. 1(1), pp. 61-67, Oct.- Dec. 2011.

There are two types of in-fiber gratings; fiber Bragg gratings (FBGs) with periodicities of the order of optical wavelength and long period fiber gratings (LPFGs) with periodicities of several hundred wavelengths. Since Hill et al. **[45]** and Vengasarkar et al. **[16]** wrote the first FBG and LPFG in silica glass fibers, the fabrication and applications of in-fiber gratings have achieved rapid developments. Various fabrication methods, such as ultraviolet (UV) laser exposure [**46**], CO_2 laser irradiation [**18**], infrared femtosecond pulses [**47**], electric arc discharge [**48**], ion implantation [**49**], periodic microbends [**50**], have been demonstrated to write LPFGs in different types of fibers.

The fabrication of LPFGs relies upon the introduction of a periodic modulation of optical properties of the fiber. This may be achieved by permanent modification of the refractive index (RI) of the core of the optical fiber or by physical deformation of the fiber. The RI modification is commonly achieved by UV radiation in photosensitive fiber using wavelengths between 193-266 nm through an amplitude mask. However, RI change in UV written LPFGs is known to contain an unstable component which decays in time causing a significant change in central wavelengths of attenuation bands and in the coupling strength. These gratings are also reported to be unstable above 300 ^{0}C [**16**].

Davis et al. [**18**] reported the first LPFG written by CO_2 laser irradiation technique in conventional glass fiber in 1998. Compared with UV-laser exposure, the CO_2 laser irradiation technique is much more flexible, stable up to 600 ^{0}C and low cost because no photosensitivity or pre-treatment process are required to write gratings in any type of fiber. Another low cost technique known as arc excitation method has become popular for writing LPFGs with a period >300 μm. The gratings are reported to be stable up-to 1000 ^{0}C in some fibers.

In Section 2.2 and 2.3, we describe our experimental system for writing gratings using CO_2 laser and in Section 2.4, electric arc-induced grating writing method has been described. The modelling and fabrication of specialty gratings is described Section 2.5. Subsequently the possible mechanism of refractive index modulation in such LPFGs is discussed in Section 2.6.2.

2.2 CO_2 laser irradiation techniques

A laboratory scale CO_2 laser based LPFG writing method utilizing point by point exposure technique was developed initially. A home built CO_2 laser (max. power 20 W) is focussed onto the unjacketed fiber held between a 10 μm resolution translation stage and a fiber holder. The schematic diagram of the setup is shown in Fig. 2.1.

The fiber is exposed to a CO_2 laser for predetermined period through an electronic shutter and then translated by the required period for next exposure. This point-by-point LPFG writing method is repeated for grating length 20-30 mm as per the design. The exposure time is controlled so that minimal physical deformation of the fiber takes place. The evolution of grating is monitored on-line by observing the transmission spectrum using an optical spectrum analyser (OSA). Fig. 2.2 shows the transmission spectrum of a typical LPFG fabricated in a smf-28 fiber by point by point method. Such a LPFG fabrication system usually requires an exact control of both shutter and the translation stage to achieve reproducible results. Additionally, the vibration of the employed fiber, resulting from periodic movement of the fiber, and laser power variation affects the quality and stability of the grating.

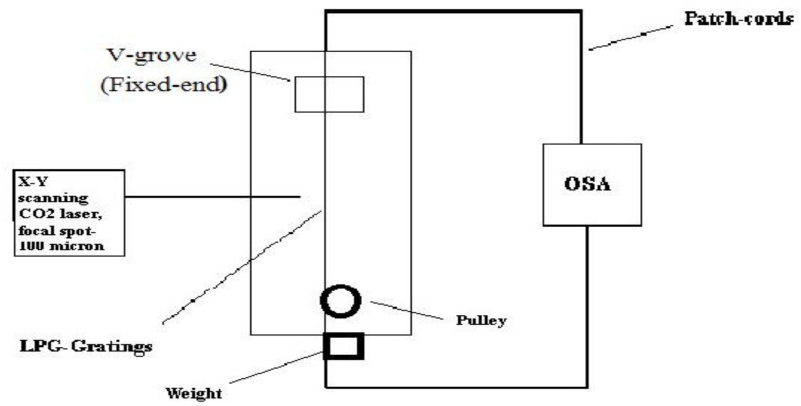

Fig. 2.1. Experimental set-up for writing LPFGs

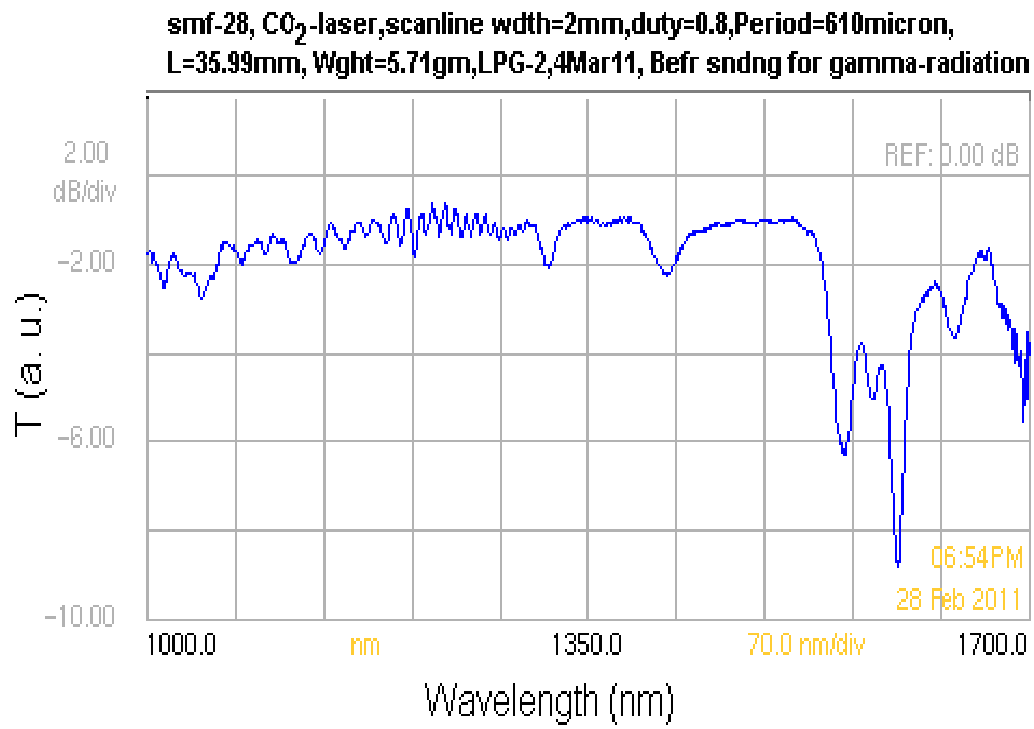

Fig. 2.2. Experimental normalized transmission spectrum of CO_2 laser LPFG in smf-28 fiber (period 610 micron)

2.3 CO_2 laser based scanning technique and fabrication of TAP-LPFG

Due to inherent constraints of the point-by-point technique, the grating writing system was upgraded with a two-dimensional scanning of CO2 laser system. The experimental setup for LPFG writing is shown in Fig. 2.3.

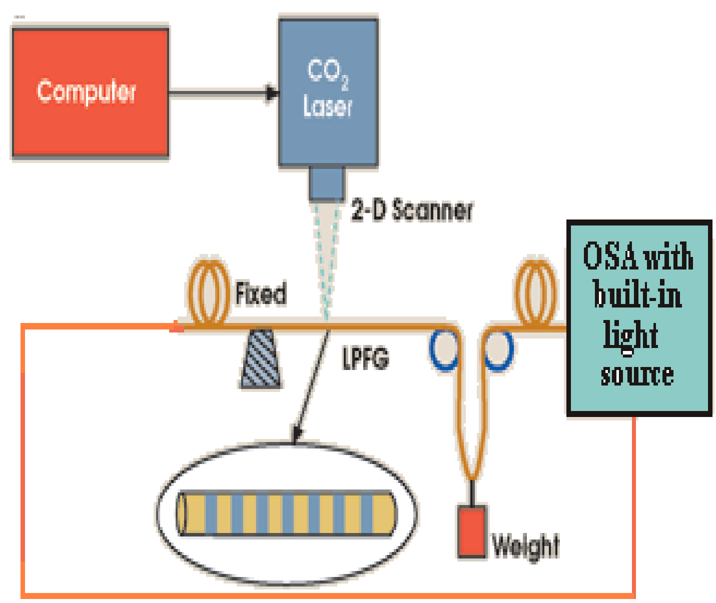

Fig. 2.3. Schematic diagram of LPFG fabrication system based on 2-D scanning of focussed CO_2 laser

One end of the employed fiber is fixed and another end is attached to a small weight to provide a constant pretension in the fiber. The focussed CO_2 laser beam is scanned periodically across the employed fiber along ‘X’ direction and then shifted a grating pitch along ‘Y’ direction i.e. the fiber axis, to create next grating period by means of two-dimensional optical scanners under a computer based supervisory control. In this technique, the fiber is not periodically moved along the fiber axis. Such a system is capable of writing high quality, high period accuracy gratings with very low insertion loss. Moreover, it can also write TAP gratings which require the exact control of grating period (better than one micron) while the period is relatively short (< 250 micron).

Fig. 2.4 shows a grating fabrication protocol file made in AutoCAD for General Laser Mark System, with a grating period of 610 µm. The laser beam automatically follows the pattern with a predetermined scans while the grating formation is monitored online. The parameters are first optimised with a chosen fiber and then fed to marker system.

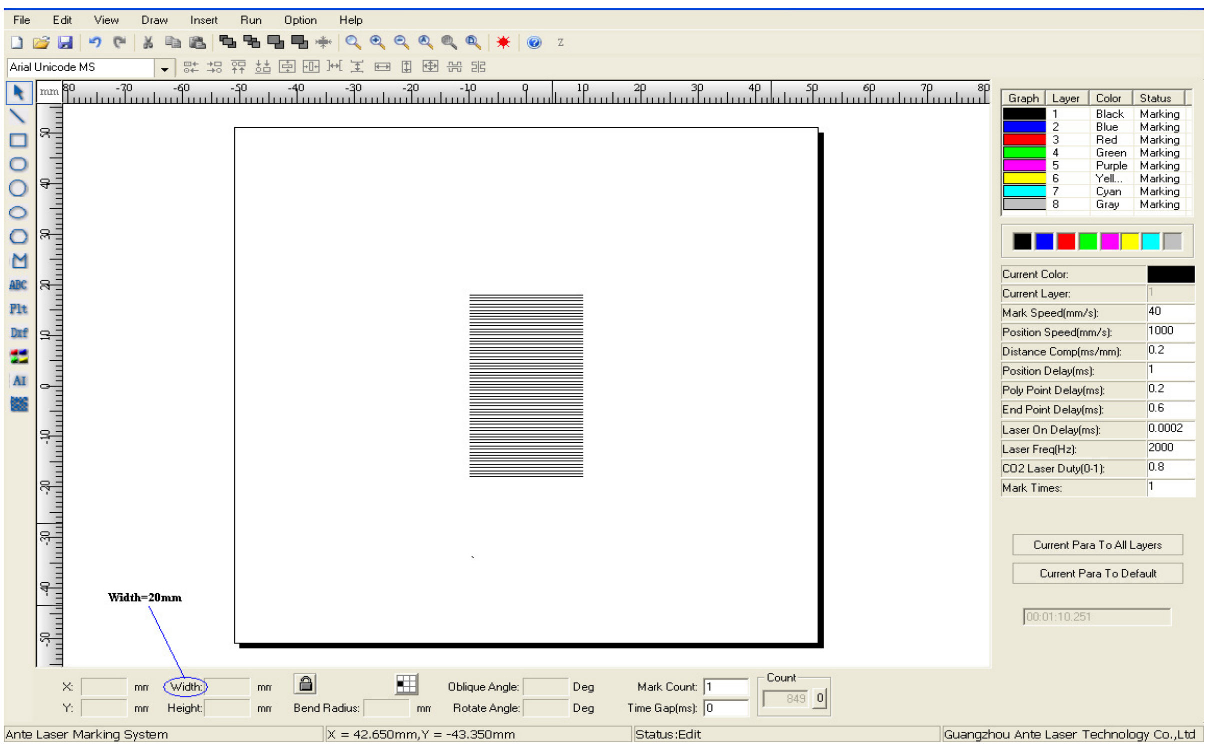

Fig. 2.4. Screen file photo of a marker system made in AutoCAD for writing LPFG with a grating period of 610µm. In this case the width of laser marking line is of only 2 mm in X direction

We have designed, modelled and fabricated speciality LPFGs such as turnaround-point LPFGs (TAP-LPFGs) in B/Ge doped fibers using this system (details in Section 2.5).

As shown in Fig. 2.5, a high quality TAP-LPFG with broad band (~ 100 nm) attenuation characteristic of TAP point for 11^{th} cladding mode has been produced. Fig. 2.6 and 2.7 also show the capability of our grating writing system whereby, near-TAP-LPFGs have been fabricated. In all figures, the green curve is the transmission spectrum of fiber before the beginning of the process of grating writing. The blue trace represents the ratio between green and black curves so as to provide sharper features with good signal to noise ratio (SNR). To further confirm the TAP-LPFG formation, we fabricated the LPFG with a grating period reduced by one micron so that we move slightly away from TAP point. We have also shown the possibility of post-fabrication tuning of TAP-LPFG by gamma dose for critical applications [**19, 22, and 51**].

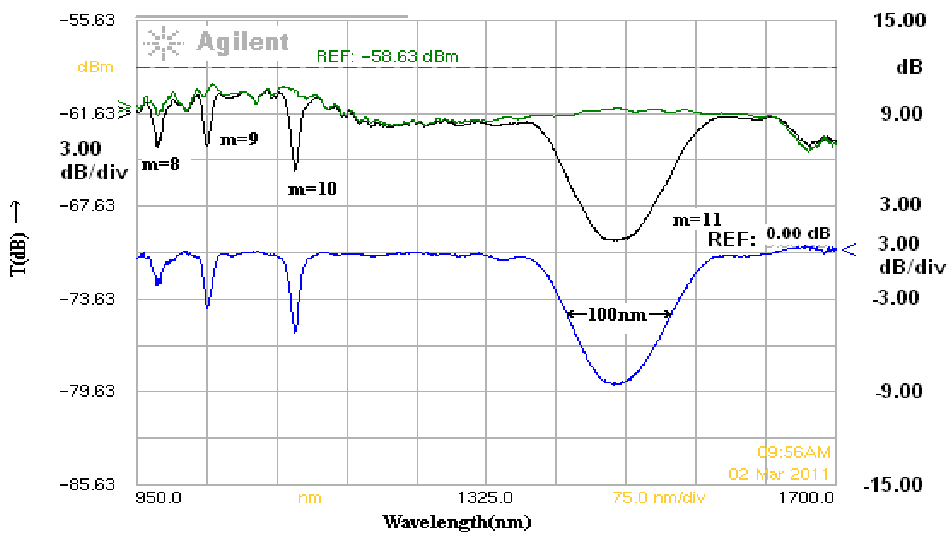

Fig. 2.5. Transmission spectra of exact TAP- LPFG in B/Ge doped fiber. Large bandwidth (~100 nm) is observed at TAP. Black curve represents spectra of inscribed LPFG and green represents spectra before LPFG was made (Top), m is the cladding mode order; Blue represents the ratio between the green and black traces (Bottom)

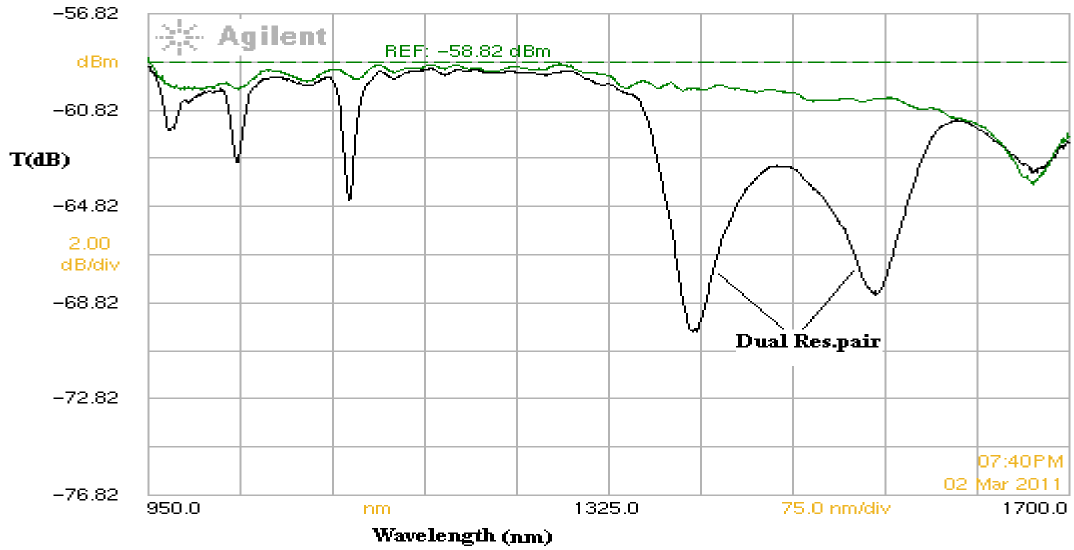

Fig. 2.6. Transmission spectra of fiber with CO_2 laser written near-TAP-LPFG (Period=207 μm)

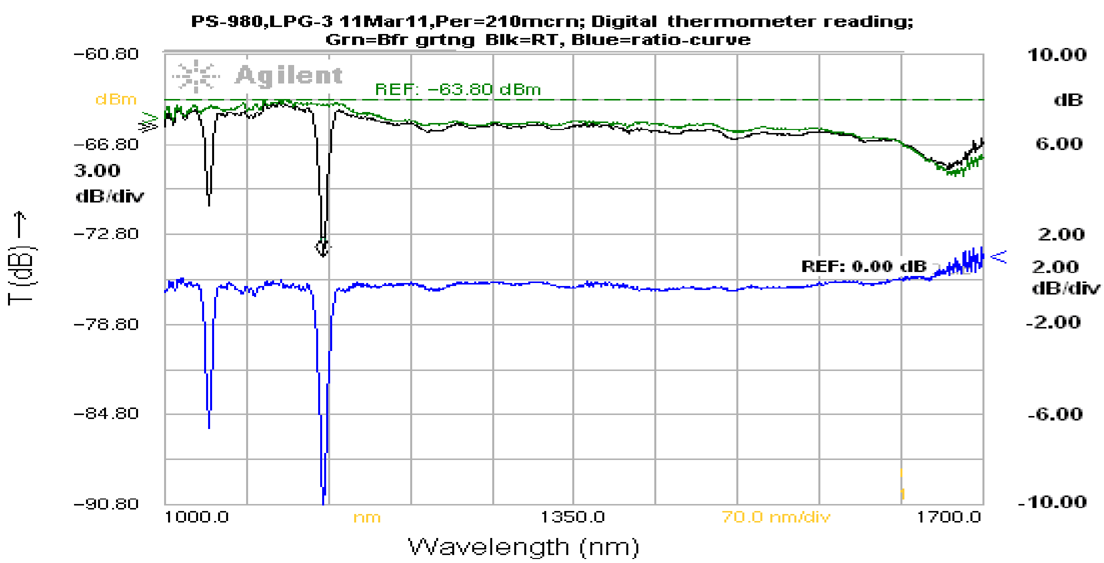

Fig. 2.7. CO_2 laser written off-TAP-LPFG in PS-980 fiber (210 μm). Black curve represents spectra of inscribed LPFG and green represents spectra before LPFG was made (Top), m is the cladding mode order; Blue represents the ratio between the green and black traces (Bottom)

2.4 Electric arc-induced LPFGs

LPFGs for our experiments were fabricated in all types of optical fibers, using a computer-assisted precision arc-discharge apparatus. The method is based on periodic melting of the fiber, while a pulling weight stretches it, thus determining a periodically tapered fiber [**52-54**]. The grating period was mainly determined by the moving step of the translation stage that was controlled by a computer and by some other factors such as arc intensity, arc duration time (τ), and pulling weight. A schematic diagram of the fabrication setup is plotted in Fig. 2.8.

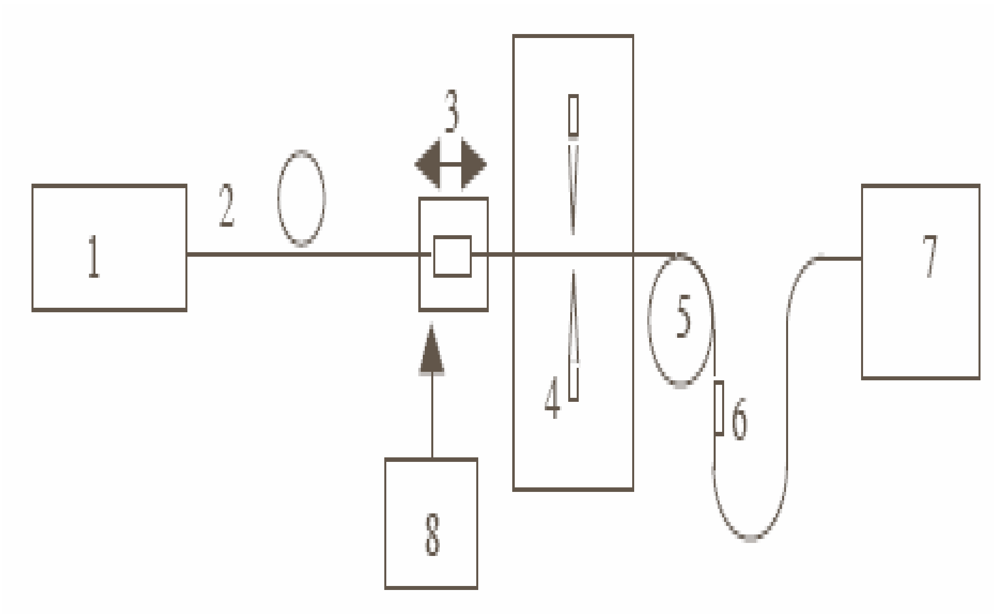

Fig. 2.8. Computer-assisted arc-discharge apparatus for manufacturing of LPFG: 1 – broadband light source, 2 – Corning smf-28 optical fiber, 3 – motorized translation stage, 4 – arc generating electrodes, 5 – pulley, 6 – weight, 7 – optical spectrum analyzer (OSA), 8 – computer.

Using this set-up LPFGs with period >300 μm were inscribed in various types of single mode fibers. The period restriction is due to wider spatial extent of arc spot on the fiber. Fig. 9 shows the transmission spectrum of one representative LPFG in B/Ge codoped fiber.

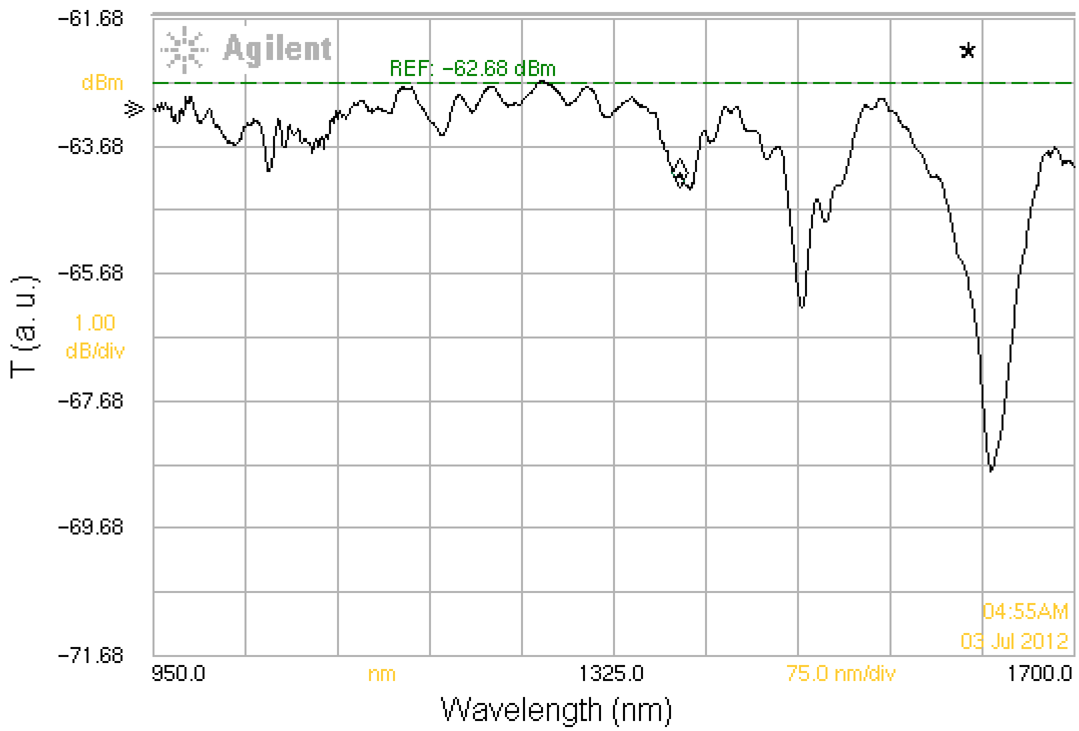

Fig. 2.9. Transmission spectrum of B/Ge codoped fiber with arc-induced LPFG.

2.5 Theory and simulation

The phase matching condition between the guided mode and the forward propagating cladding modes of an LPFG are given by expressions [**46**]

$$\beta_{01} - \beta_{cl}^{n} = \frac{2\pi}{\Lambda} \qquad (2.1)$$

$$\lambda_n = \left[n_{eff}^{co} - n_{eff}^{cl,n} \right] \Lambda \qquad (2.2)$$

where Λ is the grating periodicity required to couple the fundamental mode to the n^{th} -cladding mode; β_{01} is the propagation constant of the fundamental mode; β_{cl}^{n} are the propagation constants of cladding modes where the superscript denotes the order of the mode; n_{eff}^{co} and $n_{eff}^{cl,n}$ are effective indices of fundamental core mode and m^{th} order cladding mode, respectively. LPFGs couple light from fundamental core mode to different co-propagating cladding modes and the resonance loss wavelength λ_n is determined by phase matching condition.

The smallest transmission of the attenuation bands as given earlier by Eq. (1.8) is reproduced below [**1, 46**]

$$T_i = 1 - \left(\sin \kappa_i L\right)^2 \qquad (2.3)$$

where L is the length of the grating and κ_i is the coupling coefficient for the i^{th} cladding mode, which is determined by the overlap integral of the core and cladding mode and by the amplitude of the periodic modulation of the mode propagation constants.

The phase matching curves (PMC) for fundamental core mode and LP_{01} to LP_{013} cladding modes were calculated for B/Ge codoped single mode fiber. We have used the fiber parameters provided by the supplier in standard brochure (r_{cl} = 62.5 μm, MFD = 6 μm, NA= 0.13-0.14, cladding pure silica). It is observed that the slope of phase matching curve for 11^{th} order cladding mode at grating period 208 μm exhibits a change in sign from positive to negative with increasing wavelength (Fig. 10).

It is seen from Fig. 2.10 that for the 11^{th} mode, a given LPFG period very close but lower than TAP point (near about 207 μm) corresponds to two resonant wavelengths (~1.37 and 1.52 μm) which is characterized by dual resonant dips in the transmission spectrum. Xinwei Lan et al. [**28**] has derived the sensitivity expressions for LPFG in which the

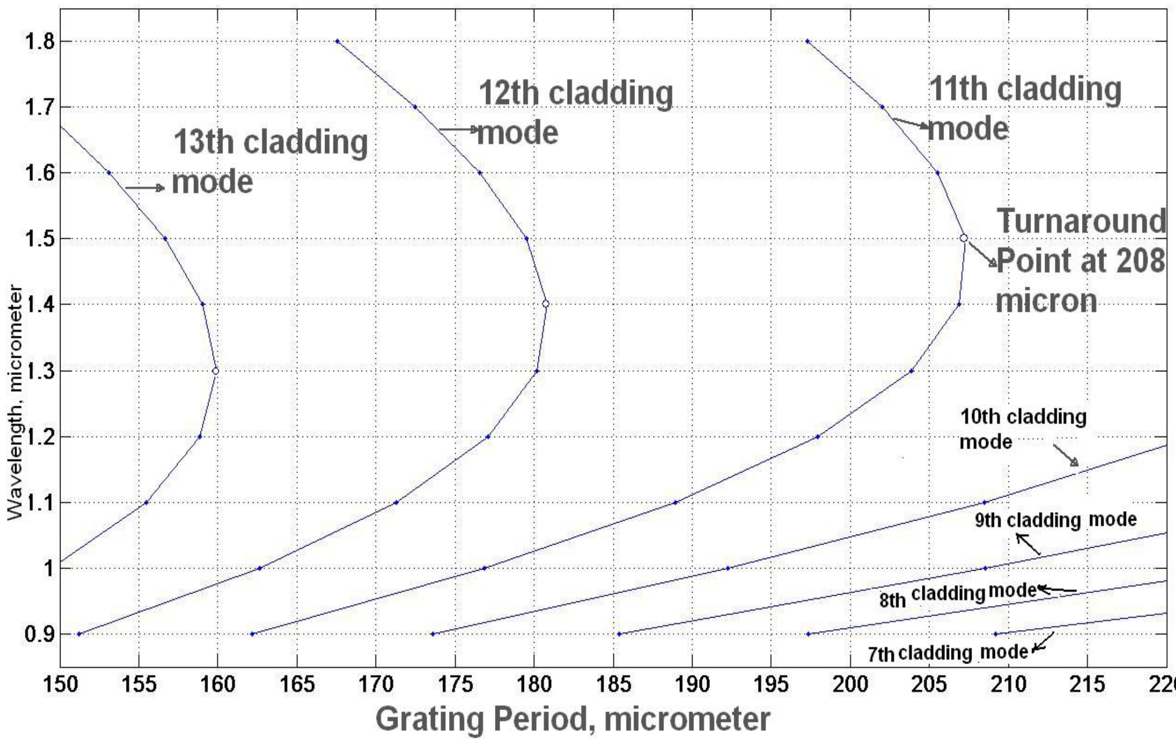

Fig. 2.10. Calculated variation of mode resonance wavelength with LPFG period for B/Ge doped fiber

general sensitivity factor γ defined by Eq. (4) [**28**]

$$\gamma = \frac{\frac{d\lambda}{d\Lambda}}{n_{core}^{eff} - n_{clad,m}^{eff}} \qquad (2.4)$$

The parameter γ is the key factor for sensitivity determination of higher order LPFG resonances. LPFG sensitivity is mainly determined by the γ factor which also describes the waveguide dispersion. For every cladding mode, γ is the key factor for sensitivity determination of higher order LPFG resonances. For every cladding mode, $\left|\frac{d\lambda}{d\Lambda}\right| \to \infty$ at turning point. Thus from Eq.

(2.4) we find that $|\gamma| \rightarrow \infty$ and so the turning point operation of LPFG determines the condition for maximum sensitivity. Our aim has been to develop high sensitivity LPFGs for nuclear and industrial applications. Accordingly, several LPFGs were fabricated with period near 208 micron to experimentally achieve Turnaround point LPFG characteristics. One representative exact-TAP-LPFG is shown in Fig. 2.11.

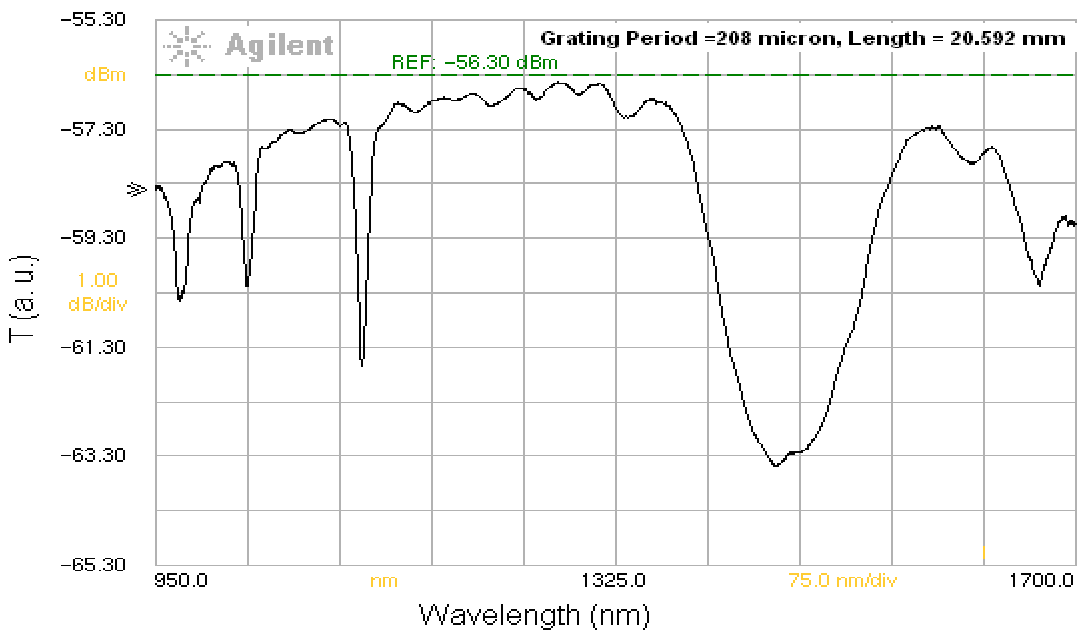

Fig. 2.11. Transmission spectrum of exact TAP-LPFG

We have previously shown in Fig. 5, 6 and 7 the transmission spectra of exact TAP, near TAP and off-TAP LPFG fabricated by scanning CO_2 laser system. Table 2.1 shows the simulated and experimentally observed resonance wavelength dips. The experimentally obtained resonances are quite close to predicted simulated values. The slight deviations are expected because the doping contents of chosen fiber are not exactly known.

We can note that the coupling of higher order cladding mode near TAP within spectral range of 950-1700 nm requires grating with relatively lower period (< 250 μm) whereas the fabrication of LPFG with resonance exactly near TAP within 900-1700 nm band requires a very robust fiber and/or laser beam movement system with a precision better than 1.0 µm. All these conditions can be met in scanning CO_2 laser based system and hence our LPFGs are reproducible and have been packaged for field applications.

Table 2.1. Comparison of simulated and experimental resonance wavelength

Grating period (µm)	Simulated λ (µm)			Experimental λ (µm) ± 0.001		
	TAP mode (11^{th} order)	10^{th} order	9^{th} order	TAP mode (11^{th} order)	10^{th} order	9^{th} order
206	1.37, 1.572	1.085	0.989	1.381, 1.565	1.115	1.024
208	1.5	1.097	0.9975	1.467	1.119	1.025

2. 6 Experimental work related to photonic crystal fiber (PCF)

Photonic Crystal Fibers (PCFs) also known as Holey fiber are a new class of optical fibers that have attracted intense scientific research during past few years. Typically, these fibers incorporate a number of air holes that run along the length of the fiber, and the size, shape and distribution of the holes can be designed to achieve various novel wave-guiding properties that may not be possible in conventional fibers. We have carried out following experimental studies related to LPFG in photonic crystal fibers (PCFs).

2.6.1 To write LPFG in endlessly single mode PCF

Various PCFs have been demonstrated so far that exhibit remarkable properties such as endlessly single mode fiber, large mode area and highly non-linear performance [**101**]. The particular ESM PCF used for this work (Crystal Fiber, ESM-1550-01) had an outer diameter of 125 µm, a core diameter of 12 µm surrounded by 54 air holes with diameters of 3.7 µm with space between adjacent holes being 8 µm (see Fig. 2.12).

Fig. 2.12. Cross-Section of the endlessly single mode PCF taken using a microscope with 20x objective lens

Formation of LPFG in pure-silica core PCF fibers is not straight forward because there is no photosenstivty provided by Ge-O_2 vacancy defect centers. The LPFGs in PCF are primarily formed due to modification of glass structure. However, any geometrical deformation results in flaws or cracks that result in fracture of the fiber and therefore LPFGs in PCF require high precision systems. Our fully automated CO_2 laser based grating writing system can set the grating period (200-800 μm) with a precision of one micron while laser intensity can be stabilized within +/- 5 %.

A LPFG with a period of 450 μm was inscribed into this PCF using the CO_2 laser technique since initial experiments showed this periodicity would yield an attenuation band at a suitable wavelength band 1500-1550 nm. Fig. 2.13 shows the transmission spectrum of the LPFG which had a length of 19 mm.

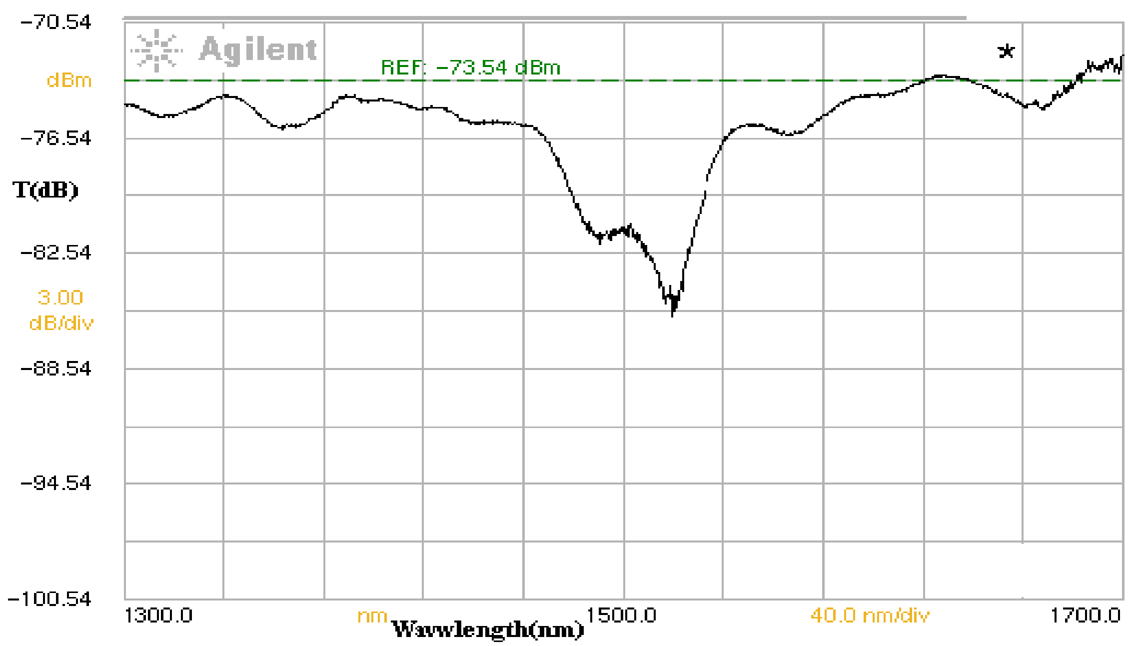

Fig. 2.13. Transmission characteristics of a LPFG fabricated on an ESM-PCF with a period of 450 μm

For the preparation of LPFG in an endless-single-mode photonic crystal fiber (ESM-PCF) both ends of the PCF are fusion spliced to SMFs. The loss for each splice is about 0.74 dB. An X-Y scanning CO_2 laser is used for the fabrication of LPFGs in the ESM-PCF. The CO_2 laser operates at a frequency of 2 kHz and has a maximum power of 10 W. The laser power is controlled by the mark-speed of the laser pulses. The typical grating length and period in our experiment is 23.4 mm and 450 μm respectively. Attenuation bands in the range of 1300-1700 nm have been investigated by an optical spectrum analyzer. The CO_2 laser based LPFGs have been reported in similar fibers [**55, 56**].

2.6.2 Mechanisms of refractive index modulation for writing LPFG

Possible mechanisms for refractive index modulation in the CO_2 laser induced LPFGs have been attributed to residual stress relaxation, glass densification and/or physical deformation [**19, 53**]. Residual stress is formed in optical fibers during the drawing process, resulting mainly from the superposition of thermal stress caused by difference in thermal expansion coefficients between core and cladding and mechanical stress caused by viscoelastic properties of the two regions. When an optical fiber is exposed to CO_2 laser pulses the compressive stress induced in the fiber core during fiber manufacturing process is relaxed [**57**]. It has been published that mechanical stress in a CO_2 laser-induced LPFG written in a B/Ge doped fiber is fully relaxed by CO_2 laser. This relaxation usually results in a decrease in refractive index in the fibers. It is also our experience that much less laser power is required to write LPFGs in B/Ge doped fiber compared to standard germanosilciate fiber which does not have Boron. Some indirect evidence is also available when the formation of grating is being monitored step by step as shown in Fig. 2.14. The resonance dips show a clear shift to blue side as the full grating is formed, due to decrease of effective index.

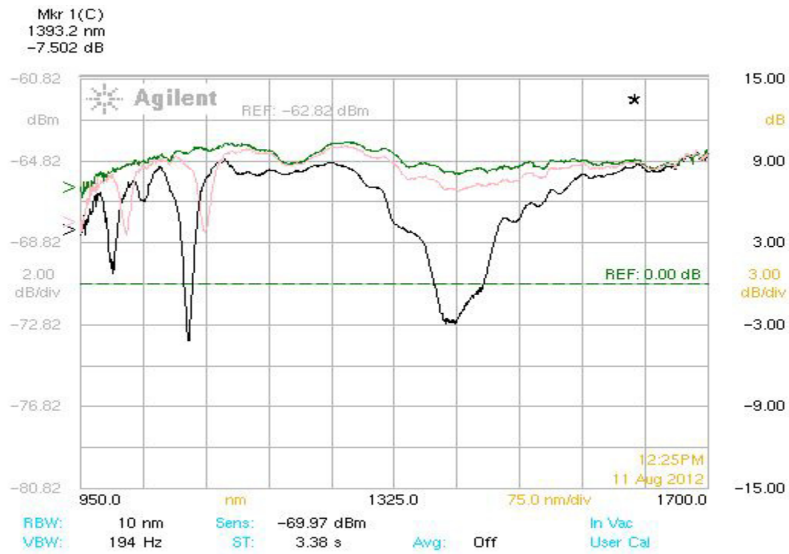

Fig. 2.14. Transmission spectrum of LPFGs fabricated with different laser dose exposures. Pink trace shows the spectrum after few laser scans (partial formation) while black trace shows the spectrum when full grating is formed.

It has been reported earlier that the Boron co-doping in fiber lowers the fictive temperature of the core substantially, and so local heating of the fiber by CO_2 laser radiation causes not only stress relaxation, but also glass structure changes in the core. However, our gamma irradiation measurements of these gratings indicate stress relaxation as the dominant mechanism of grating formation. Any other mechanism is likely to desensitize the grating for gamma-induced effects. With a low laser irradiation power, index change occurs only in the core and the resultant index distribution is axially symmetric. In this condition, the laser irradiation produces a Gaussian-shaped index perturbation profile along the axial direction (z) of the optical fiber. The low insertion loss, good quality of grating and good matching of experimental results with simulation as observed in Fig. 2.5, 2.6 and 2.7 establish the axially symmetric RI changes in B/Ge codoped fibers.

Electric arc fabrication of an LPFG relies upon a combination of up to four effects to generate the periodic modulation of the fiber properties. This includes the periodic tapering of the fiber, the diffusion of dopants, relaxation of internal stresses and glass structure change **[52]**. We do not have any direct evidence to justify any one mechanism. However, we have observed that arc-induced technique is very versatile and it is possible to write good quality LPFGs in any type of single mode fiber. We had been able to write LPFGs in B/Ge doped fibers supplied by three different manufacturers and standard smf-28 fibers which are likely to have different stresses and glass fictive temperature. Fig. 2.15**,** 2.16, 2.17 and 2.18 show the transmission spectrum of arc-induced LPFGs in different types of fibers under more or less same peak current and pulling weight/load.

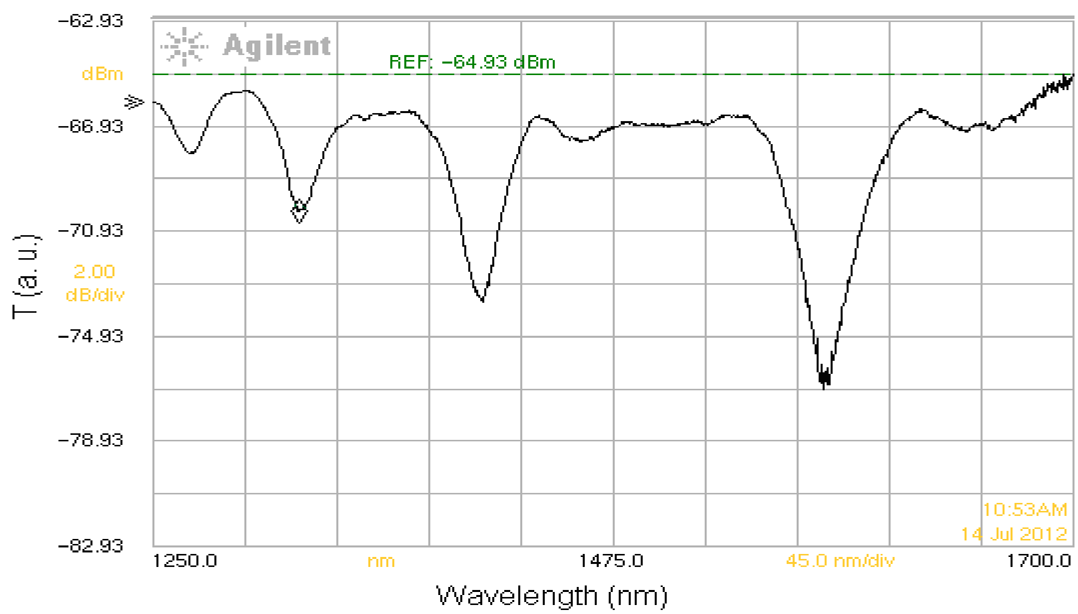

Fig. 2.15. Transmission spectrum of arc-induced LPFG in B/Ge co-doped Indian fiber supplied by CGCRI, Kolkata.

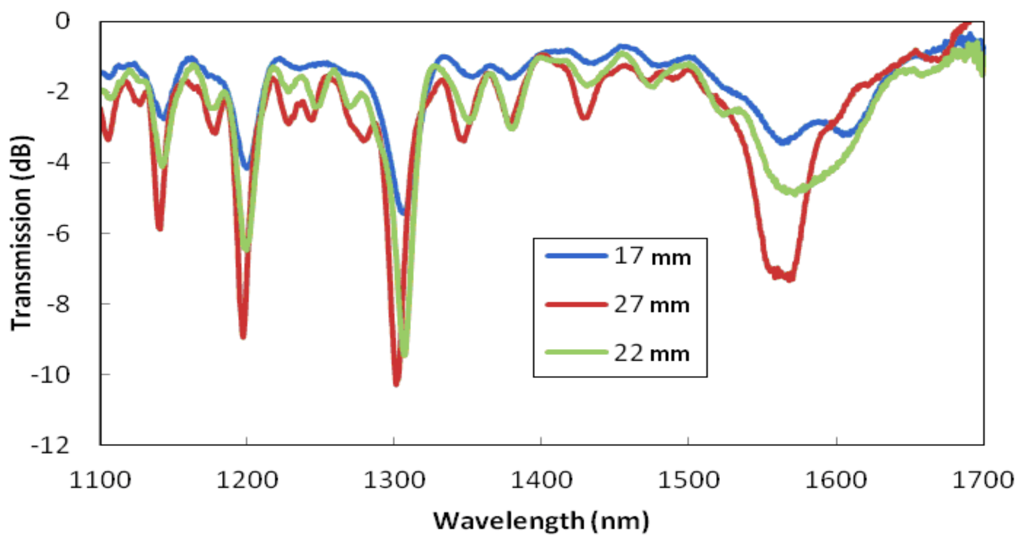

Fig. 2.16. Transmission spectrum of arc-induced LPFG in B/Ge codoped fiber from Fiber Core, UK for different grating lengths

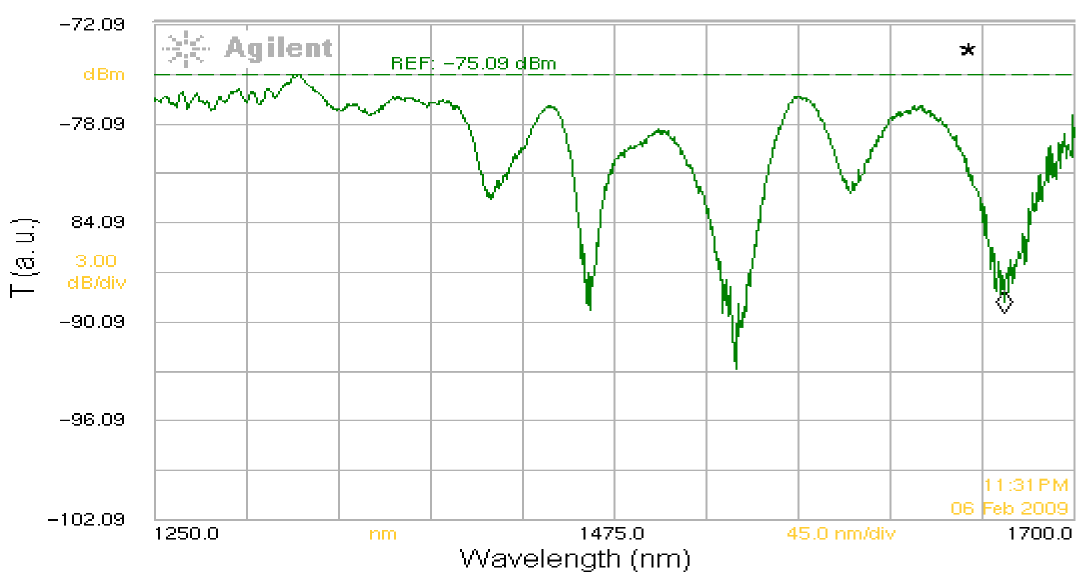

Fig. 2.17. Transmission spectrum of arc-induced grating in B/Ge doped fibers from INO, Canada

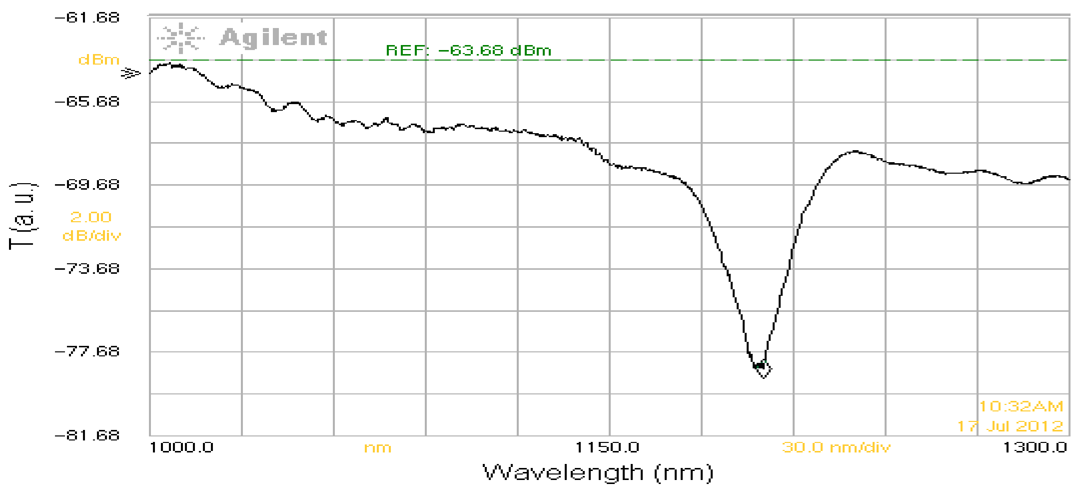

Fig. 2.18. Transmission spectrum of arc-written LPFG in standards smf-28 fiber from THORLABS Inc., USA

Fig. 2.16 indicates the effect of taper due to increase of length of the grating. We have seen that the fiber slowly gets tapered if longer grating is made by point by point arc-induced writing method. For our study, the B/Ge doped fibers were procured from different manufacturers. All Boron/Ge doped fibers are known to have high stresses. The exact concentration of Boron or Ge is not disclosed by the suppliers. They are likely to have been drawn at different drawing tension. Yet, we could make good quality gratings in all of them. These results strongly implicate the role of stress relaxation as the main mechanism of grating RI modulation with some role of densification. Gamma dose studies of these gratings do not indicate any significant role of dopant diffusion.

2.7 Conclusion

We have designed and developed long period fiber gratings using CO_2 laser based irradiation and arc-induced method. These techniques are very versatile, require no photosensitivity in the fiber and the grating parameters like grating depth and spectral shapes of resonances are stable at least up to 300 °C. For an LPFG in step index fiber, we have calculated the dispersion of propagation constant for the fundamental core mode and the cladding modes. The simulations have predicted the occurrence of first Turning point for 11^{th} order cladding mode within operating range of 0.9-18 μm. Accordingly, higher order mode and turnaround-point (TAP) LPFGs were fabricated in B/Ge doped fibers for the first time using scanning CO_2 laser system. It was shown that with this method, TAP-LPFGs working under various circumstances can be easily fabricated by adjusting the inscription period.

We obtained very close agreement between the results of theoretical calculations and experiments for TAP-LPFGs [**43, 58, and 59**]. The technique for writing LPFGs in Photonic crystal fibers has been developed. The principle advantages of PCF-LPFG are:

- They have negligible temperature sensitivity
- They are nuclear radiation resistant
- They offer flexibility for low cost PCF-based devices

The LPFGs were written by arc-induced method virtually in all types of fibers which led us to shed some light on possible mechanisms of grating modulation (refractive index profile) in LPFGs. These investigations have provided a foundation for design, development and fabrication of fully packaged devices based on fiber gratings.

CHAPTER 3

SPECIALTY GRATINGS FOR SENSITIVITY ENHANCEMENT OF DIFFERENT PHYSICAL PARAMETERS

3.1 Introduction

Long period fiber gratings (LPFGs) that can couple light between the core and cladding modes of an optical fiber have become popular for applications in lasers, optical communication and sensing. Since the coupling is wavelength-selective, the fiber grating acts as a wavelength-dependent loss element. Various LPFG devices have been demonstrated for use as band rejection filters, erbium doped fiber amplifier, gain equalizers, mode converters and sensors for physical parameters such as temperature, strain, bending and refractive index. In all fields of sensing applications, the knowledge of sensitivity of LPFG to the parameters of its physical environment is clearly important. Besides, the full characterization of the sensitivity of LPFG is an important precursor to practical device design.

The phase matching condition between the guided mode and the forward propagating cladding modes of an LPFG is given earlier by Eq. (2.1) and (2.2) and are reproduced below [**2, 16**]

$$\beta_{01} - \beta_{cl}^{n} = \frac{2\pi}{\Lambda} \qquad (3.1)$$

The part of the results reported in this chapter has been published in the following paper: S. Chaubey, Sanjay Kher, S. M. Oak, "Radiation and taper tuning of long period grating for high sensitivity strain measurement", IEEE proceedings of WFOPC, 2011, July 2011, ISSN: 1927-5056, pp. 1-4, Dec. 2011.

$$\lambda_n = \left[n_{co}^{eff} - n_{cl,n}^{eff} \right] \Lambda \qquad (3.2)$$

Where Λ is the grating periodicity required to couple the fundamental mode to the nth-cladding mode; β_{01} is the propagation constant of the fundamental mode; β_{cl}^{n} are the propagation constants of cladding modes where the superscript denoted the order of the mode. The characteristics of LPFGs are affected by external perturbations such as strain, temperature and bends. The effect is primarily due to a differential change induced in two coupled modes. More specifically, since the propagation constants of fundamental core mode β_{01} and coupled cladding mode β_{cl}^{n} undergo dissimilar changes owing to a change in external conditions, the difference between the two modes $\Delta\beta$ is altered. This results in a shift in the wavelength of resonant coupling as per Eqs. (3.1 and 3.2).

Temperature sensitivity of LPFGs inscribed in standard telecommunication fiber and B/Ge co-doped fibers have been studied to design a high resolution thermal sensor operating at a particular wavelength band.

We have designed and fabricated LPFGs in metal coated smf-28 fiber, recoated grating zones with thin gold layer for temperature sensing applications. Section 3.2 describes high temperature characterization of such gratings and describes the features of a packaged probe. Further, in Section 3.3, specialty gratings such as TAPLPFGs have been designed, fabricated and characterized for high sensitivity strain sensing applications. We have demonstrated such sensors based on intensity and wavelength modulation principal in Section 3.4. In Section 3.6, we describe LPFGs in PCF fibers for temperature-insensitive strain applications in nuclear environment.

3.2 Temperature sensitivity

The origin of the temperature sensitivity may be understood by Eq. (1.10) which is reproduced below [**1**].

$$\frac{d\lambda}{dT}=\frac{d\lambda}{d(\delta n_{eff})}\left\{\frac{dn_{co}^{eff}}{dT}-\frac{dn_{cl,i}^{eff}}{dT}\right\}+\frac{\Lambda}{L}\frac{d\lambda}{d\Lambda}\frac{dL}{dT} \tag{3.3}$$

where λ is the central wavelength of the attenuation band, T is the temperature, n_{eff} is the effective refractive index of the core mode, n_{cl} is the effective refractive index of the cladding mode, $\delta n_{eff}=n_{co}^{eff}-n_{cl,i}^{eff}$, L is the length of the LPFG and Λ is the period of the LPFG.

The first term on the right-hand side of Eq. (3.3) is the material contribution, and is related to the change in the differential refractive index of the core and cladding arising from the thermo-optic effect. This contribution is dependent upon the composition of the fibre and is strongly dependent upon the order of the cladding mode. For coupling to low order cladding modes (accessed using longer periods, Λ > 100 μm), the material effect dominates. For coupling to higher-order cladding modes (accessed using shorter periods, Λ < 100 μm), the material effect for standard germano silicate fibres can be negligible. The second term is the waveguide contribution as it results from changes in the LPFG's period. The magnitude and sign of the term depend upon the order of the cladding mode.

For coupling to low-order cladding modes $\frac{d\lambda}{d\Lambda}$ is positive, while for the higher-order cladding modes this term is negative. Thus, by an appropriate choice of LPFG period it is possible to balance the two contributions to the temperature sensitivity to produce a temperature-independent attenuation band and also to produce attenuation bands with temperature sensitivities (positive or negative) appropriate to specific applications.

At room temperature, the temperature response of the wavelengths of the attenuation bands' is linear. However, it has been shown that the response becomes non-linear at cryogenic temperatures, below 77 K. LPFGs fabricated in standard telecommunications fiber exhibit temperature sensitivities in the range of 3 nm/100 °C to10 nm/100 °C [**23**]. This is an order of magnitude larger than the sensitivity of FBG sensors. Metal coated fibers have high gamma radiation resistance [**60**]. In this work, we have developed technology to write LPFGs in copper/carbon coated fibers for their temperature sensing applications up to 300 °C for usage in nuclear power plants. The Cu/C-coated fiber (IVG Fiber, Cu1300) has a carbon coating for the first layer and copper coating for the second layer. The carbon layer (hermetic coating) improves the reliability of the fibers, thereby preventing strength degradation caused by moisture attack on the fiber surface and preventing the diffusion of hydrogen into the core of the fiber [**60**].

Fig. 3.1 shows the transmission curve of grating formation during grating writing process. Fig. 3.2 shows the measured temperature response of the LPFG when mounted on a micro-heater for thermal characterization. Clear shift of resonance bands can be seen due to increase of temperature. Fig. 3.3 shows the sensitivity curve of the radiation hardened fiber. The response is linear up to 300 °C and slightly non-linear beyond. It has been observed earlier that radiation-induced resonance dip shifts of LPFGs written in smf-28 fibers are saturated above a gamma dose of 100 kGy [**88**]. The results of Fig. 3.3 also show that temperature sensitivity (0.08 nm/

°C) of LPFG in copper coated fibers is not remarkably affected by gamma radiation and hence temperature sensors can be developed for nuclear environment.

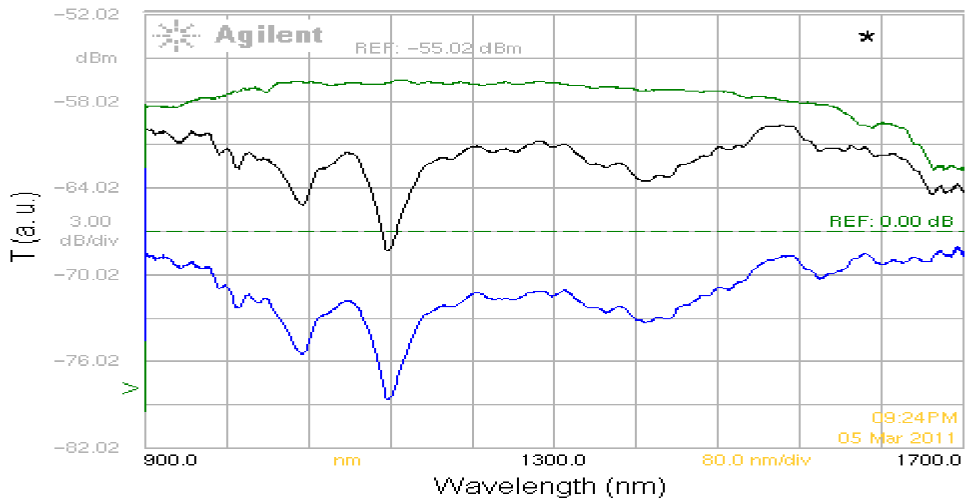

Fig. 3.1. LPFG transmission spectrum in Copper-coated smf-28 fiber as recorded by optical spectrum analyzer (OSA); Green: Source spectrum, Black: LPFG spectrum, and Blue: Normalized LPFG spectrum.

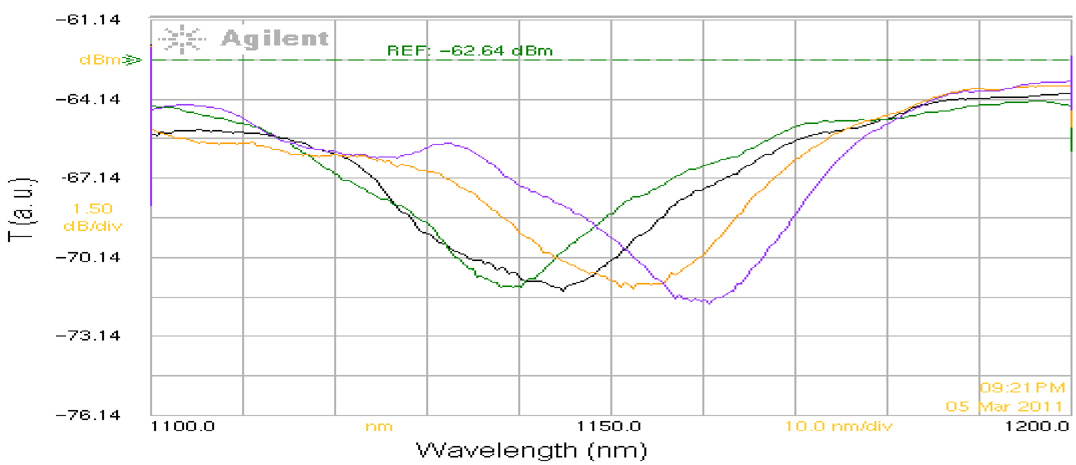

Fig. 3.2. Measured temperature dependent transmission spectrum of LPFG (period 610 µm) in Cu-coated smf-28: Green: 36 °C, Black: 100 °C, Orange: 200 °C, and Violet: 300 °C

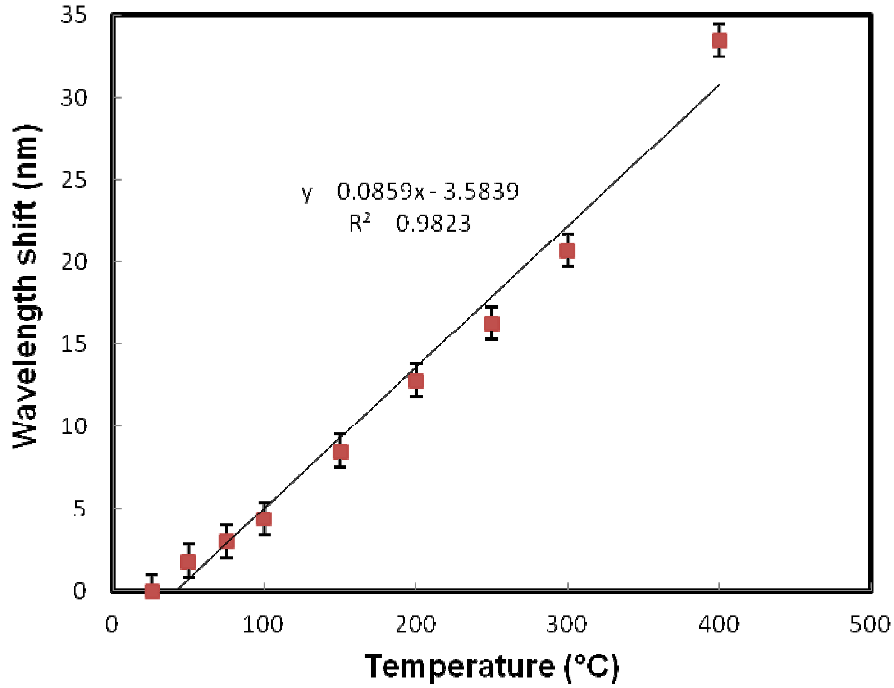

Fig. 3.3. Temperature sensitivity of LPFG inscribed by arc discharge in smf-28 fiber exposed to radiation dose of 100 kGy, before inscription.

For the fabrication of high resolution temperature sensors, a number of techniques for further enhancing the sensitivity have been investigated by us. Altering the fibre composition, such that the thermo-optic coefficient of the core is either larger or smaller than that of the cladding, can also be used to obtain the required temperature sensitivity. Since Boron doping significantly increases the thermo-optic coefficient of the core, the LPFGs in these fibers offer high temperature sensitivity. We have studied LPFGs written in various B/Ge doped fibers supplied by different manufacturers. Based on optimum dopants and resonance wavelength, we have designed a fully packaged temperature sensor probe.

The salient features of the device (Fig.3. 4) are listed below:

- Temperature range: 25 - 90 °C
- Accuracy: ± 0.5 °C
- Resolution: 0.2 °C
- Linear thermal response and thermal sensitivity = 0.38 nm/ °C.

It is significant to note that the sensitivity of our LPFG based device is an order of magnitude higher than standard fibre Bragg grating sensors with reported nominal sensitivity of 0.011 nm/°C [**67**].

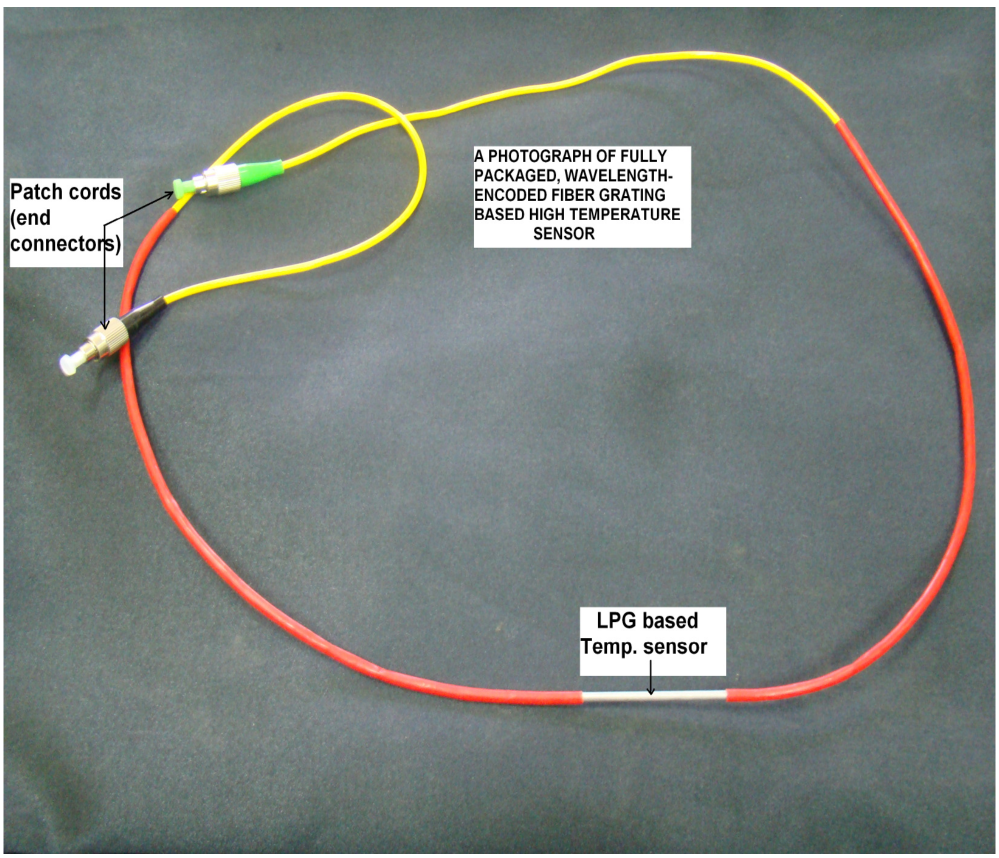

Fig. 3.4. Photograph of packaged sensor probe

Further, by careful choice of order of cladding mode [**28**], TAP-mode (Phase matching turning point) and operating wavelength, LPFGs fabricated in photosensitive B-Ge co-doped optical fibers have been shown to offer sensitivities of up to350 nm/100 °C (near TAP-mode) [**61, 62**]. Our results on these specialty gratings are described below.

The design and operation of TAP-LPFG has been explained earlier in Chapter 2. Briefly, the phase matching curves (PMC) for fundamental core mode and LP01 to LP013 cladding modes were calculated for B/Ge codoped single mode fiber. It is observed that the slope of phase matching curve for 11th order cladding mode at grating period 208 μm exhibits a change in sign from positive to negative with increasing wavelength (Fig. 3.5). Thus for this mode, a given LPFG period very close but lower than TAP point (near about 207 μm) corresponds to two resonant wavelengths which is characterized by dual resonant dips in the transmission spectrum (shown earlier as Fig. 2.10).

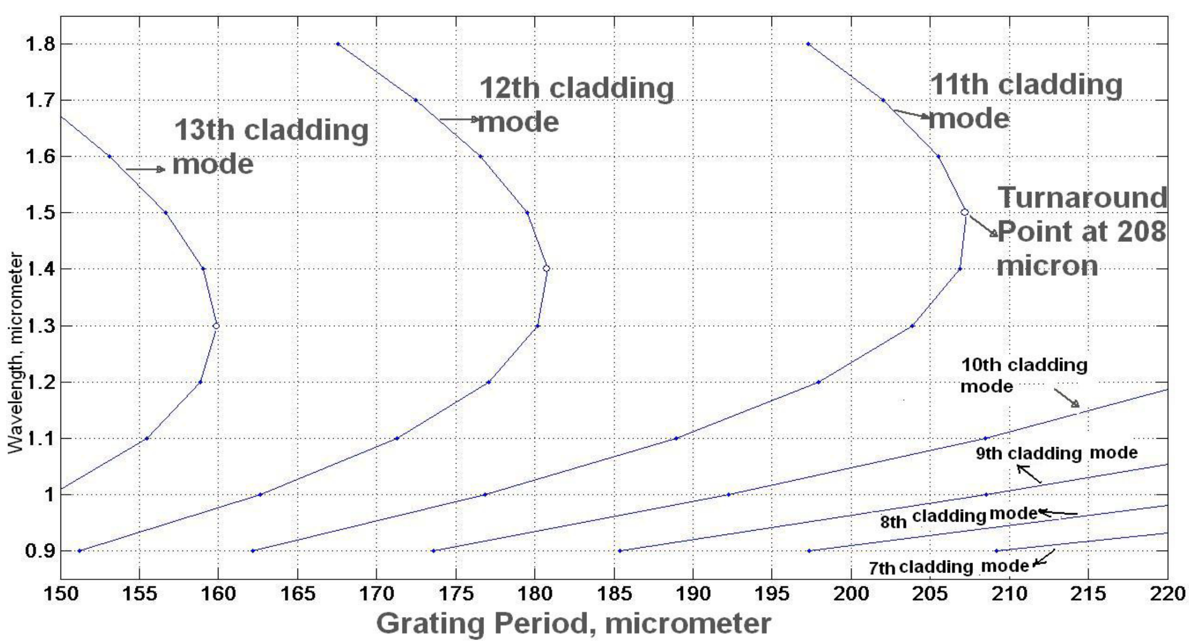

Fig. 3.5. Phase matching curve for B/Ge doped fiber.

It is shown (Fig. 3.6) that the main effect of temperature is the wavelength shift of dual band and the amplitude changes are not significant.

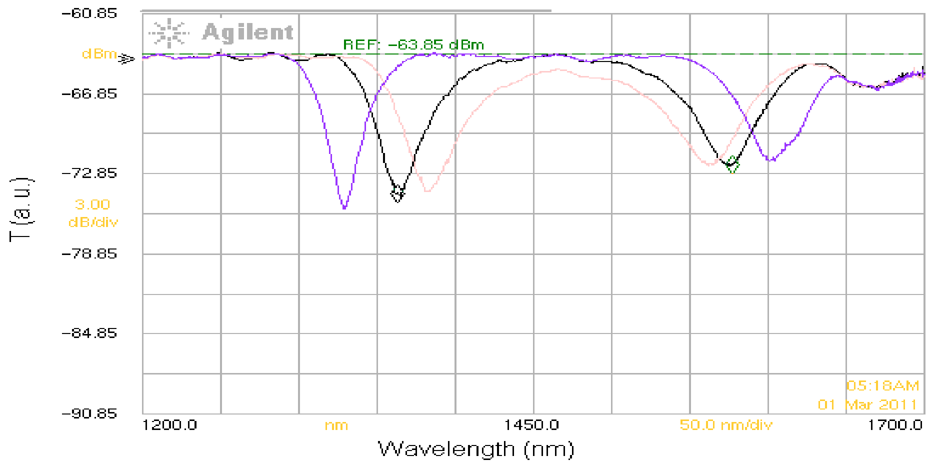

Fig. 3.6. Measured temperature responses of near TAP-LPFG. (a) Transmission spectrum of the grating at different temperatures; Pink: 26 ^{o}C, Black: 40 ^{o}C, Violet: 80 ^{o}C

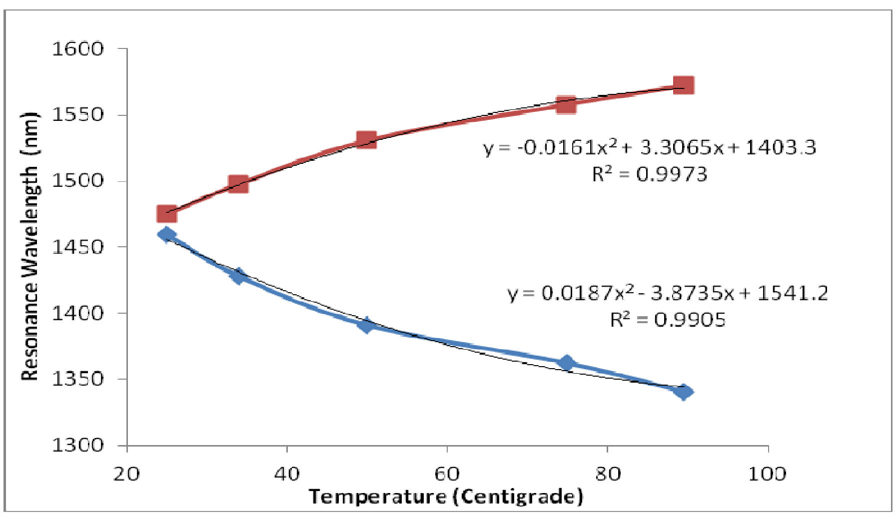

Fig. 3.7. Measured temperature response of near TAP-LPFG: temperature dependent variations of 11th cladding dual mode

Thermal response of near-TAP-LPFG in B/Ge doped fibers was studied. For the study, grating zone was kept in a micro heater system with temperature stability of ±0.5 C ° and heated up to 80 °C. The response is shown in Fig. 3.6. It is seen that high temperature sensitivity of each of the two peaks of the dual resonances are +3.3 nm /C and -3.87 nm/ °C, respectively, in 25-40 °C. The origin of non-linearity is readily visible in Fig. 3.7 which originates due to rapid reduction of γ factor for wavelengths away from turning point. These gratings were reproducible when CO_2 laser technique was used. Such gratings will find immense potential for commercialization of LPFG based very high sensitivity sensors.

3.3 LPFG based strain measurements: Strain sensitivity

The axial strain sensitivity of LPFGs may be assessed by Eq. (1.11) reproduced below [**16**].

$$\frac{d\lambda}{d\varepsilon} = \frac{d\lambda}{d(\delta n_{eff})}\left\{\frac{dn_{co}^{eff}}{d\varepsilon} - \frac{dn_{cl,i}^{eff}}{d\varepsilon}\right\} + \Lambda\frac{d\lambda}{d\Lambda} \qquad (3.4)$$

Again, the sensitivity comprises material and waveguide effects, the material effects being the change in dimension of the fibre and the strain-optic effect, with the waveguide effects arising from the slope of the dispersion term $\frac{d\lambda}{d\Lambda}$. For LPFGs with periodicity >100 μm, the material contribution is negative, while the waveguide contribution is positive. Appropriate choice of grating period and fibre composition will thus allow the generation of attenuation bands with positive, negative or zero sensitivity to strain.

By use of CO_2 laser method, a LPFG sensor with strain sensitivity -0.45 pm/με and a temperature sensitivity of 59.0 pm/ °C was written in Corning SMF-28 fiber. It has been published earlier that the strain sensitivity of the LPFG in these fibers can be effectively increased (-7.692 pm/με) by creating a particular tapering profile [**38**]. We have developed a technique to fabricate a taper region in about 50 mm zone of a fiber. Usually a taper zone is created in a fiber after removing the coating and the grating is written over this taper zone. The microscopic image of the tapered region of the 610 μm period long period grating is given in the Fig. 3.8. The strain response of such LPFG sensors is shown in Fig. 3.9.

Such devices offer the strain sensitivity of ~7.8 pm/με, in the strain range of 10-1500 με. However, they are not amenable to production due to difficulty of making a reproducible tapering profile over a grating zone. Therefore, we have investigated alternative methods to improve the strain sensitivity of LPFGs**.**

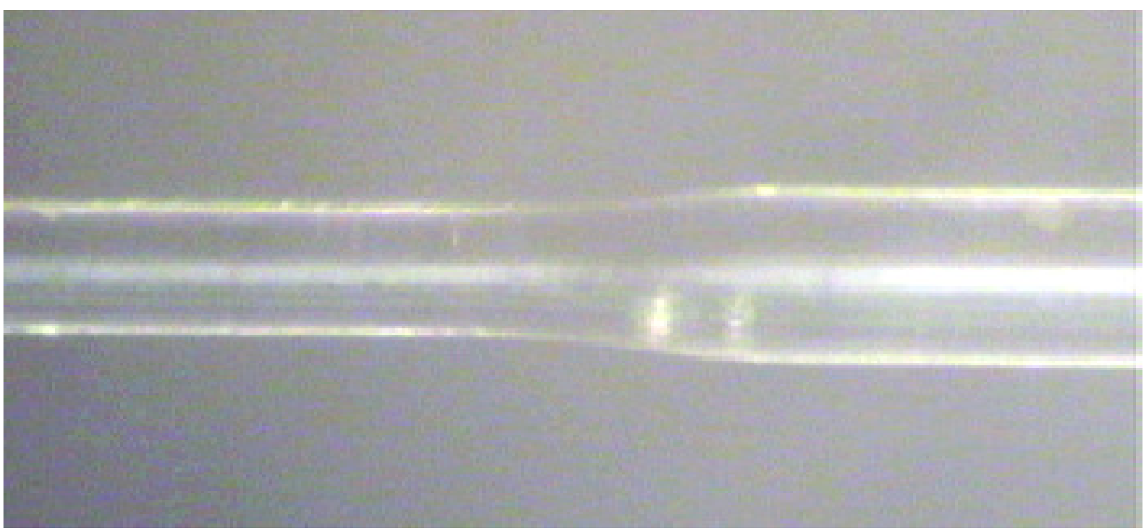

Fig. 3.8. Microscopic image of a taper region made by CO_2 laser based technique

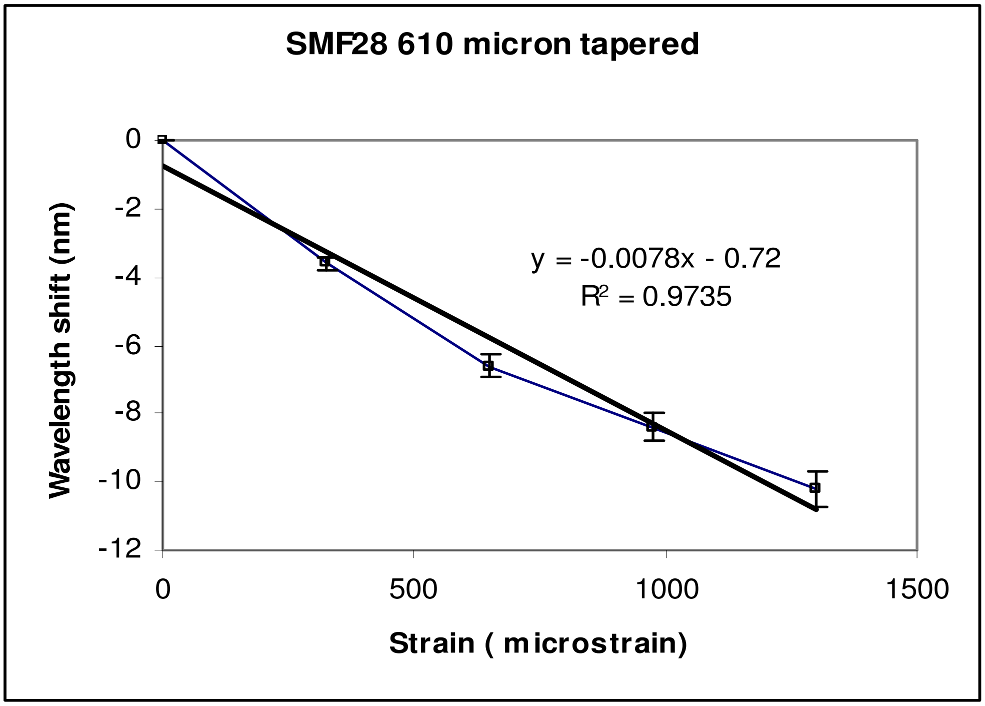

Fig. 3.9. Measured strain response of tapered long period fiber grating (LPFG) - Variation of dip wavelength shift corresponding to different tensile strength applied to LPFG.

3.4 Design, development and characterization of high sensitivity specialty gratings for strain sensing applications

We have investigated specialty LPFGs for: (1) Amplitude modulated high sensitivity strain sensors; (2) wavelength encoded high sensitivity strain sensors; (3) Temperature-insensitive strain sensors. Their detailed description is as follows.

Modeling and simulation studies (earlier shown in Table 2.1) are reproduced in Table 3.2 for the sake of completeness. This study identified the grating period at 208 μm + 0.5 μm for 11th order

TAP-Mode (Fig. 3.5). Accordingly, LPFGs were written by CO_2 laser based method for exact TAP and near TAP for amplitude modulated and wavelength encoded operation.

Table 3.1 Comparison of simulated and experimental resonance wavelength

Grating period (μm)	Simulated λ (μm)			Experimental λ (μm) ± 0.001		
	TAP mode (11^{th} order)	10^{th} order	9^{th} order	TAP mode (11^{th} order)	10^{th} order	9^{th} order
206	1.37, 1.572	1.085	0.989	1.381, 1.565	1.115	1.024
208	1.5	1.097	0.9975	1.467	1.119	1.025

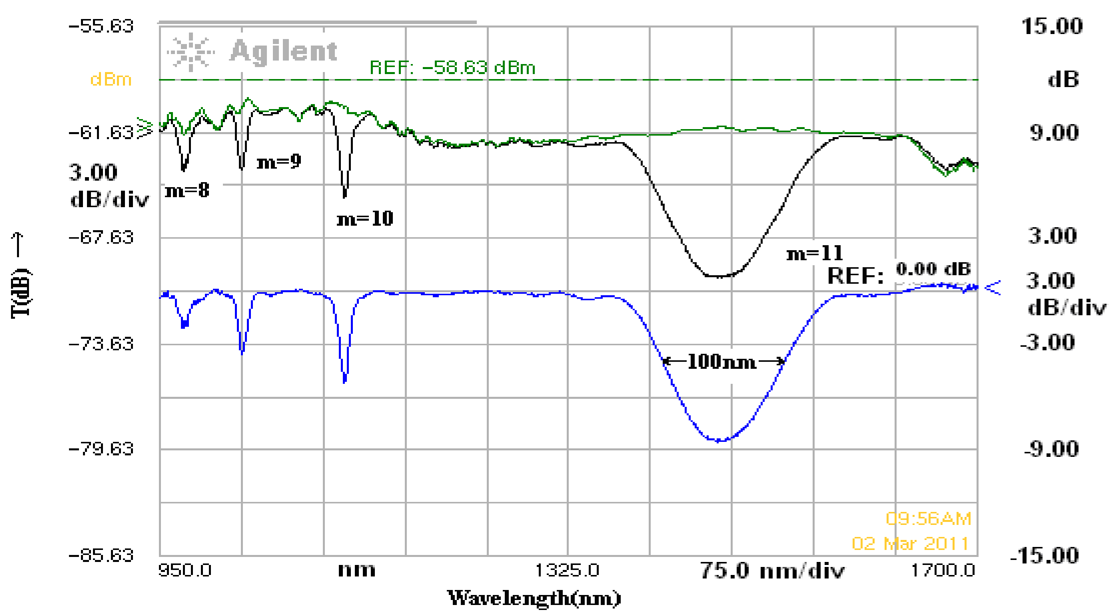

Fig. 3.10. Transmission spectra of exact TAP- LPFG in B/Ge doped fiber. Large bandwidth (~100 nm) is observed at TAP. Black curve represents spectra of inscribed LPFG and green represents spectra before LPFG was made (Top), m is the cladding mode order; Blue represents the ratio between the green and black traces (Bottom)

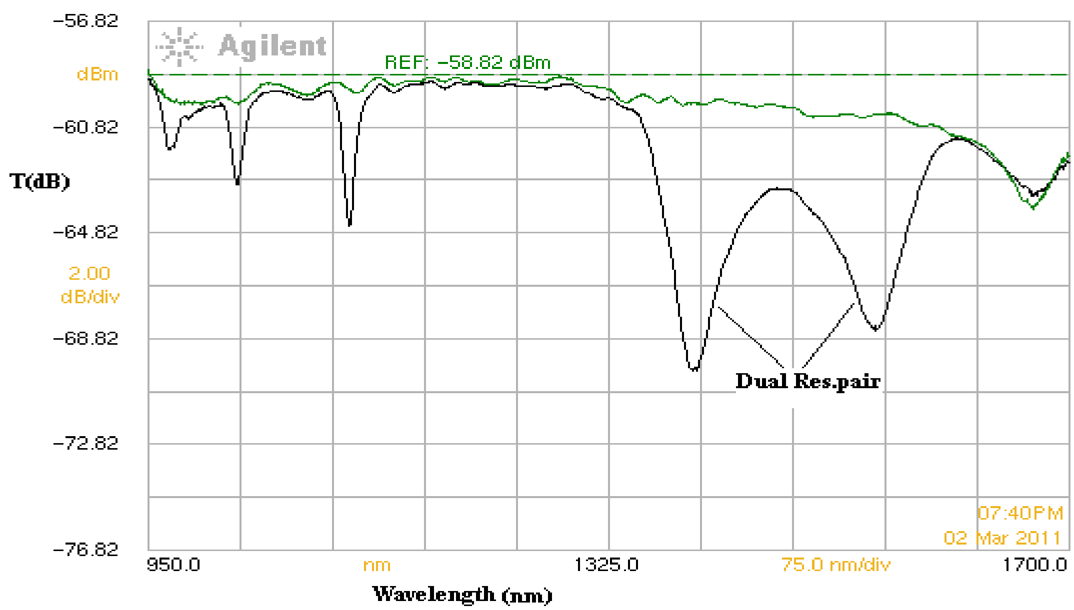

Fig. 3.11. Transmission spectra of LPFG near TAP point; bi-furcated resonance pair at 1400 nm and 1525 nm can be seen. Black represents spectra of inscribed LPFG and green represents spectra before LPFG was made

Fig. 3.10 and 3.11 show the characteristics of such gratings.

3.4.1 Intensity modulated strain sensors based on exact TAP-LPFG

We have developed high sensitivity long period fiber gratings (LPFGs) in B-Ge co-doped fiber for strain sensing application. These LPFGs are shortest grating period (180μm) LPFGs inscribed in B-Ge co doped fiber, using CO_2 laser based grating inscription set up. Strain sensitivity of 1.77 dB/mε has been obtained for attenuation band corresponding to turn around point mode. TAP operation of LPFG facilitates intensity based detection using simple optical power meter instead of wavelength based detection.

It has been previously reported that higher order mode resonances and operation near turn around point (TAP) of LPFG offers ultra-high sensitivity [**38**]. However, such investigations were done using UV induced index changes in the core of a single mode photosensitive fiber. The UV based gratings are known to have refractive index changes in time, causing a significant change in central wavelength of attenuation bands and coupling strengths. Therefore, we have used CO_2 laser based grating inscription technique to inscribe TAP-LPFGs. The technique is simple and amenable to all types of fibers. Theoretical simulation of phase matching curve for selected fiber helped in initial prediction of grating period to obtain TAP within our source wavelength band (950-1700 nm).

Basically, sensing mechanism of the grating depends on the wavelength shift due to the change of environmental parameters and requires bulky wavelength interrogation instruments. However, for field application, intensity based detection is preferred for simple and compact devices. Earlier, several methods have been reported for converting the wavelength shift of LPFG to intensity changes, such as FBG interrogated by LPFG and using a core mode blocker [**63**]. However, using additional components in such configuration increases the cost of the setup and the sensitivity obtained is also less.

In this report, we present CO_2 laser inscribed, intensity based, and highly sensitive method for strain measurement using a turnaround point (TAP-LPFG) in B-Ge co-doped fiber. This is the shortest grating period LPFG inscribed using CO_2 laser in B-Ge doped fiber as per our knowledge. Since Boron doping increases the attenuation near 1550 nm, it is necessary to design

TAPLPFG near 1400nm. This requires grating period lower than 190 µm which is difficult to achieve with grating writing techniques such as arc induced modulation method [**64, 65**].

This LPFG can also be used as an ultra broadband loss filter in wavelength range 1300 -1500 nm with maximum loss at 1400 nm > 5dB.

3.4.2 Principle and theory

LPFGs couple light from fundamental core mode to different co propagating cladding modes and the resonance loss wavelength λ_{res} is determined by phase matching condition,

$$\lambda_n = \left[n_{eff}^{co} - n_{eff}^{cl,n} \right] \Lambda \qquad (3.5)$$

where Λ is the grating period and n_{eff}^{co}, $n_{eff}^{cl,n}$ are effective indices of fundamental core mode and m^{th} order cladding mode respectively. The ratio of power coupled into i^{th} cladding mode to initial power contained in guided LP_{01} mode is given by Eq. (1.8) which is reproduced below **[17]**

$$T_i = 1 - \left(\sin \kappa_i L \right)^2 \qquad (3.6)$$

where L is the length of the grating and κ_i is the coupling coefficient for the i^{th} cladding mode, which is determined by the overlap integral of the core and cladding mode and by the amplitude of the periodic modulation of the mode propagation constants.

Shu et al. [**62**] have derived the analytical expressions for temperature, strain and surrounding RI for LPFGs where-in the general sensitivity factor (γ) is defined by Eq. (2.4) and is reproduced below

$$\gamma = \frac{\frac{d\lambda}{d\Lambda}}{n_{core}^{eff} - n_{clad,m}^{eff}} \qquad (3.7)$$

where, γ is the key factor for sensitivity determination of higher order LPFG resonances. LPFG sensitivity is mainly determined by the γ factor which also describes the waveguide dispersion. For every cladding mode, $\left| \frac{d\lambda}{d\Lambda} \right| \rightarrow \infty$ at turning point. Thus from eq. (7) we find that $|\gamma| \rightarrow \infty$ and so the turning point operation of LPFG determines the condition for maximum sensitivity.

3.4.3 Experiment and results

For the present work, standard photosensitive fiber (B-Ge co doped photosensitive fiber, Fiber core, UK) has been used. The schematic diagram (shown earlier as Fig. 2.3) of grating inscription setup based on two dimensional scanning of CO_2 laser beam is shown below.

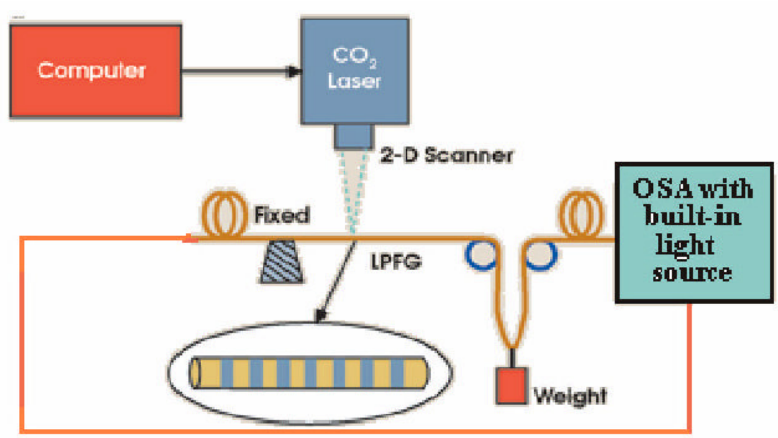

Fig. 3.12. Schematic diagram of CO_2 Laser based LPFG inscription system

The sharply focused CO_2 laser pulses are scanned across the fiber by means of a two-dimensional automated scanner and the transmitted LPFG spectrum in the wavelength range

950-1700nm is monitored online using an optical spectrum analyzer (OSA model Agilent 86146B) with a wavelength resolution of 0.1 nm. The line speed of scanning laser is 60 mm/s, pulse repetition rate is 2 kHz and the average output power is about 1 W. The scanning process is repeated until the LPFG with sufficient strength is formed. Phase matching curves (PMC) for fundamental core mode and LP_{01} to LP_{013} cladding modes were calculated (Fig. 3.5) for B-Ge co doped single mode fiber using fiber parameters provided by the supplier in the standard brochure (r_{cl} = 62.5 µm , MFD at λ_{op} = 6µm, Numerical Aperture = 0.13-0.14, cladding pure silica). Simulations showed that ~180µm grating period LPFG operates at turn around point having broadband loss centered at 1400nm. Accordingly, experimental set-up was used to inscribe an 180µm grating period, 20 mm length LPFG in B-Ge doped fiber (Fibercore, UK) to achieve TAP-LPFG for 12th order cladding mode.

The insertion loss was < 0.5 dB for this LPFG. Fig. 3.13 shows the changes in transmission spectrum of TAP-LPFG when it was fixed over two translation stages and strain was applied gradually by pulling one of the stages. Fig. 3.14 shows the linear fit of the values obtained for different strain applied to the LPFG. Strain sensitivity of 1.77 dB/mε was obtained. These observations show that a TAP-LPFG in B-Ge co-doped single mode fiber can form an excellent intensity detection based strain sensor without requiring any wavelength based demodulation instrument.

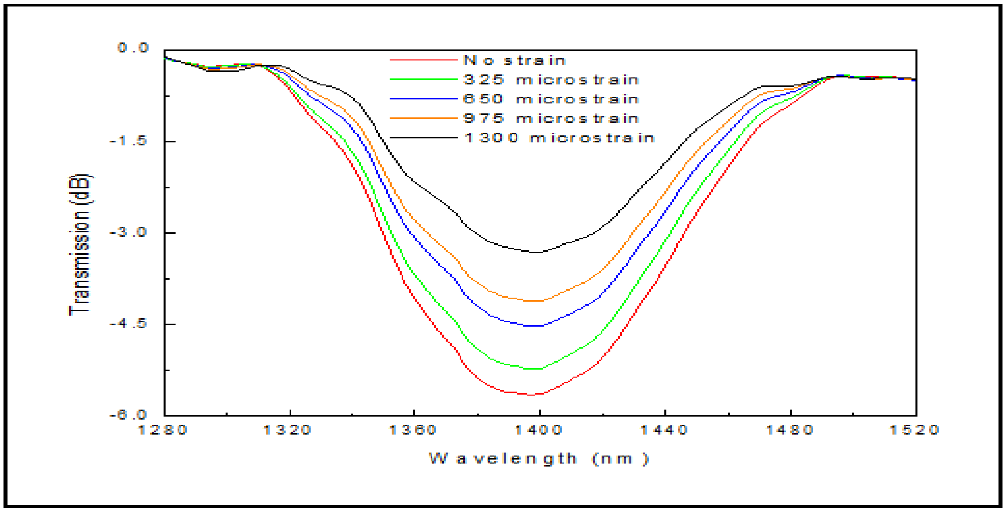

Fig. 3.13. Measured strain response of a TAP-LPFG (180μm grating period). Transmission spectrum of the grating corresponding to TAP mode (12th) at different applied longitudinal strain

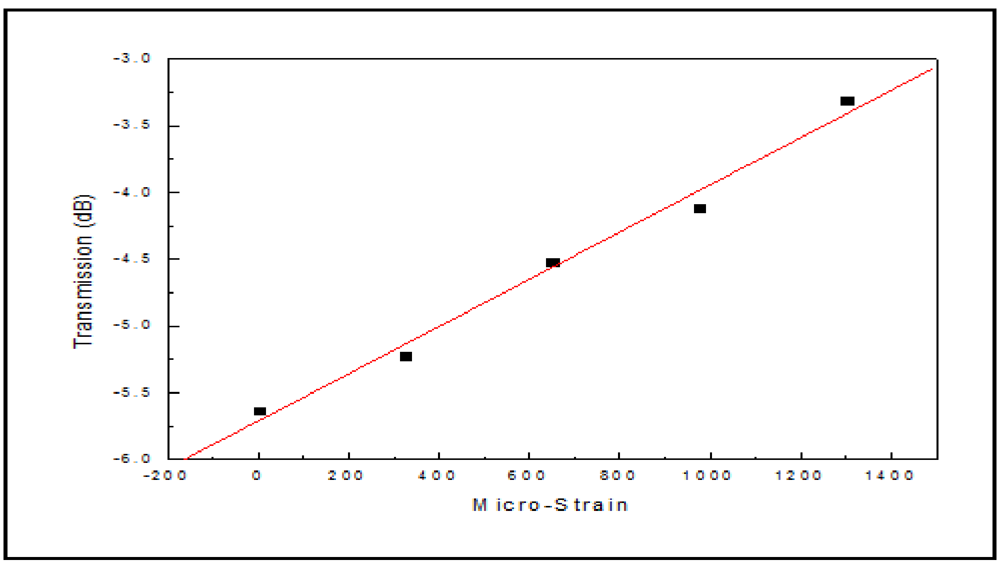

Fig. 3.14. Amplitude based strain calibration curve: Decrease in transmission loss at 1400 nm with increase in longitudinal strain for strain in the range 0-1300 με

In conclusion, we have designed highly sensitive intensity based TAPLPFG strain sensor with sensitivity 1.77 dB/mε which is at least 5 times larger as compared to earlier reported values.

Intensity based detection opens up new areas for simple, fiber based, and sensitive strain sensing devices. This LPFG can also be used as broadband loss filter in the wavelength range 1300-1500 nm with strain tunable transmission.

3.5 Wavelength encoded strain sensors using near TAP-LPFG

Fig. 3.15 illustrates the strain response of near TAP-LPFG. As axial strain is increased, the individual response dips as shown by pink trace were observed to move closer (black trace).

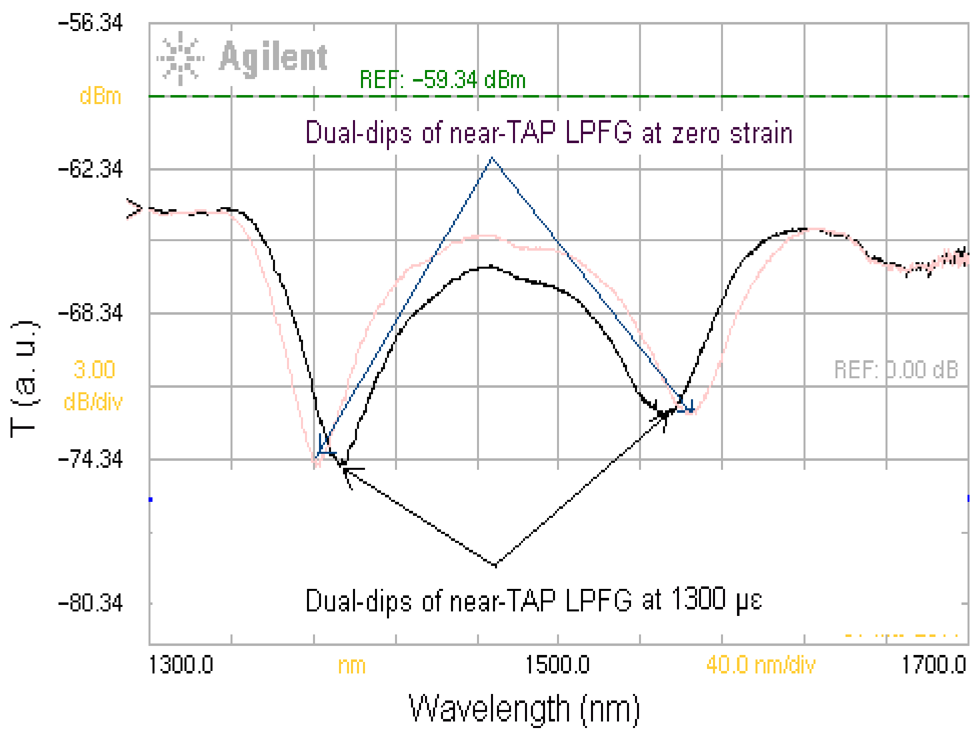

Fig. 3.15. Measured transmission function of near TAP-LPFG with and without strain: pink: 0 με and Black: 1300 με

The strain is increased in steps of 300 με and the resonance dip shifts of dual TAP mode were recorded with auto-dip measurement system of OSA.

The strain sensitivity calculated from the slope of the best fit line through the measured data (Fig. 3.16) for dual peaks is 11 nm/ 1000 με for 1560 nm peak and 10 nm/ 1000 με for 1380 nm peak.

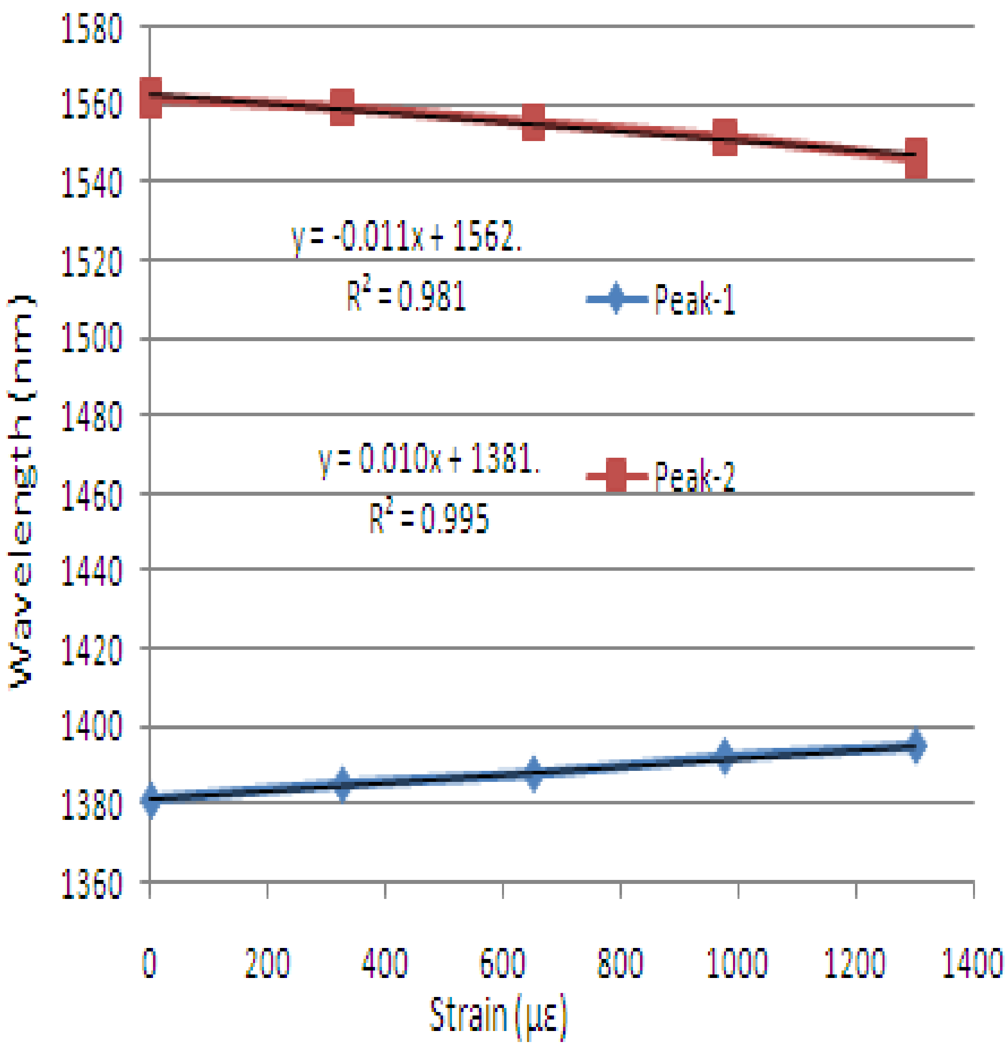

Fig. 3.16. Measured strain response of dual peak (Strain dependent wavelength variations of 11th mode)

3.6 Temperature-insensitive strain sensors based on LPFG in PCF fibers

During application of LPFG based strain sensors, one of the main difficulties is the cross sensitivity between strain and the temperature. The common methods for cross sensitivity reduction are using temperature compensation and simultaneous strain and temperature measurement [**66, 67**]. Conventional fibers contain at least two different glasses, each with a different thermal expansion coefficient, thereby giving rise to high temperature sensitivity.

Technology has been developed for demonstration of temperature-insensitive, strain sensors for use in nuclear environment. They are based on long period fiber gratings in Photonic crystal fibers which are inherently insensitive to temperature due to single material construction.

The fiber grating based strain sensors with a strain sensitivity of 2.0 pm/ $\mu\varepsilon$ covering axial strain range of 50-1300 $\mu\varepsilon$ can be used up to 75 kGy gamma dose environment without any deterioration in sensitivity. They can be used in secondary loops of nuclear reactors and are not commercially available. A long period fiber grating sensor in photonic crystal fiber with a strain sensitivity of -2.0 pm/ $\mu\varepsilon$ and negligible temperature sensitivity is fabricated by use of CO_2 laser beam. Such a strain sensor can effectively reduce the cross sensitivity between strain and temperature. They have been shown to be resistant to nuclear radiation and are thus useful for applications in secondary loops of nuclear reactors.

Photonic Crystal Fibers (PCFs) also known as Holey fiber are a new class of optical fibers that have attracted intense scientific research during past few years. Typically, these fibers incorporate a number of air holes that run along the length of the fiber, and the size, shape and distribution of the holes can be designed to achieve various novel wave-guiding properties that may not be possible in conventional fibers.

Various PCFs have been demonstrated so far that exhibit remarkable properties such as endlessly single mode fiber, large mode area and highly non-linear performance. Temperature-insensitive Long Period Gratings (LPFGs) have attracted much attention because of their potential applications in achieving stable optical filters, gain flatteners as well as in realizing temperature–insensitive sensors for Industrial and nuclear applications. Conventional fibers contain at least two different glasses, each with a different thermal expansion coefficient, thereby giving rise to high temperature sensitivity. PCFs are virtually insensitive to temperature because they are made of only one material (and air hole). This property can be used to obtain temperature- insensitive PCF based devices. LPFGs in PCF fibers have not yet been reported in India. Besides, the effect of high nuclear radiation on such PCF based grating sensors has not been reported by any group to the best of our knowledge.

3.6.1 Theory

For a long period grating with periodicity Λ, the wavelength $\lambda^{(m)}$ at which mode coupling occurs is given by Eq. (2.2) and rewritten below for convenience.

$$\lambda_n = \left[n_{eff}^{co} - n_{eff}^{cl,n} \right] \Lambda \qquad (3.8)$$

where, n_{eff}^{co} is the effective refractive index of the propagating core mode at wavelength λ and $n_{eff}^{cl,n}$ is the effective refractive index of the m^{th} cladding mode. The variation in the grating period and modal effective indices due to strain and temperature causes the coupling wavelength to shift. This spectral shift is distinct for each loss band and is a function of the order of corresponding cladding mode.

The axial strain sensitivity of LPFGs may be examined by Eq. (1.11) which is rewritten below:

$$\frac{d\lambda}{d\varepsilon}=\frac{d\lambda}{d(\delta n_{eff})}\left\{\frac{dn_{co}^{eff}}{d\varepsilon}-\frac{dn_{cl,i}^{eff}}{d\varepsilon}\right\}+\Lambda\frac{d\lambda}{d\Lambda} \tag{3.9}$$

where, $\delta n_{eff}=n_{co}^{eff}-n_{cl,i}^{eff}$ is the differential effective index, ordinal m has been dropped for the sake of simplicity. The two terms on the right side can be divided into material (first term) and waveguide (second term) contributions. The temperature sensitivity of LPFG grating is given by Eq. (1.10) which is represented below for ready reference.

$$\frac{d\lambda}{dT}=\frac{d\lambda}{d(\delta n_{eff})}\left\{\frac{dn_{co}^{eff}}{dT}-\frac{dn_{cl,i}^{eff}}{dT}\right\}+\frac{\Lambda}{L}\frac{d\lambda}{d\Lambda}\frac{dL}{dT} \tag{3.10}$$

where, *λ* is the central wavelength of the attenuation band, *T* is the temperature, *L* is the length of the LPFG and *Λ* is the period of the LPFG. For standard long period gratings with periodicity of hundreds of micrometers, the material effect dominates the waveguide contribution. Hence only first term in Eq (3.9) and (3.10) are considered for evaluation of sensitivity. For photonic crystal fibers which are single material fibers, the first term in Eq. (3.10) becomes negligible, resulting in very low temperature sensitivity. This term is an order smaller than that of B-Ge doped photosensitive fiber. This opens-up the field for PCF based temperature-insensitive sensors. By use of CO_2 laser method, a LPFG sensor with strain sensitivity -0.45 pm/με and a temperature sensitivity of 59.0 pm/°C was reported in Corning SMF-28 fiber. Another LPFG with a strain sensitivity of -0.19 pm/ με and temperature sensitivity of 10.9 pm/ °C was described in PCF fiber [**25**]. In this paper, we present a LPFG-PCF sensor fabricated in endlessly single mode photonic crystal fiber (ESM-PCF) with a high strain sensitivity (-2.0 pm/με) and negligible temperature sensitivity.

3.6.2 Experiment

Inscription of LPFGs have been demonstrated using various techniques such as UV treatment, heat treatment with a CO_2 laser or by applying mechanical pressure [**23**]. Formation of LPFG in pure-silica core PCF fibers is not straight forward because there is no photosensitivity provided by Ge-O_2 vacancy defect centers. The LPFGs in PCF are primarily formed due to modification of glass structure. However, any geometrical deformation results in flaws or cracks that result in fracture of the fiber and therefore LPFGs in PCF require high precision systems. Our fully automated CO_2 laser based grating writing system can set the grating period (200μm-800μm) with a precision of one micron while laser intensity can be stabilized within ±5 %.

Fig. 3.17 shows the cross Section of ESM-PCF. The PCF used in our experiment is an ESM-12-02 (Endlessly single-mode 12μm) fiber made by Crystal Fiber, Denmark. This fiber exhibits low loss across the widest possible wavelength region from 600 nm to above 2000 nm while keeping an almost constant mode field diameter. The fiber is endlessly single-mode (i.e. it has no higher order mode cut-off) and, therefore, delivers pristine mode quality at all wavelengths. The ESM-12 has a standard 125 μm outer diameter and is compatible with all common fiber tools.

For the preparation of LPFG in an ESM-PCF both ends of the PCF are fusion spliced to SMFs. The loss for each splice is about 0.74 dB. An X-Y scanning CO_2 laser is used for the fabrication of LPFGs in the ESM-PCF. The CO_2 laser operates at a frequency of 2 kHz and has a maximum power of 10 W. The laser power is controlled by the mark-speed of the laser pulses. The typical grating length and period in our experiment is 23.4 mm and 450 μm respectively. Fig. 3.18 shows the transmission characteristics of a LPFG fabricated on an ESM-PCF. Attenuation bands in the range of 1300 -1700 nm have been investigated by an optical spectrum analyzer.

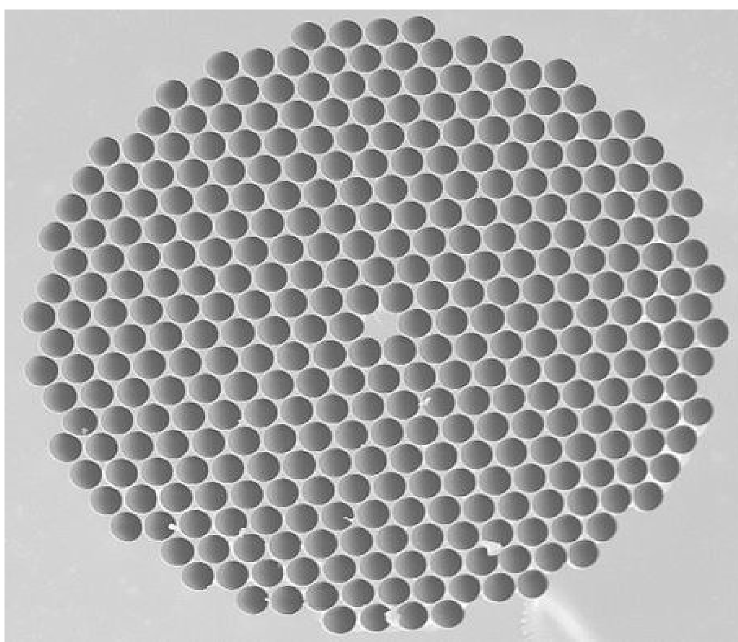

Fig. 3.17. Cross Section micro-profile of PCF fiber (taken from www.wikepedia.com)

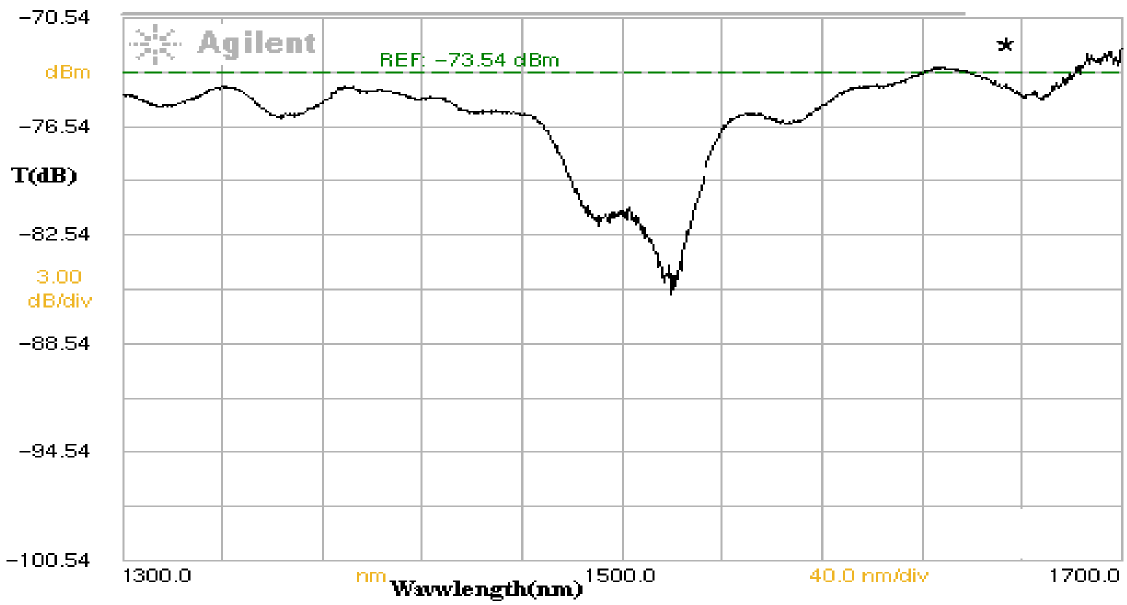

Fig. 3.18. Transmission characteristics of a LPFG fabricated on an ESM-PCF with a period of 450μm

3.6.3 Results and discussion

The strain characteristics were measured by giving a known axial strain. The thermal properties are reordered by keeping the sensor in a heated oven**.** Fig. 3.19 shows the strain response of LPFG. It shows that the resonance wavelength varies due to applied strain. There is also slight change in resonance strength. Fig. 3.20 shows the sensitivity curve for LPFG. A linear best fit to the experimental observations provide the strain sensitivity of -2.0 pm/ με over 0-1300 με.

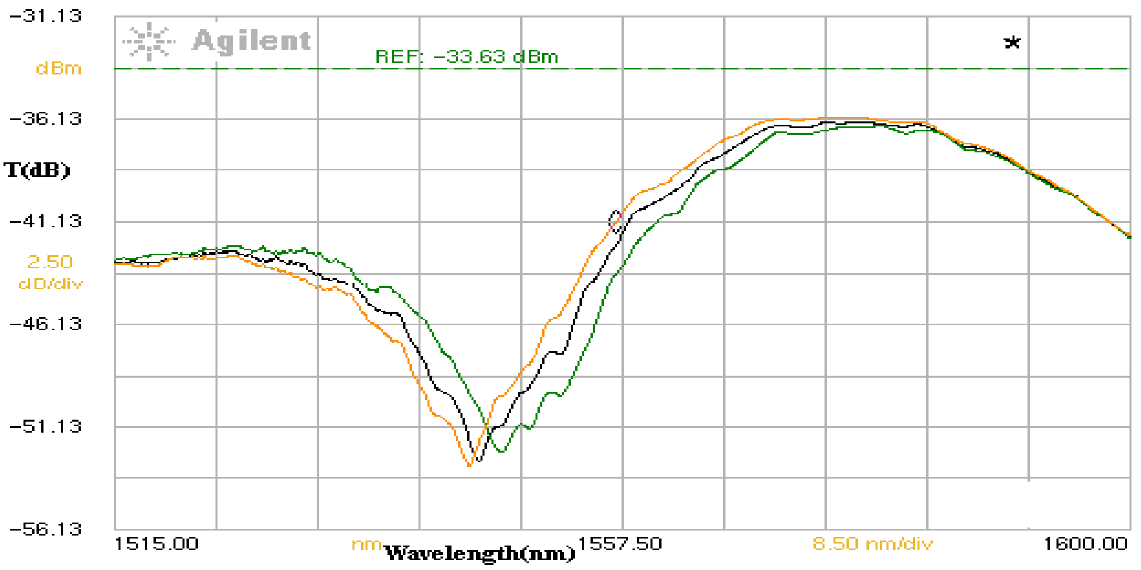

Fig. 3.19. Strain response of a LPFG fabricated on an ESM-PCF; Green=0 με, Black=650 με and Orange=1300 με

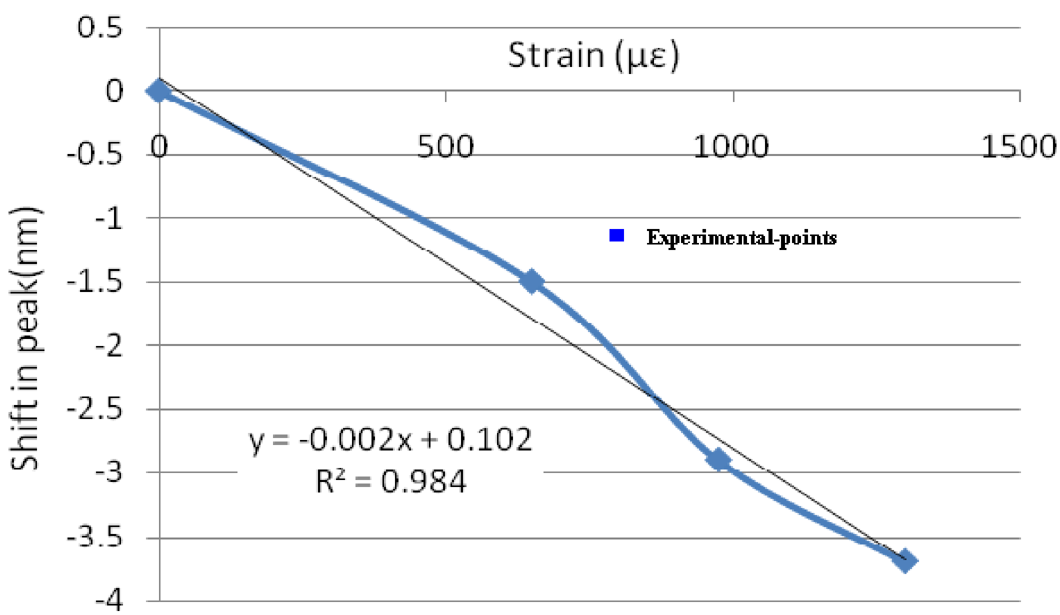

Fig. 3.20. Strain dependent wavelength shift of LPFG

Fig. 3.21 shows the thermal response of LPFG fabricated in an ESM-PCF. It clearly shows that there is negligible variation in the spectral response of LPFG even though the sensor is heated up to 100 ºC. The estimated thermal sensitivity is 0.004 nm/ ºC.

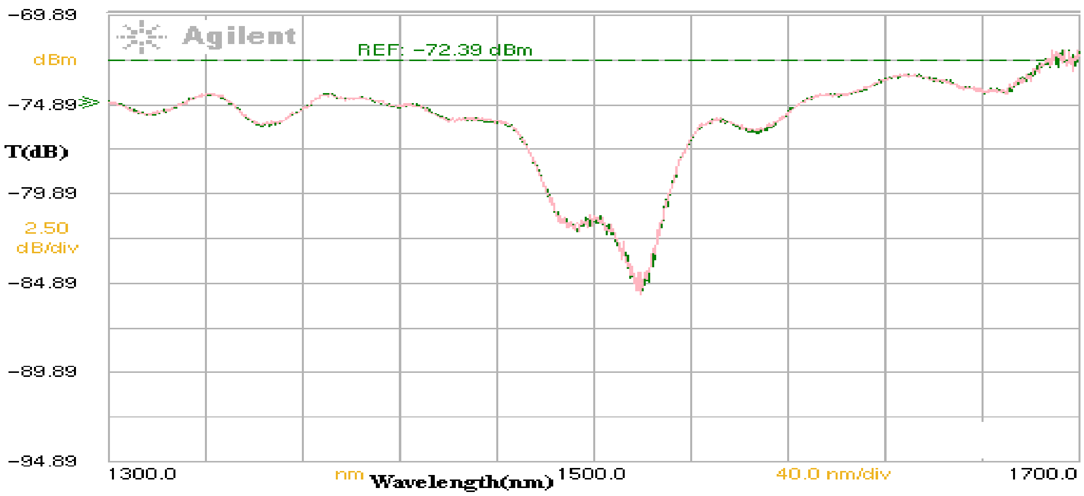

Fig. 3.21. Thermal response of a LPFG fabricated in an ESM-PCF; Green: 24.5 ºC and Pink: 100 ºC

To test the sensor performance in nuclear environment, the device was kept in gamma chamber for total dose of 75 KGy. After the dose, the device was taken out from gamma- chamber and was re-mounted on test setup. The spectral response and strain response was measured again. Fig. 3.22 shows the spectral response characteristics. By comparing Fig. 3.18 and Fig. 3.22, it can be seen that there is no spectral change (resonance dip, dip-strength) in the transmission characteristics of LPFG due to irradiation of intense gamma- dose.

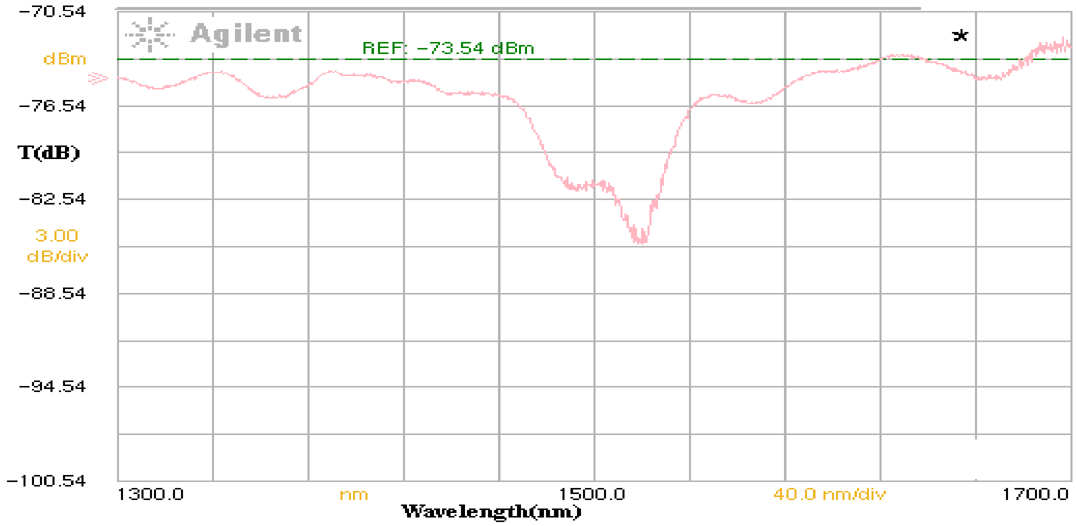

Fig. 3.22. Transmission characteristics of a gamma-irradiated LPFG fabricated in an ESM-PCF

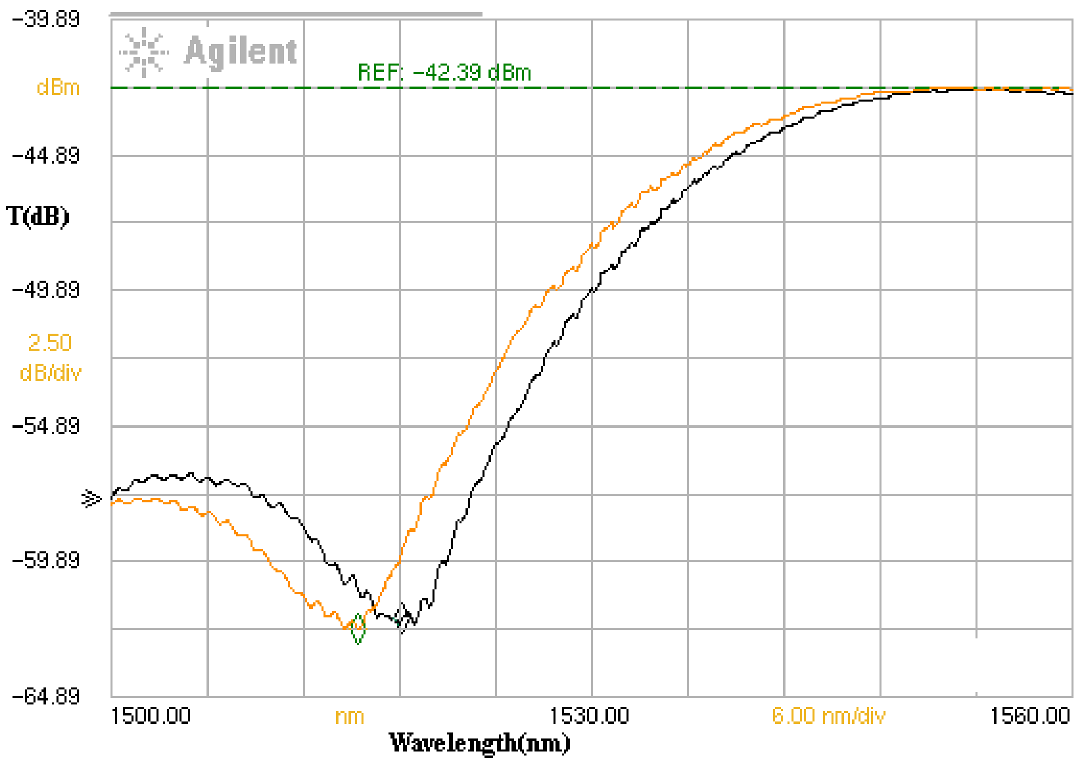

Fig. 3.23. Strain response of a LPFG fabricated on an ESM-PCF after nuclear dose of 75 kGy; Black=0 με and Orange=1300 με

Fig. 3.23 shows the strain characteristics of irradiated LPFG. By comparing Fig. 3.19 and Fig. 3.23, it is clear that there is no effect on strain sensitivity of LPFG device due to gamma-dose. The sensitivity is found to be - 2.12 pm/με which is almost equal to the sensitivity observed without irradiation.

3.7 Conclusion

High sensitivity TAP-LPFGs have been fabricated previously by UV radiation based technique. However, such gratings are known to contain an unstable component, which decays in time causing a significant change in central wavelengths of attenuation bands and in the coupling strength. They also have stability problems above 250 °C and can not be used for high temperature applications. We have shown that LPFGs written by CO_2 laser and arc induced technique are stable up-to at least 400 °C (limit due to heating oven rating) and can be used in Fast breeder reactors for coolant monitoring. Both CO_2 laser and arc-Induced technique are flexible, require no photosensitivity in the fiber for grating inscription and are capable of writing LPFGs in any type of fiber including in PCF fibers.

We have studied the effect of mode order and operation of TAP-LPFGs for high sensitivity measurements. We have verified the theoretical descriptions with good accuracy and have confirmed the presence of turning points. Highly sensitive sensors for each variable have been demonstrated. These studies have resulted in sensors operating on simple intensity measurements as well as wavelength modulated principle. Gratings for temperature sensing applications have also been packaged for rugged operation. To protect the gratings against moisture and environmental chemicals, a process has been developed to deposit gold coatings through vacuum thermal deposition. Technology has been developed for writing LPFGs in PCF fibers for temperature-insensitive strain sensing applications in nuclear environment.

We have also shown that long period gratings in ESM-PCF offer high strain sensitivity. Such sensors can effectively reduce cross sensitivity between temperature and strain. They can work reliably in 50-1300 με ranges with a resolution of 25 με even in thermally unstable environment of ±10 °C. Moreover, these sensors are resistant to gamma radiation up to at least 75 kGy and thus have potential for applications in particle accelerators, secondary loop of nuclear reactors and waste treatment facility.

CHAPTER 4

APPLICATION OF FIBER OPTICS SENSORS FOR TRANSPORTATION FUEL MONITORING

4.1 Introduction

Recent years have witnessed dramatic progress in the design and development of fiber optic chemical sensors as detection of chemical species is important in many industrial, environmental and chemical processes. The fiber optic sensors being chemically inert and immune to EMI are especially useful for applications in hazardous environment of hydrocarbons. Such sensors include refractometric sensors and evanescent wave absorption sensors. Precision refractive index (RI) sensing based on accurate determination of RI of an analyte, is critical for biological and chemical sensing, since a number of substances can be detected through measurement of the RI. In RI measurement, the coupled output power varies due to variation of numerical aperture (NA) of the fiber due to analyte presence in the sensing region where the fiber cladding has been removed. The evanescent wave sensors are based on change in transmitted power due to effect of absorbing species on evanescent field. This in turn depends on exposed fiber length and anlayte

---

Part of the results reported in this chapter has been published in the following paper: Sanjay Kher, Smita Chaubey, Jai Kishore, S.M.Oak, "Detection of fuel adulteration with high sensitivity using turnaround Point long period fiber gratings in B/Ge doped fibers," IEEE Sensors Journal, vol. 13, no. 11, 2013, pp. 4482-4486.

concentration [**68**]. The RI change can also result in shifts in resonance peaks due to variation in phase matching condition of a fiber grating. We have investigated the effect of external liquid RI change on characteristics of LPFGs. Using this effect, we have shown the application of such gratings for monitoring the adulteration of gasoline fuel. Automobile fuel industry is an area which is in constant search of sensors for in-situ monitoring of quality control and adulteration detection. The use of alternative and renewable energy sources has also drawn attention in international sphere for conservation of fuel oil by mixing/blending ethanol. Adulteration of petroleum products especially petrol {Motor gasoline (MS)} and diesel {high speed diesel (HSD)}, has become a serious problem, particularly in Asia.

Kerosene is the most important domestic fuel for economically weaker Sections of society and is highly subsidized. The large differences in the price of petrol, diesel and kerosene compounded with easy miscibility of kerosene makes its adulteration a very plausible proposition. Such practices result in damage to automobile engines and increased environmental pollution.

One of the main factors responsible for adulteration is non-availability of any standard technique that can be universally adopted for on-the-spot detection of adulteration level. There have been number of methods proposed for checking adulteration of transportation fuel (TF) such as filter test, checking properties like density, viscosity, flash point, ultrasonic techniques [**69**] American standards for testing materials (ASTM) distillation, titration techniques [**70**] and chemical markers. All the above methods suffer from limitations in terms of accuracy, real-time on-site detection and sensitivity in determining adulteration levels.

Anhydrous ethanol is blended with gasoline due to their octane-enhancing and pollution-reducing capabilities. The combustion of ethanol-gasoline blend provides significant reduction in air pollutants such as CO, CO_2 and hydrocarbons reducing green house effect and global warming. Ethanol is a renewable energy source produced from sugarcane and corn which also provides a good income source for farmers. The exact volumetric concentration of ethanol in fuel is specified by respective governments, and up to 20 % V/V ethanol blending is permitted in some countries. So it is important to monitor ethanol content in fuel to comply with regulations. Moreover, the adulteration of water in ethanol (high hydrated alcohol) causes engine damage and possible damage to environment. Therefore, a careful monitoring of water content in ethanol is necessary to minimize problems when using ethanol fuel or gasoline-ethanol fuel blends in vehicle engines. Efficient monitoring of these parameters requires high sensitivity ambient refractive index (RI) sensors. Several high sensitivity RI sensors based on Microstructure-FBGs [**71**], surface plasmon resonance (SPR) [**72**], metal clad waveguides [**73**] and long period fiber gratings (LPFGs) [**74, 64**] have been reported.

In FBG sensors, the coupling occurs between the forward propagating core mode and backward propagating core mode. FBG sensors suffer from low external medium index sensitivity because of confinement of modal fields within the core [**75**]. As the core mode is not sensitive to surrounding refractive index, the fiber cladding of the FBG is often polished or etched to increase the evanescent field interaction with the surrounding material. This results in reduced mechanical strength of the sensor.

Various optimization techniques such as FBGs in three-hole, six-hole PCF fibers have been demonstrated to measure RI with sensitivity (~ 1500 nm/ RIU where RIU stands for refractive index unit). However, hydrogen-loading and FBG writing in micro-structure fiber is a complex process which increases the overall cost of the sensor. SPR based technique requires nano-meter thick precision metallization but offers high sensitivity (~ 2000 nm/RIU). LPFGs have found large interest as emerging devices for fuel adulteration due to their sensitivity to surrounding refractive index (SRI). The LPFG based sensors are compact, easy to fabricate and do not need any metallization. Other major advantage of LPFG sensors is the possibility to tune the resonance wavelength anywhere in the electromagnetic spectrum including the highly sensitive infrared region. The effect of uniform fiber thinning (tapering) on the spectral characteristics of UV-induced LPFGs has been investigated in recent years. LPFG chemical etching was proposed by Vasilev et al. [**76**] as a post fabrication resonant peak positioning of the attenuation bands. The detailed analysis of the sensitivity enhancement in thinned LPFGs inscribed in SMF-28 corning fiber was reported by Agostino Ladicicco et al., [**77**]. They observed six times enhancement in sensitivity for sixth order mode by reduction of fiber diameter from 125 µm to 104 µm in SRI range from 1 to 1.45. Qing-Li Jin et al., [**78**] have presented an optimal design of a temperature-insensitive LPFG with a reduced cladding radius of 27 µm. The resonant wavelength shift was 86 nm for SRI range of 1-1.45 and temperature sensitivity of 0.008 nm/ C. The best reported value using LPFGs for fuel adulteration of kerosene in petrol is 0.06 nm/% change of kerosene for 0-10% range [**74**], and the sensitivity for SRI is 1700 nm/RIU (refractive index unit) in the RI range of 1.3611-1.476 for ethanol-kerosene samples **[79**]. For ethanol-gasoline blend the best reported RI sensitivity is approx. 250 nm/ RIU in 10-20% blend [**80**].

We have conducted systematic studies [**29**] for applicability of LPFG as a sensor device to assess fuel conformity for transportation purposes. In Section 4.2 we describe the principle and probe calibration studies while in Section 4.3 and 4.4, we provide the device testing and experimental results. We further describe surface plasmon resonance (SPR) based technique for comparison in Section 4.6.

4.2 Principle of operation

The adulteration of kerosene in gasoline changes the refractive index of pure gasoline and therefore, optical fiber based sensors capable of measuring the refractive index changes can be used for detection of adulteration. The same physical principle is applicable for ethanol blending and detection of water content in ethanol.

The refractive index sensitivity of LPFG arises from the dependence of the phase matching condition upon the effective refractive index of the cladding modes. The effective indices of the cladding modes are dependent upon the difference between the refractive index of cladding and that of the ambient medium surrounding the cladding through evanescent wave interaction. The central attenuation bands thus show a dependence (shift) upon the refractive index of the medium surrounding the cladding.

It is well known that resonance wavelength λ_{res} of a LPFG with period Λ is determined by phase matching condition [**76**]

$$\lambda_{res} = \left[n_{core}^{eff} - n_{clad,m}^{eff} \right] \Lambda \qquad (4.1)$$

where, n_{core}^{eff} and $n_{clad,m}^{eff}$ are effective indices of the fundamental core mode and the m^{th} cladding mode, respectively.

According to [**62**], the sensitivity of LPFG for SRI is defined by

$$\frac{d\lambda_{res}}{dT} = \lambda_{res}.\gamma.(\alpha + \Gamma_{temp}) \qquad (4.2)$$

where γ describes the waveguide dispersion and is a general sensitivity parameter for LPFG. General sensitivity factor γ is defined by following expression which is same as Eq. (2.3) [**62**]

$$\gamma = \frac{\frac{d\lambda}{d\Lambda}}{n_{core}^{eff} - n_{clad,m}^{eff}} \qquad (4.3)$$

Here, Γ_{surr} describes the SRI dependence of the waveguide dispersion which includes the effect of cladding diameter; γ is the key factor for sensitivity determination of higher order LPFG resonances. Fig. 4.1 shows the refractive index sensitivity of a LPFG written by CO_2 laser in a photoensitive fiber. For the SRI measurement range of 1.33 to 1.43, the sensitivity is 165 nm/ RIU. For lower order modes (up to six), the general sensitivity factor γ is <2, hence typical LPFG sensitivity is relatively smaller (< 700 nm/ RIU) compared to SPR based sensors.

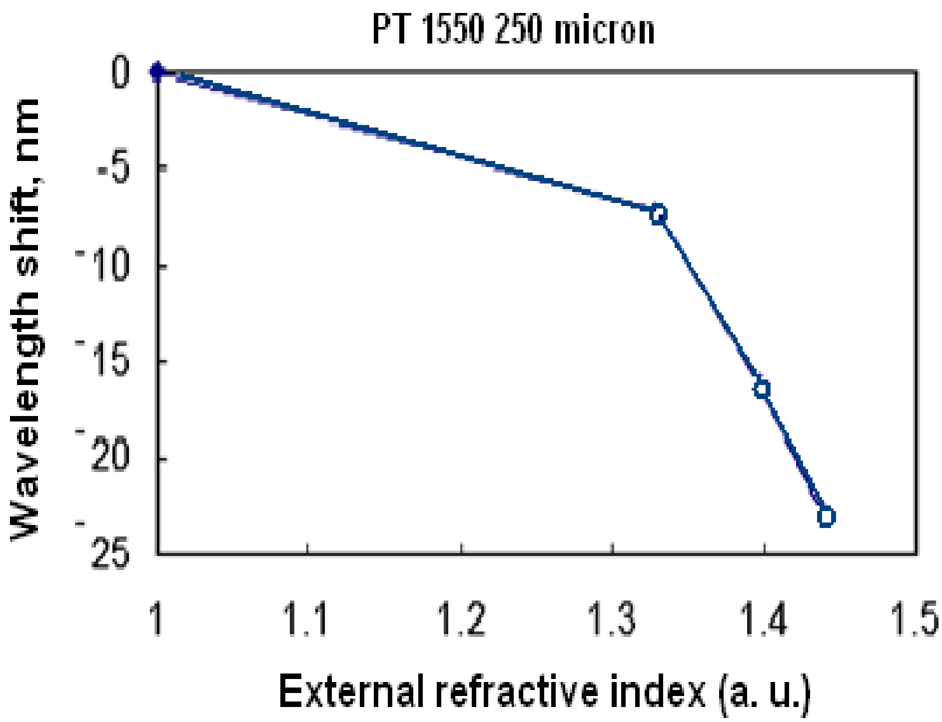

Fig. 4.1. Refractive index sensitivity of a typical LPFG

It has been reported that the shift in the resonance wavelength corresponding to the changes in surrounding refractive index (SRI), increases with increasing mode order (effect of γ) , coupling to asymmetric modes and reduction of fiber diameter [**77**]. It is well known that higher the cladding mode order, larger would be the corresponding evanescent field in the region outside the fiber, higher would be the sensitivity of the sensor. Also, the cladding mode distribution is dependent on the geometrical features of the fiber. This means that fiber cladding reduction/modification induces modifications in the distributions of cladding modes, leading to changes in spectral characteristics. This aspect is useful for post fabrication tuning. Thus, for high sensitivity applications, it is desirable to work with the highest-order cladding mode that falls within the bandwidth of the light source used to interrogate the grating.

4.3 Properties of general sensitivity factor for increased sensitivity to SRI

Eq. (4.1) shows that the effective refractive indices of both core and cladding modes are functions of the wavelength, so there is a particular relation between resonant wavelength and grating period for given structural parameters of the fiber. For our chosen fiber (parameters explained in Chapter 2) co-doped with B/Ge, we have calculated the Phase matching curves as shown in Fig. 2.10 earlier. It shows that for lower-order cladding modes (up to 10), the curves exhibit positive slopes throughout wavelength range of 900-1800 nm, the resonant wavelengths increase monotonically with the increment of grating period. Therefore, there is only one interSection between each PMC and a vertical line representing a specific grating period. This case thus explains the conventional LPFG that are characterized by a single attenuation peak for each cladding mode. For a higher-order cladding modes (>10), the phase-matching condition maps out quadratic curves. The slopes of the curves for cladding modes (>10th cladding mode) change their signs from positive to negative with increasing wavelength at the points denoted by open circles near some specific grating periods (occurrence of turning points). Further, for a given period and a selected cladding mode, a vertical line may intersect a PMC twice. In other words, the phase matching condition may be satisfied at two different wavelengths. This is the case of dual-peak resonance which has been exploited for increased SRI sensitivity.

It can be seen from Eq. (4.3) that for a TAP-LPFG, grating sensitivity is mainly determined by the γ factor which also describes the waveguide dispersion. For every cladding mode, at the turning point, we can see (Fig. 4.1) that $\left|\frac{d\lambda}{d\Lambda}\right| \to \infty$; thus from Eq. (4.3) we find that $|\gamma| \to \infty$

and so the turning point operation of LPFG determines the condition for maximum sensitivity. In our design, we have discussed the properties of 11^{th} cladding mode near turning point for detection of fuel adulteration with improved sensitivity.

4.4 Design and experiments

Our fabrication system, based on two dimensional scanning of a CO_2 laser beam (as shown earlier in Fig. 2.3) is reproduced below for elaboration. The fiber is fixed at one end and the other end is attached to a small weight to provide a constant pre-strain in the fiber. The sharply focused amplitude modulated CO_2 laser beam is scanned across the fiber transversely (X direction) and then advances along the fiber (Y direction) with a step equal to the grating period. This is achieved by means of two-dimensional scanners under computer control, while monitoring the grating formation in real time. Such a precision controlled system where the fiber is not periodically moved, can write high quality LPFG with a nearly zero insertion loss**.** It may be noted that the TAP-LPFG requires not only a short period (< 250 µm for resonance in 1400-1500 nm) but also a precision of ±1µm, for our chosen fiber [**29**].

In our experiments, the diameter of the focused CO_2 laser beam spot is about 100 µm, the line speed is 60 mm/s, the pulse repetition rate is 2 kHz and the average output power is about 10 W. Attenuation bands in the range of 950-1700 nm have been investigated by an optical spectrum analyzer (OSA) (Model: 86146B, Make: Agilent) with a wavelength resolution of 0.1 nm. It is observed that the slope of the phase matching curve for the 11^{th} order cladding mode at a grating period of 208 µm exhibits a change in sign from positive to negative with increasing wavelength at the point marked by an arrow (exact TAP). Thus for this mode, a given LPFG period very close but lower than TAP point (near about 207 μm) corresponds to two resonant wavelengths (1.37 and 1.572μm) which is characterized by dual resonant dips in the transmission spectrum. This condition is achieved if the SRI is slightly increased compared to air. Accordingly, a precise LPFG period of 208 μm was selected so as to experimentally achieve exact TAP-LPFG for the 11^{th} order cladding mode.

An average of ten OSA traces in the wavelength range of 1200-1700 nm was calculated and the 'pit search' utility of OSA was used to locate the resonance dip. Standard deviation obtained for measurement of ethanol was 0.33 nm at mean λ_{res} of 1413.22 nm (at 25 ± 0.2 ºC) and 0.47 nm at mean λ_{res} of 1413.35 nm (at 25± 0.4 ºC).

To reduce the temperature sensitivity, all efforts were made to conduct the experiments at constant temperature of 25±0.2 ºC. To minimize systematic errors and to clean the measurement system, ethanol was introduced into the Teflon cell and cleaned several times after draining out samples from the cell. The LPFG resonance wavelength position relative to ethanol was used as the reference for ensuring cleanliness of the LPFG.

For refractive index measurements, the LPFG was passed through a specially designed Teflon cell (approximately 20 ml volume). The fiber was fixed at one end and the other end was kept under tension as shown in Fig. 4.2. This reduces the errors due to the LPFG sensitivity to strain and bending. The Teflon cell has inlet and outlet valves to fill in and drain out liquid samples. All standard liquids were of spectroscopic grade, purchased from Merck (India).

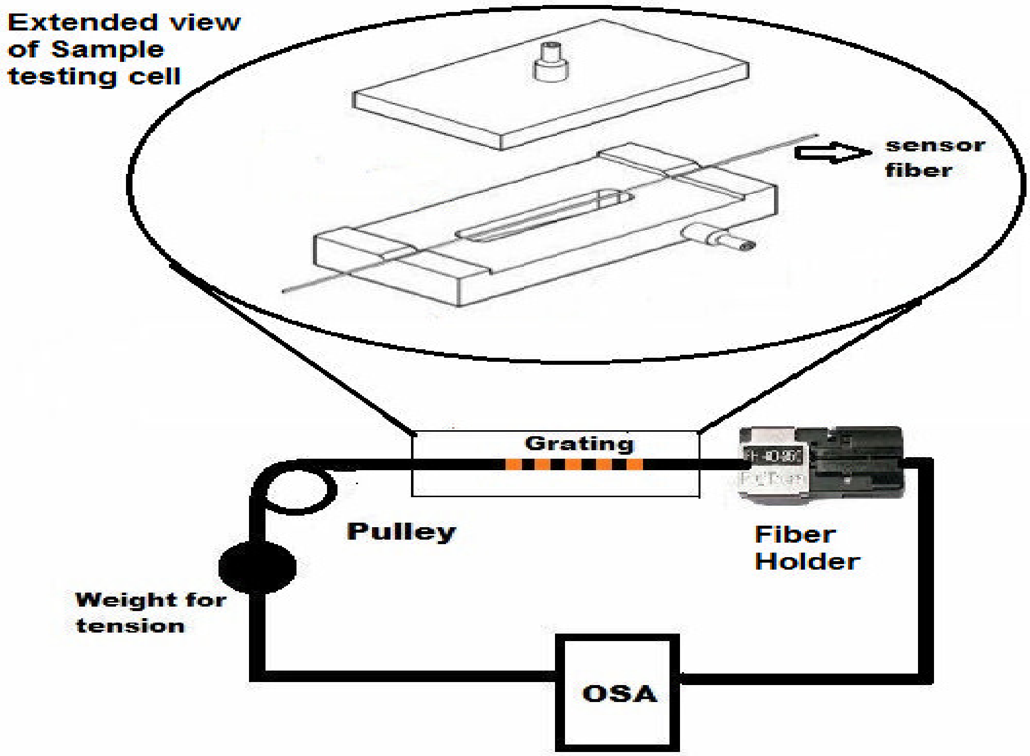

Fig. 4.2. SRI measurements: Experimental layout for SRI measurements

4.5 Experimental results and discussion

The TAP-LPFG (208 μm grating period, 20 mm length, B/Ge doped fiber) was calibrated for refractive index sensing by determining the shift of the resonant peak for known samples of standard solutions of methanol, ethanol, octanol, nonanol and decanol used as SRI medium. Fig. 4.3 shows the calibration curve while the values are tabulated in Table 4.1. As per the linear curve fitting, the TAP-LPFG offers a sensitivity of 1666 nm/RIU in the RI range 1.3977 – 1.4372. This is then used for measurements related to detection of fuel adulteration. Several samples with known adulteration of kerosene were prepared and analyzed using TAP-LPFG. These samples were transferred one after the other into the cell and the LPFG response was recorded. Initially pure petrol (RI= 1.419), 10% adulterated petrol, 50% adulterated petrol with kerosene and pure kerosene samples (RI=1.436) were used for this experiment. Fig. 4.4 shows the spectral changes observed in transmission spectrum of TAP-LPFG due to change in the surrounding medium from pure petrol to pure kerosene. The significant shift of 9.8 nm for 10% adulteration provided a boost to investigate the device applicability for measuring concentrations in 0-10% adulteration range.

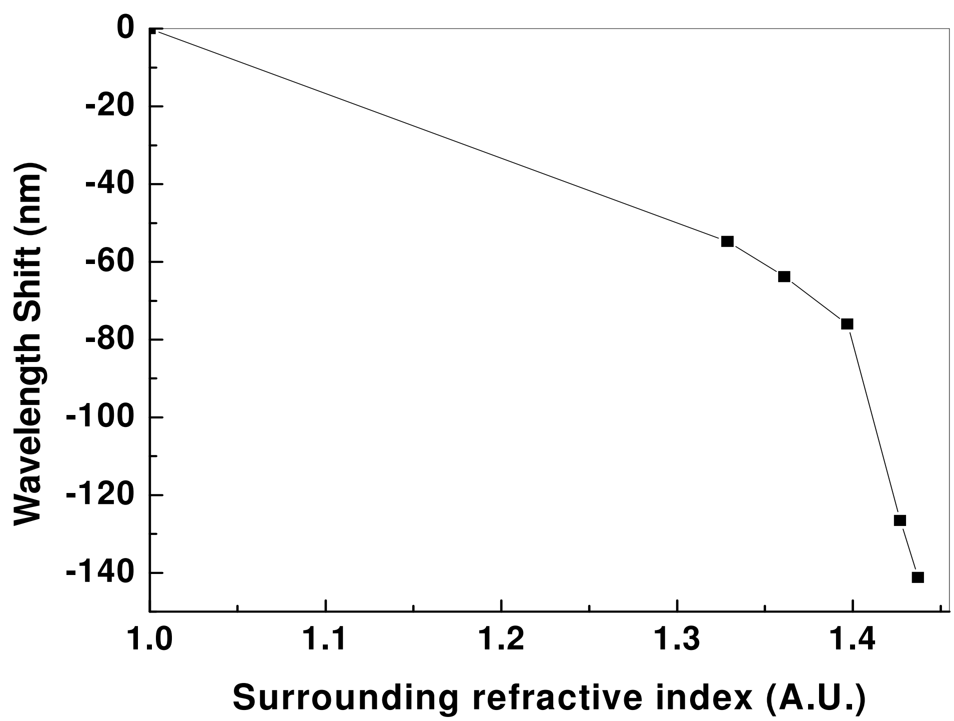

Fig. 4.3. Calibration curve for SRI measurements using TAP-LPFG as the sensor

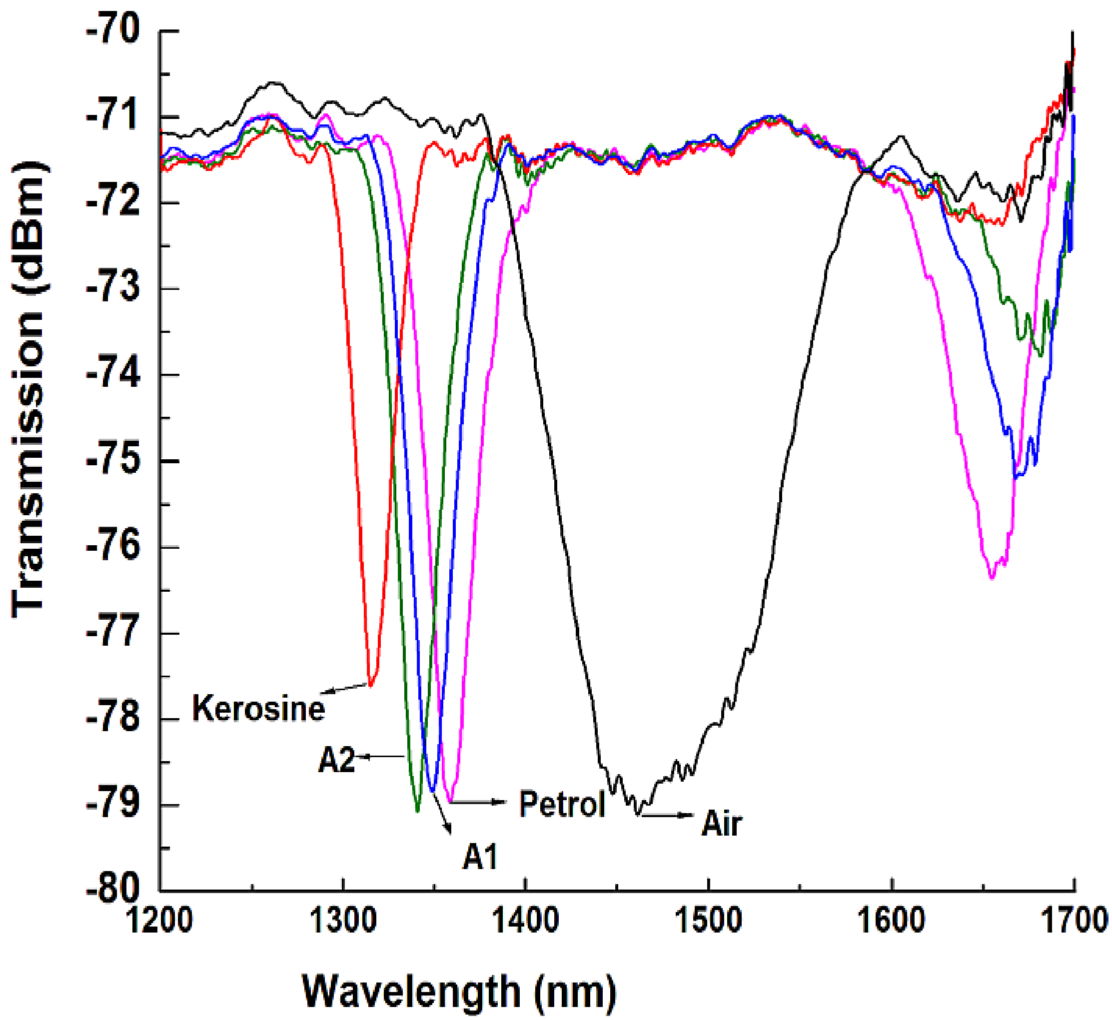

Fig.4. 4. Changes in exact-TAP LPFG transmission spectrum due to adulteration of kerosene in Petrol. The curves show change in transmission spectrum when the measurement cell is filled with petrol (Petrol), 10% kerosene added in petrol (A1), 50% kerosene added in petrol (A2) and kerosene

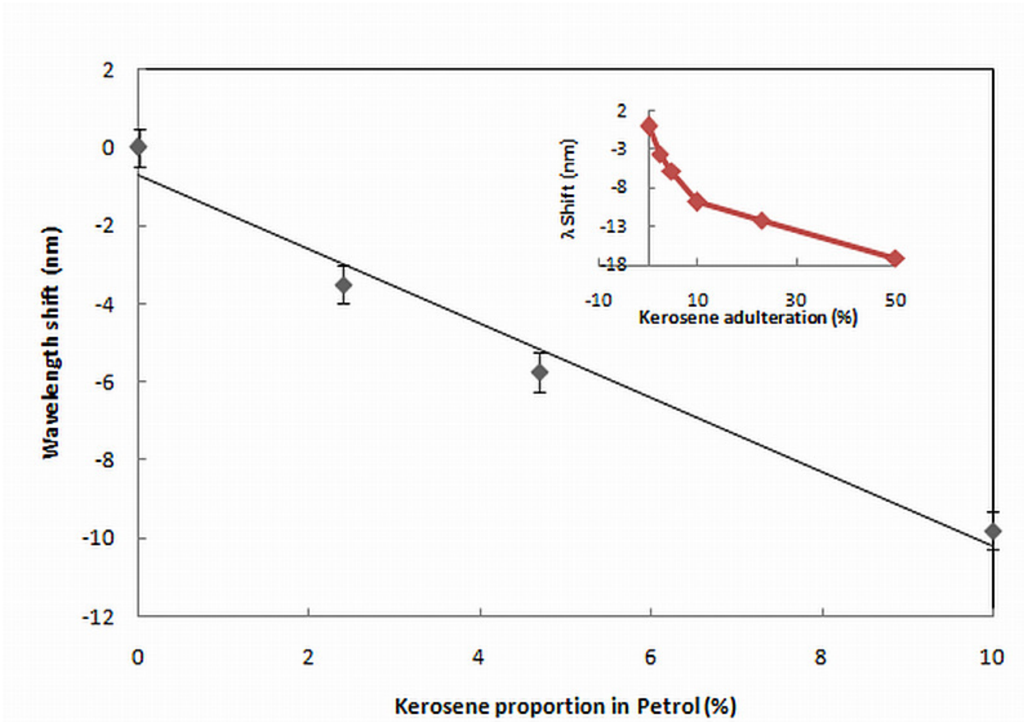

Fig. 4.5. Shift in TAP-LPFG resonance peak as a function of kerosene concentration in petrol (0-10%). Inset shows the wavelength shifts observed for kerosene adulteration samples up to 50% adulteration

To analyze the samples with lower adulteration of kerosene in petrol, samples in the range 0-10% were prepared and analyzed. The measured response of TAP-LPFG mode for increasing adulteration is plotted in Fig. 4.5 while the experimental results are tabulated in Table 4.2. The sensitivity dλ/ % change of kerosene in petrol (adulteration) calculated from the best fit straight line through the measured data is 0.949 nm/% change of kerosene in petrol up to 10 % of kerosene which allows us to easily measure 1 % adulteration of kerosene in petrol with an OSA of modest resolution.

The inset shows the plot for wavelength shifts observed in TAP resonance peak for kerosene adulteration up to 50 %. For a higher kerosene adulteration leading to higher SRI, the sensitivity reduces remarkably (0.18 nm/ % change of kerosene in petrol for 10-50 % adulteration range). One possible reason for this can be attributed to the rapidly reducing value of general sensitivity factor γ (Eq. 4.2) as dual resonance wavelengths move away from the turning point due to an increase in the value of SRI. However, this does not affect the analysis presented here or the final results as we can use the calibration curves for quantitative determination of adulteration. It can be inferred from exact TAP measurements that a slightly off TAP-LPFG (period > 208 μm) can be used for amplitude based detection of fuel adulteration where changes in SRI are reflected as changes in transmitted output signal level at the resonance wavelength.

TABLE 4.1 - WAVELENGTH SHIFT INDUCED BY VARIOUS STANDARD REFRACTIVE INDEX LIQUIDS IN NEAR TAP-LPFG WRITTEN BY CO_2 LASER IN B/GE DOPED FIBER

S.No.	Medium	RI	Wavelength shift(nm) (TAP mode)
1	Air	1	0
2	Methanol	1.3288	-54.7
3	Ethanol	1.3611	-63.8
4	Butanol	1.3977	-76
5	Nonanol	1.427	-126. 5
6	Decanol	1.4372	-141. 2

TABLE 4.2- WAVELENGTH SHIFT INDUCED BY VARIOUS CONCENTRATION COMBINATION OF KEROSENE-PETROL IN TAP-LPFG WRITTEN BY CO_2 LASER IN B/GE DOPED FIBER

S.No.	Kerosene adulteration in Petrol (%)	Wavelength shift(nm) (TAP mode)
1	0	0
2	2.4	-3.5
3	4.7	-5.75
4	10	-9.8
5	23	-12.2
6	50	-17
7	100	-38.5

Fig. 4.6 shows the capability of near TAP-LPFG for Ethanol-Petroleum blend analysis. It is clearly possible to detect ethanol blending level of 9% and 16%. The maximum permitted level for ethanol blending as per existing norms is less than 10%. These results clearly establish the superior performance of LPFGs operating near the turnaround point for development of high sensitivity sensors.

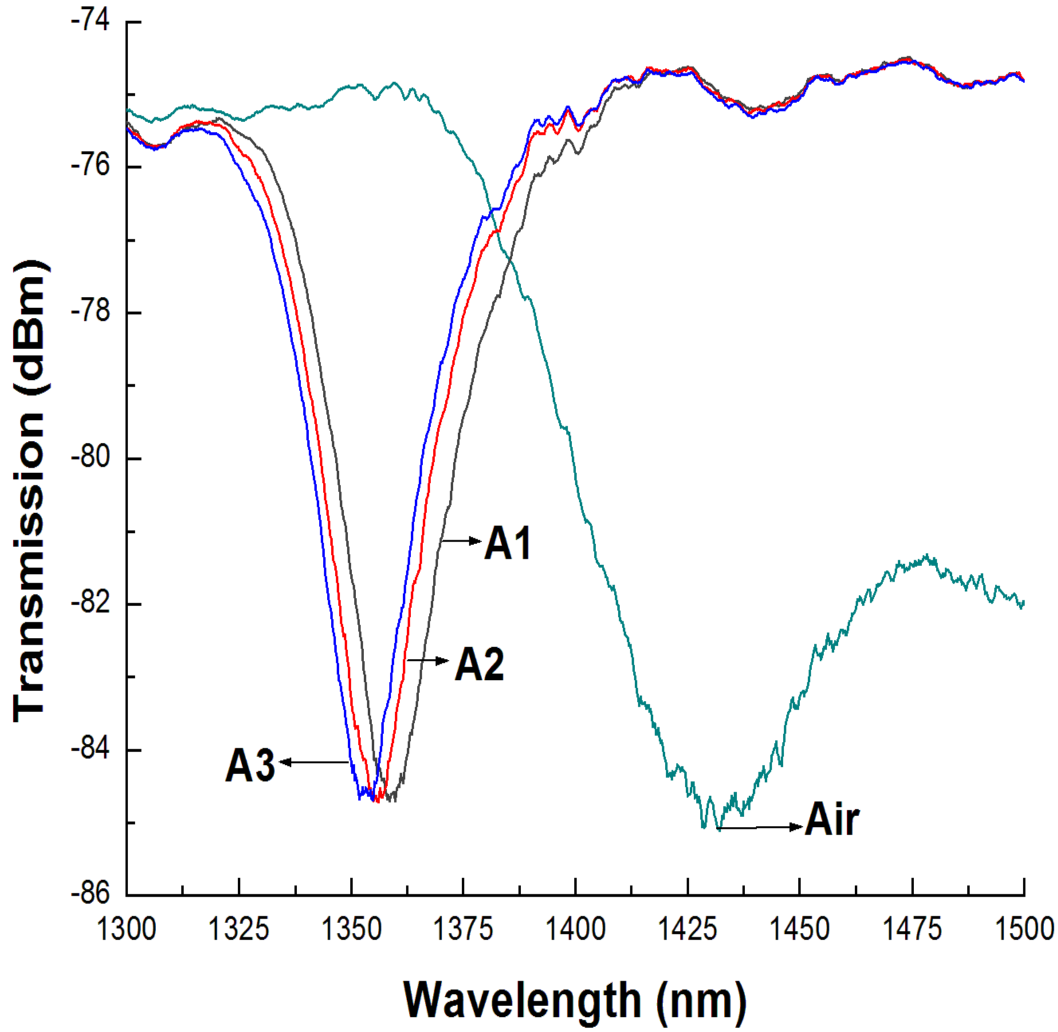

Fig. 4.6. Changes in transmission spectrum of near TAP-LPFG (206 μm grating period) in B/Ge codoped fiber due to ethyl alcohol blending of Petrol. The curves show change in transmission spectrum when the measurement cell is filled with petrol (A1), 9% ethyl alcohol added in petrol (A2) and 16 % ethyl alcohol added in petrol (A3)

We have presented CO_2 laser written exact TAP-LPFGs in B/Ge doped fibers for fuel adulteration detection. An average grating sensitivity of 1635 nm/ RIU for SRI in the range

1.397 to 1.4372 has been demonstrated. Further, we have demonstrated a very high sensitivity of 0.949 nm/% change of kerosene in petrol up to 10% of kerosene, which is significantly high compared to any previously published values [**29**]. Compared with the UV written LPFGs, these specialty LPFGs offer the advantages of lower cost, tailorability and greater potential for fuel adulteration detection, fuel blending for octane enhancement and identification of hydrocarbons in pipelines.

4.6 Study of surface plasmon resonance (SPR) based fiber optic sensors for fuel adulteration

Surface Plasmon resonance (SPR) sensors are widely used in biological, medical and environmental sensing. Surface plasmon resonance is a phenomenon which involves the absorption of a p-polarized light by the surface electrons of a metal film under specific resonance conditions determined by the dispersion relations of surface plasmons [**67, 81**]. We have also studied the evanescent wave propagating along the core/cladding interface to excite SPR at metal-air and metal/external chemical medium interface of the optical fiber and recorded SPR signals for gold nano-meter thick films coated on optical fibers.

4.6.1 Introduction and principle of SPR for SRI detection

Surface plasmon resonance (SPR) is a prominent optical phenomenon, which involves resonant excitation of electromagnetic surface waves coupled with collective oscillations of free electrons in metal. When excited over a metal/liquid interface, the plasmons offer attractive applications in food quality testing and bio-sensing [**67**].

To miniaturize SPR sensor, several Fiber/waveguide-based systems have been proposed [**72**]. In such integrated SPR sensors, one launches light into a fiber optic core and then uses coupling of fundamental core mode with the plasmon propagating over a thin film deposited onto some part of the same fiber.

In this configuration, cladding is etched off and core is symmetrically coated with metal. The phase matching condition for surface plasmon wave (SPW) in such case is given by [**98**]:

$$\frac{2\pi}{\lambda(n_{co}\sin\theta)} = \mathrm{Re}\left[\frac{2\pi}{\lambda\left(\frac{\varepsilon_s\varepsilon_m}{\varepsilon_s+\varepsilon_m}\right)^{\frac{1}{2}}}\right] \qquad (4.4)$$

where n_{co} is the fiber core refractive index, θ is the incident angle, ε_s is the dielectric function (permittivity) of the sample/analyte medium and ε_m is the permittivity of metal. Since SPWs are on the boundary between the metal and the sample medium, their excitation condition is very sensitive to any change in the boundary condition such as adsorption to the metal surface. A change in the refractive index in the sample medium produces a change in propagation constant of SPW. This change alters the coupling condition between a light wave and SPPs, which can be observed as a change in the wavelength of the optical wave that interacts with SPWs. Such sensors employ a white light source to monitor the resonance wavelength.

4.6.2 Experiment

In a fiber optic SPR sensor, the optical fiber is uncladded from a middle portion and coated with a thin film which is surrounded by the sensing medium. Light from a polychromatic source is launched from one end of the fiber while the SPR spectrum is recorded at the other end of the fiber. For fiber optic based wavelength interrogation method, a multimode plastic clad silica fiber was used as sensor. About 20 mm length of fiber cladding of a plastic coated multi-mode silica fiber is removed by chemical etching method. This small Section is then coated with nano-meter thick gold film (20-80nm) using vacuum evaporation method. A high power UV-Visible pulsed Tungsten-Halogen lamp with wide spectral emission range (220-750 nm) is used as broadband source. The Fig. 4.7 shows the schematic diagram of this setup.

Ethanol has become a widely used bio-fuel due to limited quantity of gasoline, diesel and other fossil fuels. The production of ethanol at a big scale is also possible because it can be derived from molasses, which is a by-product in the process of making sugar or other starch products. But since ethanol is cheaper than gasoline, the fuel may be adulterated by increasing the proportion of ethanol in order to maximize the profit. Therefore, sensors for ethanol-gasoline blending analysis are of great interest. Pure petrol has the RI of 1.41 while the refractive indices of 10 %, 20% and 40 % ethanol blended petrol are 1.405, 1.397 and 1.37 respectively. Fig. 4.8 shows the results of these measurements and provide clear evidence that SPR can provide a sensitivity of 4.25 nm/ (V/V%) of ethanol blending in petrol. For SRI, this sensitivity corresponds to about 1480 nm/ RIU.

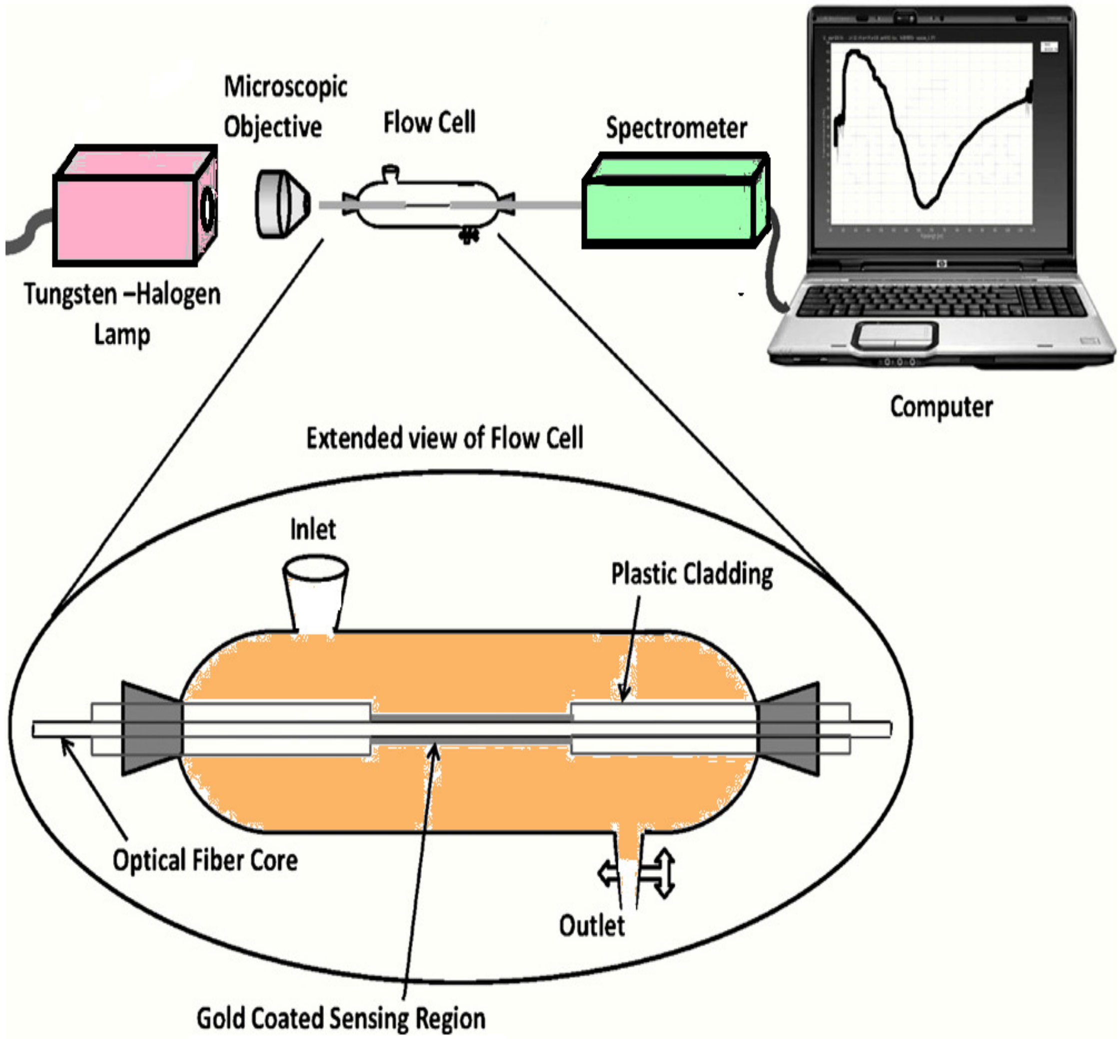

Fig. 4.7. Schematic diagram of fiber Optic SPR system

It may be noted that metal layer thickness in SPR system is an important parameter which determines the sensitivity, resonance coupling and robustness of the sensors [**82**].

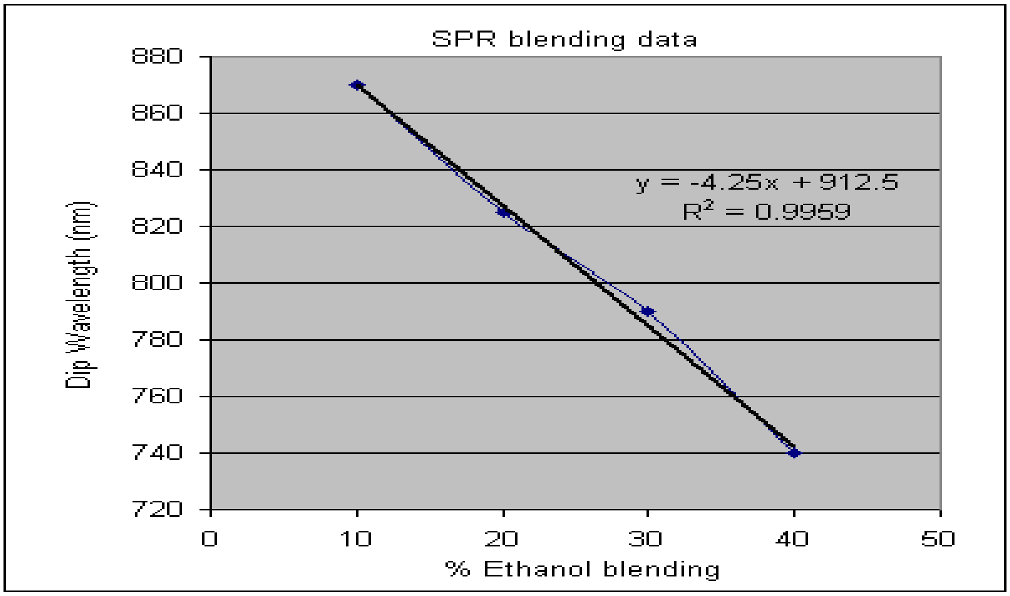

Fig. 4.8. Shift in SPR dip as a function of ethanol concentration in petrol

4.7 Conclusion

We have studied the sensing responses of long period fiber gratings (LPFGs) to the external refractive indices. The primary effect of change in the ambient index is the change in the resonant wavelength of various cladding modes of the LPFG. Such sensors have a multitude of important applications in basic research, environmental monitoring, biodefense and medicine. The development of smart sensors for Monitoring of transportation fuel adulteration, blending proportions in petrol-ethanol fuel and the quality of ethanol assume a great importance. In this study, we have designed and utilized Turnaround-point LPFGs (TAP-LPFGs), which possess far greater sensitivity than standard LPFGs.

For TAP-LPFG, an average grating sensitivity of 0.99×10^{6} pm/RIU (refractive index unit) for external refractive indices ranging from 1.36 to 1.45 has been demonstrated. Further, we have shown a very high sensitivity of 0.96 nm/V% for adulteration of kerosene in petrol up to 10 % adulteration which is significantly high compared to previously published values. These gratings offer the advantages of lower cost and greater potential for fuel adulteration detection, fuel blending and identification of hydrocarbons in pipelines. With modern grating demodulation systems, they can be employed for on-site road measurements.

CHAPTER 5

STUDIES ON EFFECT OF GAMMA RADIATION ON OPTICAL FIBERS AND FIBER GRATINGS

5.1 Introduction

Nuclear and Defense industry shows a growing interest for the possibilities offered by the fiber optic technology for both data communications and sensing applications. Optical fiber along with other optoelectronic components are of great interest for remote control and monitoring associated to nuclear environments, nuclear reactors, particle accelerators, space applications, fusion installations and management of nuclear waste sites. The light weight, immunity to EMI and large information capacity of glass optical fibers fit the mobile requirements of military. On the other hand, the possibility of distributed and point sensing for hazardous locations, possibility to carry multiplexed signals, availability to be incorporated in the structure give them an edge for nuclear applications. The interaction of ionizing radiation with optical fibers leads to a variety of physical processes as mentioned below.

(a) Radiation induced attenuation (RIA) i.e. increase in fiber attenuation due to induced optical absorption.

The part of the results reported in this chapter has been published in the following papers: (a) Sanjay Kher, Smita Chaubey, Raman Kashyap, S. M. Oak, “Turnaround-Point long period fiber gratings (TAP-LPFG) as high radiation dose sensors”, IEEE-Photonics Tech. Letters, Vol. 24, issue 9, 2012, pp. 742-744. (b) Sanjay Kher, Smita Chaubey, S.M.Oak, A. Gusarov, “Measurement of gamma-radiation induced refractive index changes in B/Ge doped fiber using LPFGs,” IEEE-Photonics Technology Letters, Vol. 25, issue 21, Nov. 1, 2013, pp. 2070-2073.

(b) Radiation induced luminescence (RIL) i.e. increase and generation of luminescence scattering especially Cerenkov light.

(c) Thermo luminescence (TLS).

(d) Optically stimulated luminescence (OSL) and

(e) Induced change of refractive index (RI).

The RIA effect distorts the transmitted spectra as in some spectral bands the attenuation becomes radiation dependent. On the other hand the RIL effect deteriorates the signal-to-noise ratio (SNR) because an additional signal is superimposed on the signal to be measured.

We have done extensive measurements for development of gamma dose sensors which are described in Section 5.3.2. Long period gratings were written in various commercially available single mode fibers using CO_2 laser and arc-induced technique. We report our discovery of Boron as a critical dopant for high sensitivity gamma dose sensing applications in Section 5.3.3. We also report our prediction of a physical mechanism for RI changes due to gamma radiation in Section 5.4. Optimally designed devices were packaged for field applications and are reported in Section 5.5.

5.1.1 The Radiation induced attenuation (RIA) effect

Radiations generate, at the microscopic scale, point defects in silica matrix network through ionization or knock-on processes. These point defects, or color centers induce the appearance of new energy levels located inside the band gap of the silica glass (α-SiO_2). As a consequence, the defect containing glass absorbs some part of transmitted signal leading, at the macroscopic scale, to an increase in attenuation of the fiber waveguide. The increase in absorption is called Radiation induced attenuation (RIA). The RIA is expressed by [**37**]

$$RIA(\lambda,t) = -\frac{10}{L}\frac{P(\lambda,t)}{P(\lambda,t_0)} \qquad (5.1)$$

where, λ is the wavelength, t is the irradiation time, L is the length of the fiber, P is the optical power in W and t_o is the irradiation start time.

The amplitude and time kinetics of these macroscopic changes depend on the nature, concentration and stability of point defects. Therefore, the radiation response of the fibers depends on composition of the silica glass (choice of core and cladding dopants, impurity levels, stoichiometry), physical properties of the glass (fictive temperature, strain) and strongly on fabrication parameters (preform deposition and drawing processes). Since, these intrinsic optical fiber parameters are not disclosed by manufacturers, the quantitative influence of each of these parameters is still an open problem.

The majority of nuclear decays are accompanied by emission of gamma rays. Hence the effect of gamma rays on various materials has gained prime importance. The RIA in the near-IR region is small compared to UV-visible region. The absorption peaks responsible for RIA in UV-visible regions are associated with the formation of color centers such as non-bridging oxygen hole centers (NBHOC) with a band at 630 nm, oxygen vacancies (E' centers) with a band at 215 nm, point defects related to defects in silica like chlorine with a band around 330 nm, germanium related defects with a band at 475 nm and many others. In near-IR regions, for high-OH fibers, the excitation of the OH vibration band is responsible. For low-OH fibers, UV-visible absorption band tails, the presence of color centers in upper end of near-IR (>1800 nm) and self trapped holes with a band at 1800 nm are believed to be responsible for RIA in near-IR regions. It is now possible to produce extremely pure synthetic silica with both low OH and Cl ion contents. Such fibers are nuclear radiation resistant and can be used for fibroscopy. Recently, hollow core Photonic band gap (PBG) fibers have been shown to be resistant to radiation dose up to 10 GGy **[83]**.

5.1.2 Nuclear environment and possible applications

The damaging effect of radiation on materials and biological systems has been a subject of intense investigation to find out the nature and extent of damage. Most living tissues are susceptible to damage under low dose of radiation (below 50 Gy). During full course of radiotherapy treatment, a patient will typically receive between 20-40 Gy in 15-20 sittings. During fission reactor maintenance, total dose of about 10 kGy is expected while for spent fuel manipulation, the expected dose is 100 kGy to 1 MGy. The severe reactor accidents may provide the dose of 100 kGy during intervention period while in core-containment buildings, the accidental dose exceeds 1.5 MGy. During the plasma burn in the International Thermonuclear Experimnetal Reactor (ITER), the diagnostic systems installed inside the vacuum has to withstand typical total gamma doses approaching 1 GGy (i.e. 10^{9} Gy). During shutdown period of such reactors, replacement of heavy in-vessel components will have to be performed in environment of typical total gamma dose of 1 MGy.

5.2 Real-time fiber optic radiation dosimeters for monitoring around thermonuclear reactors

Optical fibers offer a unique capability for monitoring radiation effects remotely in materials and tissues under a variety of environmental conditions that would preclude or limit the use of other dosimetry techniques. The sensor may be located several hundred meters from control electronics and in some case may be multiplexed so as to permit a single control unit to monitor a large number of fiber dosimeters. The ideal radiation sensing probe should be electrically passive, easy to calibrate and selectively radiation sensitive with high survivability in harsh nuclear environment. Some methods are suited primarily to very high-dose environment and others are appropriate for low doses. In order to measure the entire range of doses that may be encountered, roughly from 10^{-4} Gy for personal dosimetry to 10^{8} Gy for reactor dosimtery, more than one method may be required. This chapter will describe several different approaches to optical fiber dosimtery with a special emphasis on design, development and device fabrication based on long period fiber grating by the author for high-level dose measurement.

5.2.1 Dosimeter based on RIA

When a length of fiber is exposed to a radiation field, the radiation-induced darkening in the core of the fiber causes the optical transmission to be reduced. A calibration curve must be obtained for a particular fiber by measuring the change in the optical transmission at a particular wavelength, or several wavelengths as a function of dose. The fiber dosimeter should have following characteristics:

1. Low or moderate loss at expected dose level to assure reasonable SNR.
2. Darkening that is independent of dose rate and linear response over expected dose range.
3. A low fade rate and energy independent darkening response.

The fiber containing oxides of Barium, Zinc and Boron was produced and successfully tested in dose range of 0.09 Gy to 100 Gy, for the first time, in 1977 in Navigation Technology Satellite (NTS-2) which was launched in June 1977. The addition of a small amount of Phosphorous (P) to the fiber core results in enhanced attenuation during steady state irradiation while the High Ge doped fiber has an intense transient absorption for pulsed irradiation. The darkening is more pronounced at shorter wavelengths and falls of considerably beyond 800 nm. In practice, the determination of absorbed dose is complicated due to fading effect originating from thermally unstable defects and traps which anneal at room temperature. Therefore, the complex annealing process must be understood and accounted for accurate dose measurements. Choice of wavelength, core/clad composition and length of fiber can be optimized for sensitivity enhancement for a particular dose range.

A silica fiber containing 60 % PbO by weight has been developed for use in radiation therapy [**83**]. Recently, TiO_2/ GeO_2 doped single mode fibers have been found to be very suitable for dose measurements at 1310 nm wavelength for dose range of 0-10 Gy **[37]**. Plastic dosimeters combine acceptable radiation sensitivities with low recovery. For example, red-dyed PMMA sheet dosimeters type red 4304 from Harwell Dosimeters Ltd., can be used in the range of 5-50 kGy. However, they are not useful for real time dose measurements. The PMMA fibers developed by Optoelectronic manufacturing Corp. recently showed a high potential for dose measurements from 100 Gy to 30 kGy. They have a threshold in terms of dose and it was proved that high dose irradiation not only induces separation of side chains of PMMA molecule but also affect the main polymer structure [**84**]. A 20 mm length of this fiber is capable of measuring a dose of 1 Gy with a precision of about 2 %. By designing core/clad with OH ion control and monitoring absorption near 1390 nm, a dosimeter in the dose range of 2-6 MGy has been demonstrated [**86**].

5.2.2 Luminescence fiber dosimetry

Practically all glasses yield luminescence when exposed to ionizing radiation (radio-luminescence) due to the presence of native impurities or defects. In some cases, radiation-induced defects are also luminescent and formation of these centers can be monitored as a function of dose. The luminescence spectrum of a pure silica core fiber exposed to unfiltered 40 kV X-rays exhibited two distinct visible luminescence bands centered at 450 and 650 nm. The dose response curve after correction of transmission losses, shows a linear response up to 350 kGy. The real time luminescence signal from Al_2O_3 single crystal fibers were monitored during simultaneous irradiation and optical stimulation. Both radioluminescence (RL) and OSL signals were studied [**85**]. The steady state RL and OSL levels were found to be dependent on dose rate. It was shown that the total integrated dose can be determined by correcting real time OSL signal for depletion caused by laser stimulation pulse.

Since the darkening has less effect on long wavelength emission, dosimeters have been made that utilize the red or near-IR emission from rare earths. Pr^{3+} doped phosphor, attached to the end of 10 m long silica fiber was successfully tested to observe luminescence bands around 700, 765, 900 nm. The dose response curve shows that longest wavelength is least affected by darkening effect. A Eu^{3+} doped fiber was used to monitor dose up to 5 kGy by observing strong emission peak at 700 nm **[84]**.

The incorporation of rare earth ions greatly increases the darkening sensitivity. For precise dosimetric measurements, it is desirable to correct for darkening effects. The Cerenkov radiation also causes significant problems for real time dosimetry based on luminescence. Cerenkov radiation is generated in glass when the speed of incident radiation photon (~1 Mev for glasses) generated electrons in the medium exceeds the speed of light in the medium. This emission is broad-band, strongest at short wavelengths and falls off rapidly with increase in wavelength. It is also dependent upon angle of incidence of external radiation. These complicating factors and issues have not been addressed yet.

5.2.3 Thermo luminescent (TL) fiber dosimeters

This approach utilizes a TL radiation dosimeter phosphor attached to the end of a multi-mode fiber optic cable. The phosphor is heated by thermal diffusion from a near IR-laser which stimulates thermo luminescence from the sensor probe. Optically transparent glass material containing ZnS nano crystals and Cu^{1+} ions are very suitable for efficient utilization of laser energy. The local heating stimulates TL emission from metastable traps populated by exposure to gamma radiation **[84]**. A key feature of this sensor is the ability to anneal glass optically so that repeated measurements can be performed. These materials exhibit outstanding dosimetry characteristics, including a low fade rate, a linear response of over five orders of magnitude, an energy response for gamma rays and sensitivity similar to commercial TLD 100.

5.2.4 Optically stimulated (OSL) fiber dosimeter

The physics of optically stimulated (OSL) fiber dosimeter is similar to TLD except that the recombination of trapped charges is initiated by light rather than by heat. The most common materials that exhibit OSL are the family of alkaline earth sulfides such as MgS, BaS doped with activator/co-activator ion pairs like Sm and Ce or Sm. In this series Eu.Al_2O_3:C is another useful material. When materials such as these are exposed to ionizing radiation, free electrons migrate to metastable trapping centers where they remain trapped for extended periods. Near-IR light is then used to stimulate electron-hole recombination which results in visible luminescence and is used for dose measurement. A dosimeter based on an MgS:Sm, Ce phosphor has been described with a linear dose response from 8×10^{-5} to 4×10^{-2} Gy. The OSL technique has advantage in radiotherapy compared to TLD where heating of fiber tip is unacceptable.

A new optically transparent OSL glass doped with few ppm of Cu^+ ions has been reported by NRL, USA. Exposure to gamma radiation causes ionization of Cu^+ ions to produce Cu^{2+} and a free electron. The electron becomes trapped within glass at an electron deficient defect center. The trapped electrons can be simulated to recombine with Cu^{2+} using near-IR light. The recombination yields excited Cu^+ which decays radiatively with blue-green emission. A dosimeter is developed using this material for dose monitoring to patients undergoing radiotherapy in the range of 0.01 Gy-10 Gy **[84, 86]**.

5.2.5 Scintillation fiber optic dosimeter systems

Scintillating materials have been used for decades to detect ionizing radiation dose rate. Ionizing radiation will excite atoms and molecules to higher energy levels, which de-excite via radiative transitions. A CsI (Tl) crystal scintillator is mounted at the end of a long multi-mode fiber. Photon counters are used to detect weak luminescence signals at other end. Such probes show good linearity from 300 μGy/h to 3 Gy/h with a 2-sigma accuracy of 3.8 % in a response time of 1 μs.

5.3 Fiber Gratings for gamma dose sensing applications: Introduction, experimental results and analysis

It has been reported that doped fibers that show linear response with radiation dose are not useful for applications above a dose of 10 kGy due to attenuation saturation in the whole range of 650 - 1700 nm. Therefore, alternative techniques based on radiation induced refractive index change had been extensively investigated for higher dose values of 100 kGy - 10 MGy [**87**].

5.3.1 FBGs as dose sensors

Since fiber Bragg gratings (FBGs) have a great potential for use in nuclear environment and its technology is also fully developed, it was natural to study FBGs for measurement of high radiation dose. Most FBGs written in intrinsically photosensitive fibers show relatively low radiation sensitivity due to the effect that FBG writing using UV light eliminates the precursors of radiation-induced color centers. Usual experimental data show a small induced Bragg peak shift (BPS) towards longer wavelength. Short wavelength BPS has been reported on type IIa gratings, written in highly Ge doped or B/Ge doped fibers **[88]**. Recently, short-wavelength shift has also been reported for type I gratings written in intrinsically photosensitive fiber also **[89]**. The short wavelength shift of type I FBG in high Ge fiber (8 mole % GeO_2 and no Boron) indicated that the fiber properties play an important role in radiation sensitivity of FBGs. The mechanism of such effect was attributed to two different types of radiation induced defects. One type was responsible for refractive index increase while creation of defects of other type results in index decrease. However the exact mechanism of radiation effects on FBGs has not been clearly known till date. These studies also proved that the link between ionizing radiation and photosensitivity is not direct and hence more systematic studies are necessary to predict gamma induced index changes.

5.3.2 Long period fibre gratings (LPFGs) as gamma dose sensors

There exist very few publications about irradiation tests of long period fibre gratings (LPFGs). The authors of Ref. **[38]** found no clear shift with LPFGs written by UV laser in Ge-doped fibers after a dose value up to 70 kGy. The authors of Ref. [**39**] found no radiation induced spectral changes up to a dose of 0.5 MGy in LPFGs written by arc discharge technique in pure silica core fibers. Recently Henchel et al. [**40**] found high radiation sensitivity in Chiral LPFGs, written in some doped fibers. They studied the gratings up to a dose of 100 kGy but neither the fiber composition nor resonance mode orders were identified.

We have conducted systematic investigation of LPFGs written by CO_2 laser based technique and arc-induced technique. The dopants and fiber composition were clearly identified. Both real time and off line irradiation tests were conducted to identify the useful core dopants. Further, to obtain distinctly high radiation sensitivity of LPFGs, specialty Turn-around LPFGS (TAP-LPFGs) were fabricated and tested. These studies have led to development of TAP-LPFGs having highest ever gamma sensitivity of 35 nm/6 kGy **[43]**. The dose sensors have been fully packaged for dose sensing applications in reactors and accelerators.

We describe here the design, modeling and performance evaluation of TAP-LPFGs.We have designed and fabricated TAP-LPFGs in B/Ge doped commercial fiber (Fiber Core UK, PS 980) using CO_2 laser. Theoretical simulation of phase matching curve for the fiber helped in initial prediction of grating period (205-210 μm) to obtain TAP near 1.5 micron wavelength. This curve was earlier shown in Fig. 2.10 and is re-drawn in Fig. 5.1 for its special importance for gamma dose sensing applications. Good qualities LPFGs of about 20 mm length with near TAP or exact TAP configuration were fabricated. They were made in about 50 cm long sensitive fiber, fused with long nuclear resistant fiber and were mounted on a metal plate and kept inside gamma chamber for a specified duration. The gamma chamber facility provides a fixed dose of 1.3 kGy per hour. Typically, the spectral data were recorded off-line within 0.5 - 3 hours of the sample removal from gamma chamber. These experiments were repeated after few days with similar LPFG devices. The results were found to have similar trends with no major discrepancies. The error in resonance dip wavelength shift (DWS) measurement was lower than 0.8 nm for all cladding modes. Fig. 5.1 shows the calculated phase matching curves (PMC) for fundamental core mode and LP_{01} to LP_{013} cladding modes.

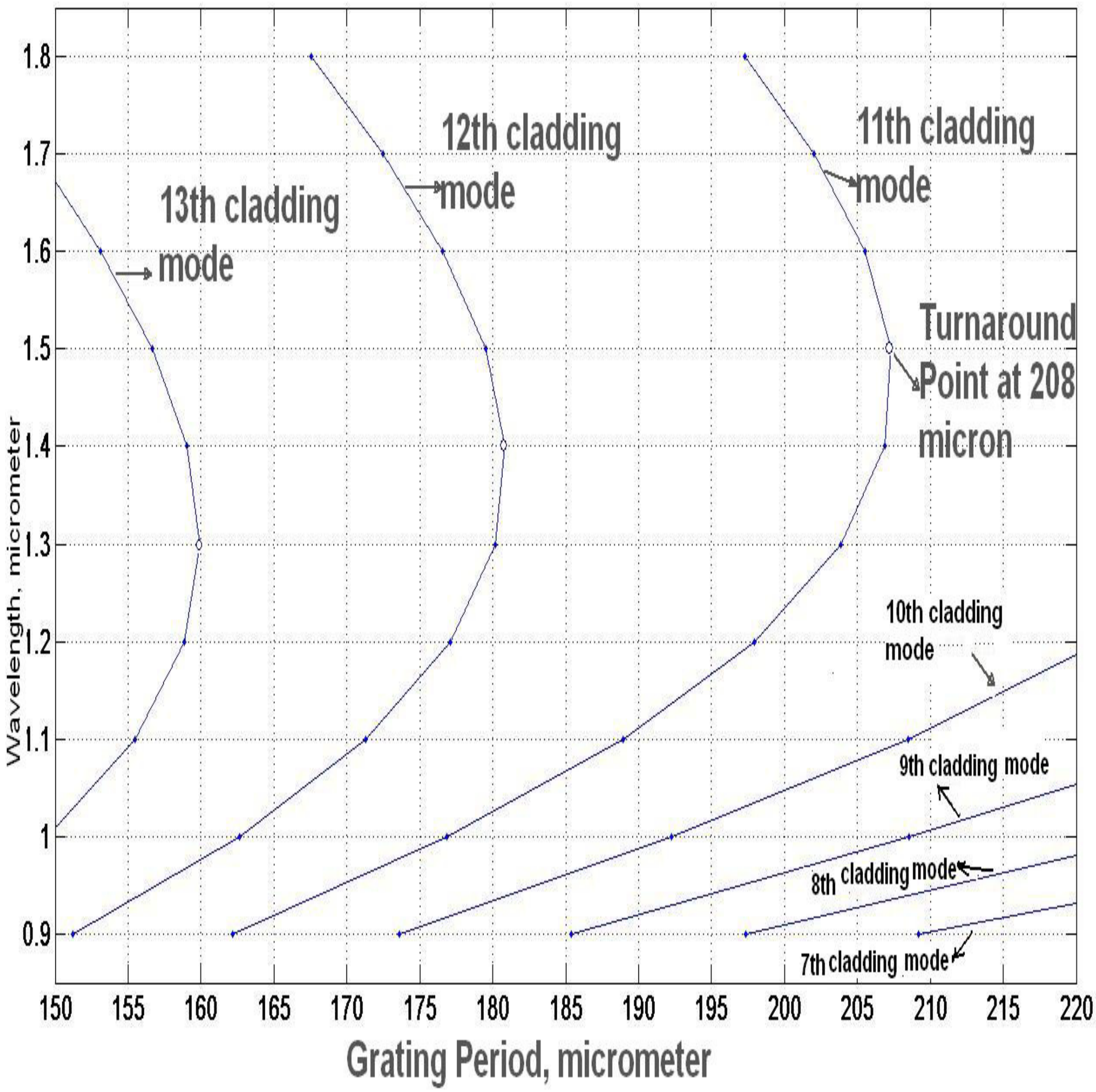

Fig. 5.1. Phase matching curve for different cladding modes of LPFG in B/Ge codoped fiber. TAP point is at cladding mode 208 µm period for 11th cladding mode

Fig. 5.2 and 5.3 show the spectral shifts due to gamma dose in near TAP-LPFG written by CO_2 laser.

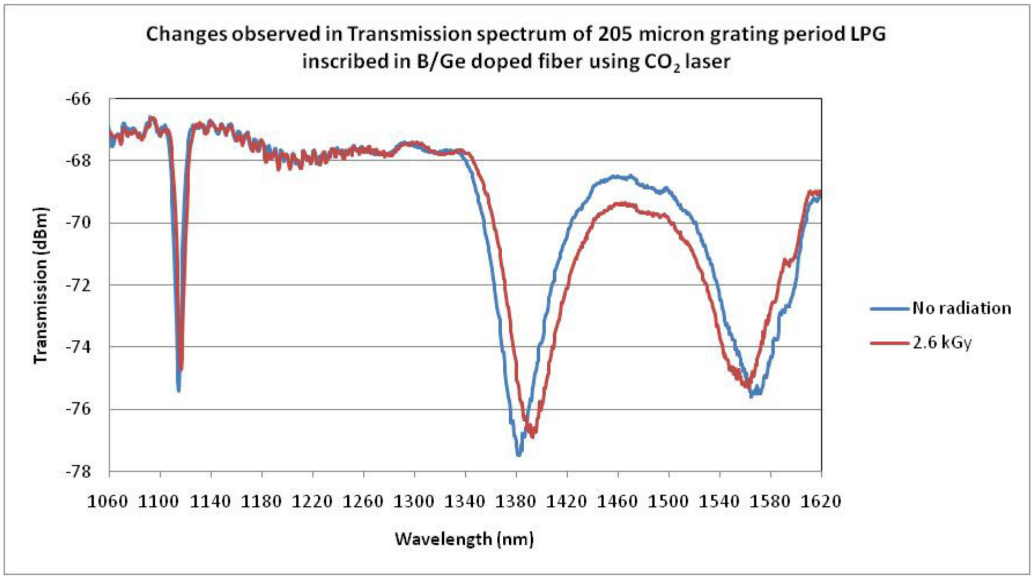

Fig. 5.2. Effect of gamma dose (2.6 kGy) on near TAP-LPFG (grating period: 205 µm)

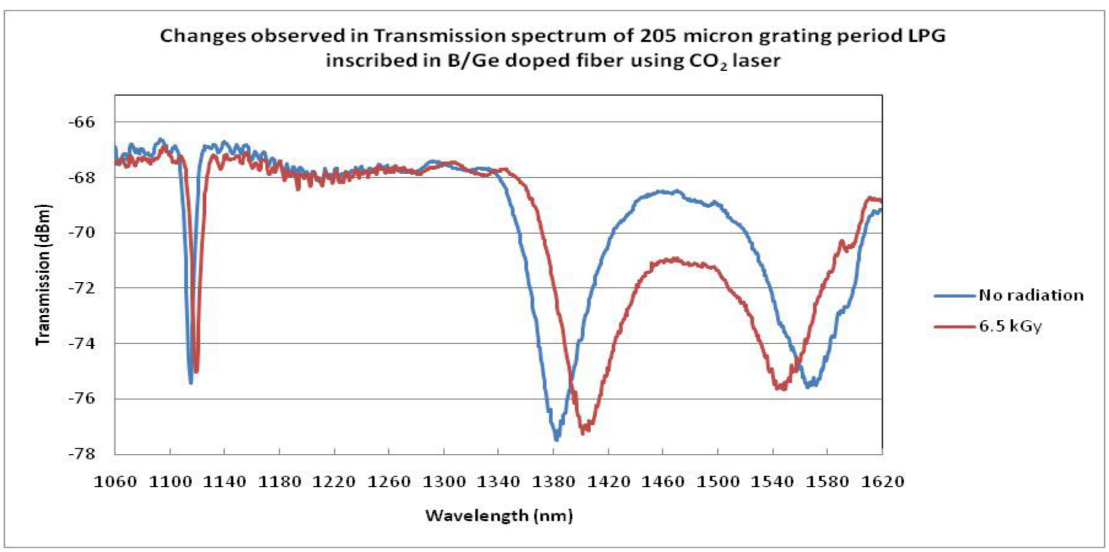

Fig. 5.3. Effect of gamma dose (6.5 kGy) on near TAP-LPFG spectrum (grating period: 205 µm)

Fig. 5.4 and 5.5 show the effect of irradiation for a near TAP-LPFG with grating period 206 micron for dose values 6 kGy and 65 kGy.

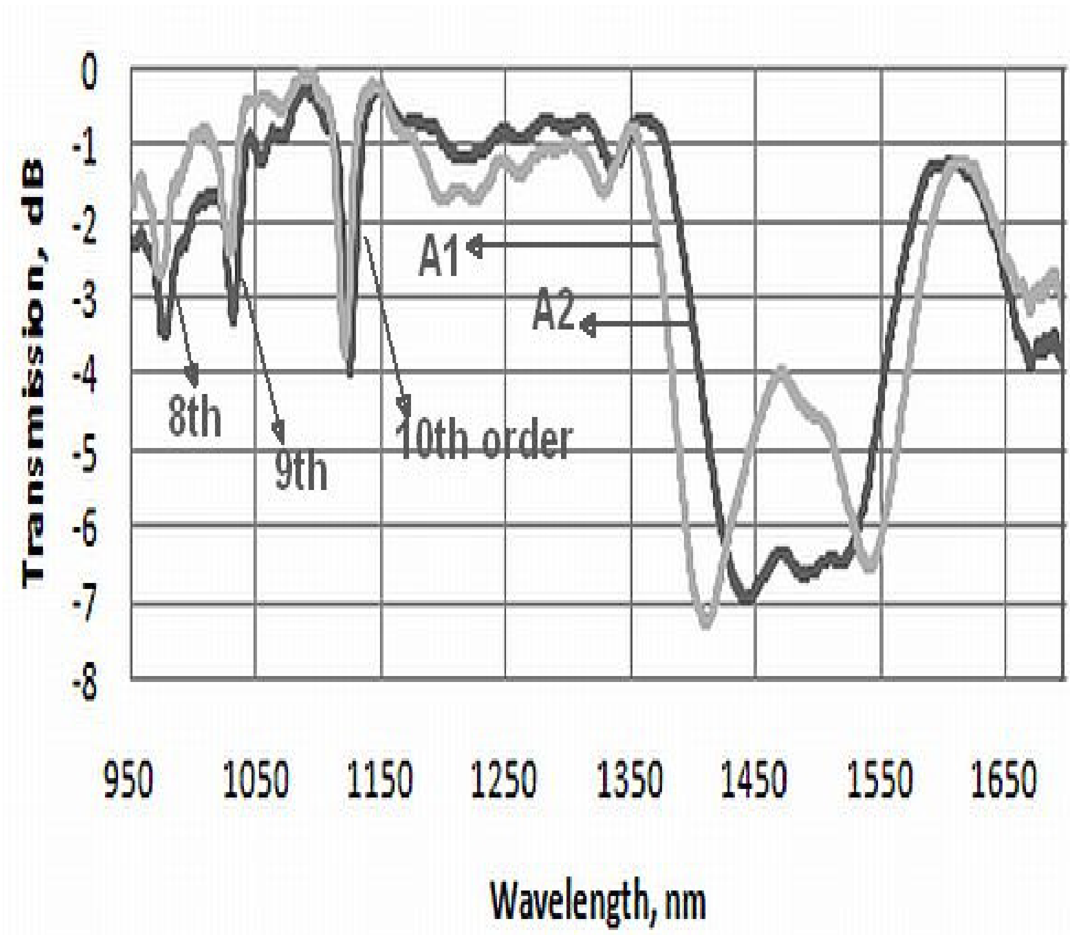

Fig. 5.4. Effect of irradiation for a near TAP-LPFG: A1 shows transmission spectrum of LPFG of period 206 μm in B/Ge codoped fiber; Dual resonance dip feature of near TAP-LPFG can be clearly seen. A2 shows LPFG spectrum after a dose of 6 kGy. The dual resonance dips come closer and nearly merge

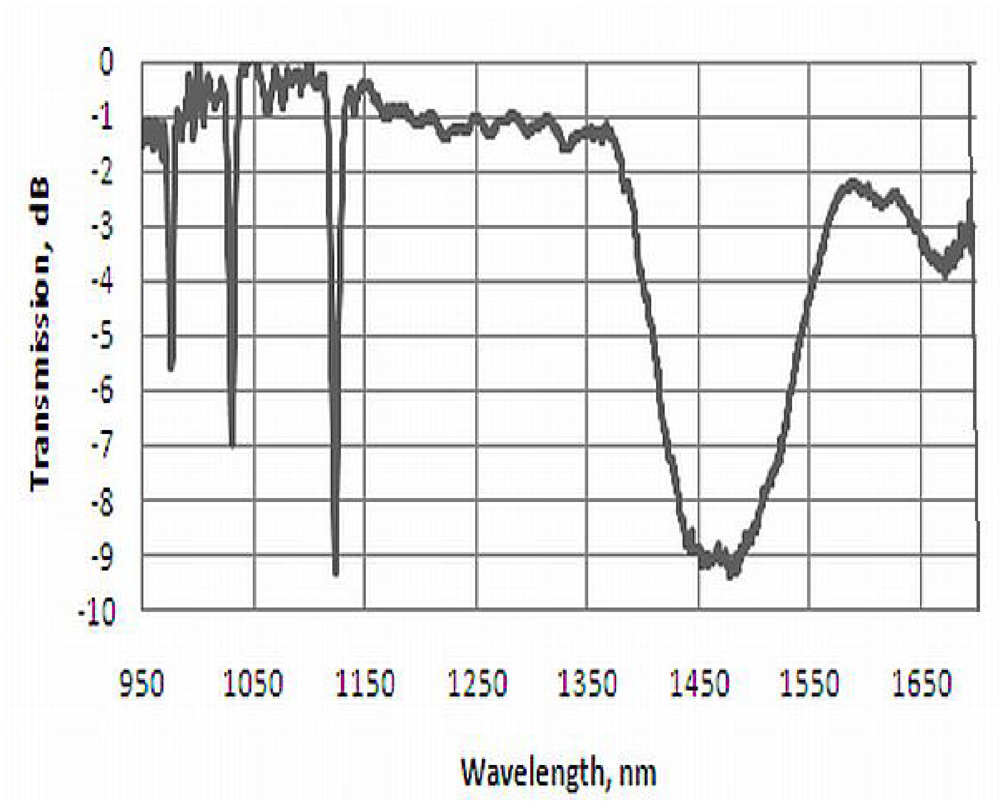

Fig. 5.5. Effect of irradiation for a near TAP-LPFG. Changes in LPFG spectrum after a dose of 65 kGy is seen. The dual resonance feature is lost and a broad dip representing exact TAP is observed

If the grating is designed for exact TAP-LPFG, we observe that the effect of irradiation results in only amplitude changes in TAP (11^{th} mode order) spectrum as per the properties of such gratings. Fig. 5.6 shows the changes in exact TAP-LPFG. These gratings are not useful for designing wavelength encoded devices but drastic amplitude changes clearly indicate the effect of gamma dose on fiber gratings. Table 5.1 summarizes the experimentally obtained wavelength shifts with different gamma radiation dose for transmission resonance dips corresponding to different cladding mode orders for near TAP-LPFG.

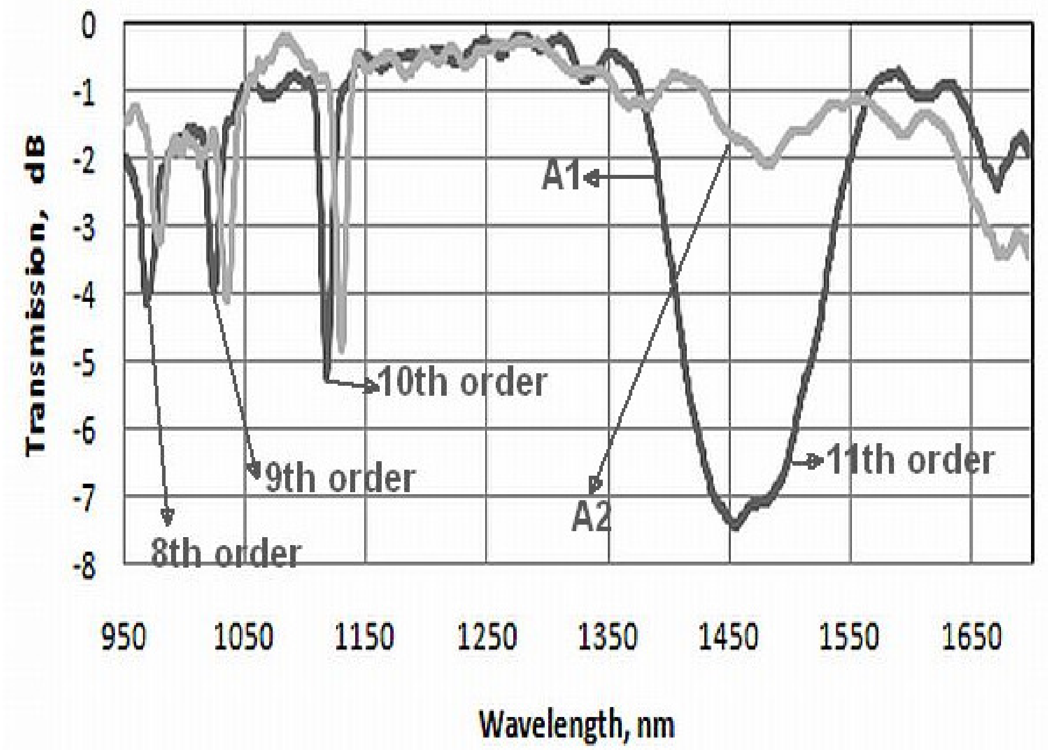

Fig. 5.6. Changes in exact TAP-LPFG. A1 shows the transmission spectrum of exact TAP LPFG in pristine fiber. A2 shows the transmission spectrum of exact TAP LPFG after 87 kGy gamma radiation exposure

The results reveal remarkably high senstivity for TAP mode and high sensivity for other higher order cladding modes. The tenth order cladding mode shows a resoance dip shift of 14.75 nm for 65 kGy dose which is highest reported ever for any type of LPFG [**43**]. Since, turning points determine the condition of maximum senstivity, our near TAP-LPFG at 11th order cladding modes exhibit very high sesnitivity (80 nm/ 65 kGy) for radiation.

The off-line studies with LPFGs written in standard smf-28 fiber, high Ge doped fibers and B/Ge codoped fibers indicated critical role of Boron in the core for achieving high sensitivity. It was also observed that grating based sensors have not been reported anywhere for dose range 100 kGy to 1 MGy. Emerging sites such as fusion reactors,

TABLE 5.1: WAVELENGTH SHIFT INDUCED BY GAMMA RADIATION EXPOSURE OF NEAR TAP-LPFG WRITTEN BY CO_2 LASER IN B/GE CO-DOPED FIBER

S.No.	Grating Period (μm)	Mode order	Dose (kGy)	Wavelength shift (nm)
1.	206	11	6	35,-38 (dual peak)
	206	10	6	3.75
	206	9	6	3
	206	8	6	1.5
2.	206	11	65	81,-90 (dual peak)
	206	10	65	14.75
	206	9	65	9.75
	206	8	65	9.75

reprocessing plants, ITER and super LHC pose a serious challenge for remote dose detectors for higher dose regime near and above 1 MGy. This is the reason why we tried to find whether long period fiber gratings can be used for measurement of dose levels above 10^5 Gy (i.e. 100 kGy). Our previous studies showed that CO_2 written long period gratings in Boron doped fiber could be a strong candidate for dose level up to 100 kGy **[43]**. Therefore, on-line studies were performed with LPFGs written by CO_2 laser and arc technique. Our present unique study based on in-situ radiation dose measurements suggest that long period gratings in Boron doped fiber can indeed be used for dose level up to 1 MGy. These studies lead to device development for high level dose applications.

5.3.3 Real time studies for high level gamma-induced effects on LPFG

In order to develop sensitive gratings suitable for very high level gamma dose measurement in the range of 10 kGy - 1 MGy, we have experimentally studied in-situ, the effect of high gamma dose on LPFG parameters such as resonance dip wavelength shifts, amplitude and width of bands, room temperature annealing and effect of mode orders. Gratings written in commercially available fibers with different dopants were also studied to get an insight into the role of fiber composition.

In order to search suitable fiber for high level dosimetry, we selected three single mode fibers with different compositions. B/Ge doped fiber (PS-980 of Fiber Core, UK) was selected due to its high photosensitivity. Photo-sensitive high Ge doped fiber SMG 652-PH (Fiber Logix, high Ge in core, Fluorine in cladding) was selected due to higher level of known defects and well known gamma induced effects in Bragg gratings written in such fibers. Radiation hard Germanosilicate fiber SMG 652 (Fiber Logix) was chosen for reference. It may be noted that other core dopants in Fiber Logix fibers are not known except the fact that they do not contain Boron. The gratings in these fibers are designated as P1, P2, F1 and F2. The fiber composition of gratings P1 and P2 is same but the grating period is 206 μm and 400 μm respectively. To study the effect of mode order on gamma sensitivity, we have written gratings P1 and P2 with period of 400 μm and 206 μm. It has been known from earlier simulation studies that coupled mode orders 3, 4 and 5 in 400 μm fiber and 10^{th} mode (highest order non-TAP cladding mode) is coupled with high efficiency in PS-980 fiber.

Table 5.2 shows the wavelength shifts observed corresponding to 65kGy gamma radiation exposure of LPFGs in different fibers for resonance loss band in the wavelength range 950-1500nm. The TAP LPFG (206 μm) P1 was relaxed at room temperature for few days to see the subtle effects of refractive index change due to radiation. This grating was then reloaded in gamma chamber and monitored for dose up to 1 MGy.

Table 5.2 also depicts that the highest wavelength shifts were obtained with LPFG P1 in B/Ge doped fiber. Table 5.1 also confirms that the gamma radiation sensitivity is more than the sensitivity of earlier reported UV written LPFGs in high Ge doped fibers. In order to investigate high level dose effects, we further exposed the LPFG in B-Ge doped fiber up to 1MGy dose levels over a period of 35 days.

It has been observed that there is a monotonous increase in resonance wavelength of the grating P1 upto total dose of 1 MGy [Fig. 5.7(a)]. It is also seen from Fig 5.7(a) that resonance peak strength (grating modulation) remains nearly constant (variation between -74.07 dBm to -74.44 dBm). Also, no remarkable changes in the spectral width of resonances were observed in spite of large dip wavelength shifts. Results up to 65 kGy in CO_2 written B-Ge fiber have already been reported for B-Ge doped fiber.

Table 5.2 GAMMA RADIATION EXPOSURE EFFECT OF 65/70 kGY DOSE ON DIFFERENT FIBER LPFGS AND MODE ORDER DEPENDENCE

No.	Fiber		Grating period [μm]	Typical mode order coupled cladding mode)	Resonance wavelength [nm]	Wavelength shift [nm]
	Manufacturer	Code				
1.	Fibercore	PS980 (P1)	205	10	1115	9.8
2.	Fibercore	PS980 (P2)	400	3	1200	8.5
3.	Fiberlogix	SM652-PH (F1)	400	6	1581	5
4.	Fiberlogix	SM652 (F2)	400	6	1522	3

For LPFGs, the sensitivity governing expression for radiation induced effects is given by the relation [**39, 43, 86, and 90**]

$$\Delta\lambda_D^i = \lambda_D^i \left(\frac{\Delta n_{co,eff} - \Delta n_{cl,eff}^i}{n_{co,eff} - n_{cl,eff}^i} + \frac{\Delta\Lambda}{\Lambda} \right) \quad (5.2)$$

where,

$\Delta\lambda_D^i$ is radiation induced wavelength shift in dip wavelength at a specific dose,

λ_D^i is dip wavelength of LPG for i^{th} order cladding mode,

Λ is grating period , $\Delta\Lambda$ is the change in grating period at a specific dose,

$\Delta n_{co,eff}$ is change in effective refractive index of core due to gamma dose,

$\Delta n^{i}_{cl,eff}$ is change in effective refractive index of cladding due to gamma dose,

$n_{co,eff}$ and $n^{i}_{cl,eff}$ are effective refractive indices of core and cladding respectively.

Comparison of gamma induced wavelength shift in F1, F2 and P1 gratings clearly shows that Boron doping plays a significant role in increasing the sensitivity. Also the results of P1 and P2 LPFGs show that even lower order coupled cladding modes show significant radiation sensitivty. This study has been continued further to investigate the effects of dose upto 1MGy.

The dose dependence has a power law dependence on wavelength shift in the radiation range 100kGy - 1000kGy as shown in Fig. 5.7. It is also observed that dip wavelength shift upto 1MGy does not saturate and there is further scope of even higher dose studies. LPFGs F1 and F2 show remarkably lower sensitivy and indicate the important role of fiber composition. It is known that F2 does not have Boron, it has high Germanium and other unknown dopants. Gamma induced wavelength shift in LPFG written in B/Ge codoped fiber as a function of dose is plotted in Fig. 5.7(b). It can be seen that induced shift with dose can be fitted as a simple power law with an exponent of 0.442 **[90]**. This is consistent with the observations of other workers. This is believed to be the first study of radiation sensitive LPFG useful for a dose level of 1MGy **[90]**. Our results are contrary to observations of Vasilev et al. **[38]** who studied CO_2 written gratings in nitrogen doped fiber but found no observable resonance shifts due to gamma radiation.

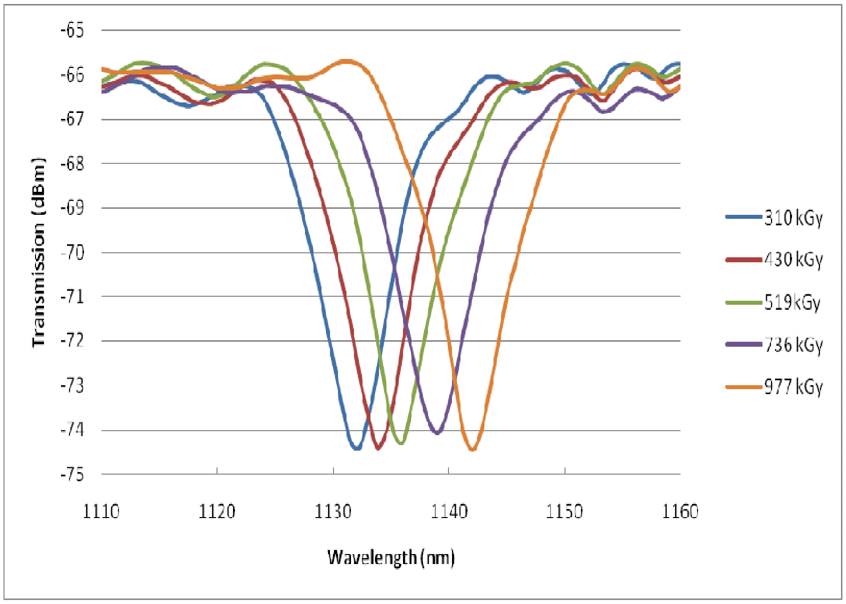

Fig. 5.7 (a)

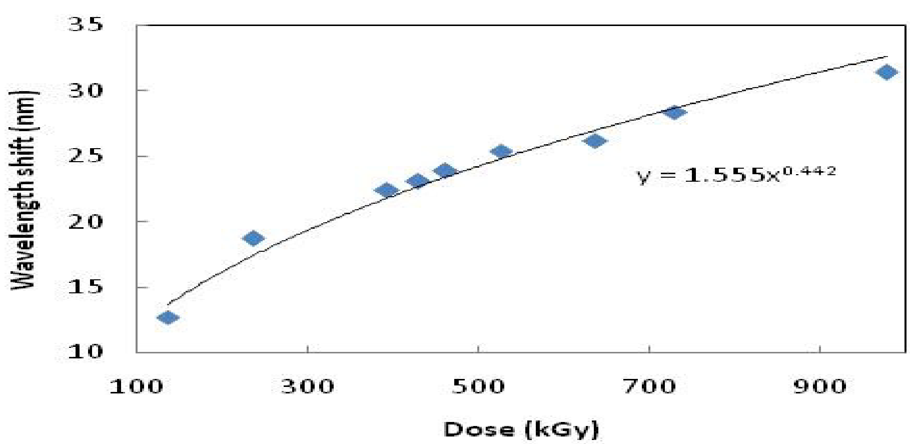

Fig. 5.7 (b)

Fig. 5.7. (a) In situ transmission spectra of P1 fiber LPFG : Wavelength shift observed in 10 th order cladding mode resonance when exposed to high dose of gamma radiation. (b) Gamma induced wavelength shift as a function of dose and the fit of the experimental data with power law

It is also observed that room temperature annealing of P1 grating for 72 hours after a dose of 237 kGy, does not change the radiation induced resonance dip wavelength shift (DWS< 8 %, Fig. 5.8). There are spectral changes in full transmission spectrum but the mode strength and dip wavelength remain nearly constant and the effect seems to be near permanent in LPFGs written in B/Ge codoped fiber.

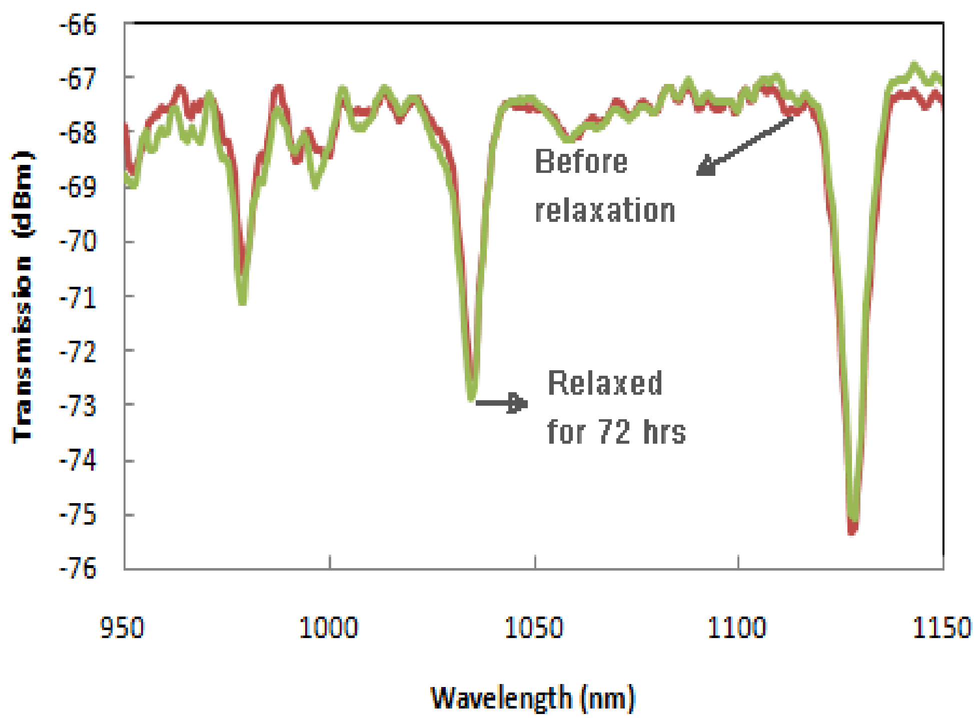

Fig. 5.8. Room temperature annealing effect on transmission spectrum of LPFG in P1 fiber after 237 kGy gamma radiation exposure

These observations were also confirmed for LPFGs written in B/Ge co-doped fibers relaxed for 67 hours after a dose of 1.54 MGy (Fig. 5.9).

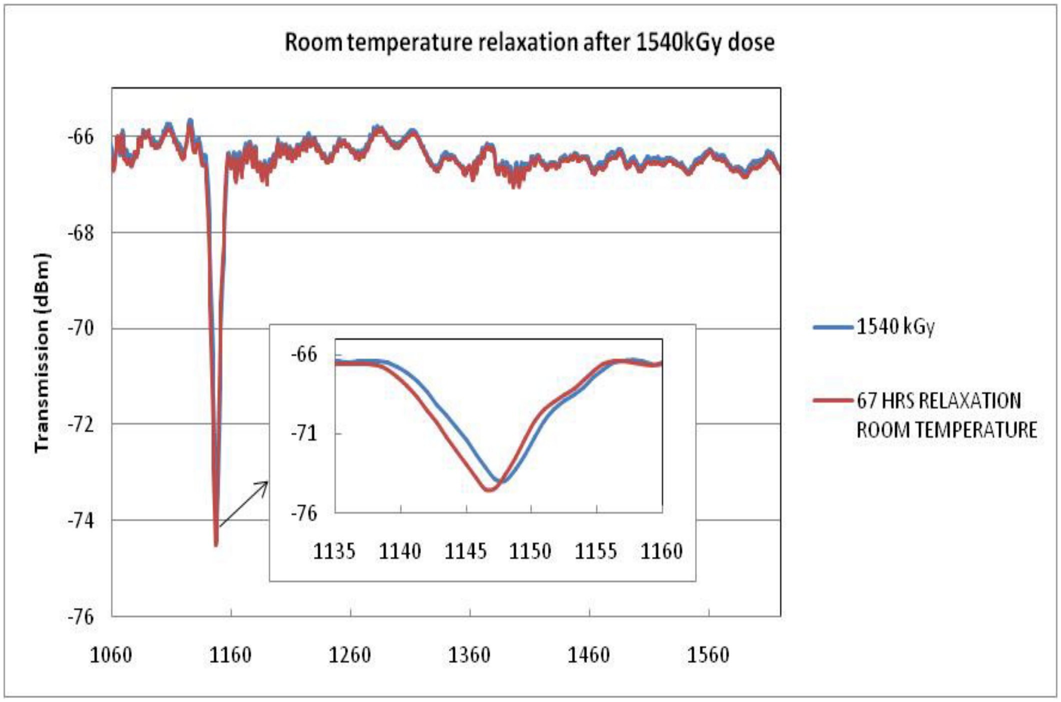

Fig. 5.9. Room temperature relaxation effect on 10th cladding mode after a dose of 1.54 MGy

5.4 Mechanism of gamma induced index change and role of fiber/grating parameters: experiments, calculations, results and prediction

Gamma-induced effects in Type I FBGs have been studied in fibers of different composition. Usually, experimental data show an induced wavelength shift towards longer wavelength. This indicates radiation induced increase in effective index of the fiber. However, recent report on high level gamma irradiation on type I FBGs written in high Ge doped fibers indicate short wavelength shift implying radiation induced decrease in effective index of the fiber **[89]**. The effect was explained on the basis of generation of different types of defects by ionizing radiation. One type is responsible for index increase while the other type could decrease the index. Similar situation exists for type IIa FBGs. The reasons were attributed to variation in fiber properties. However, no conclusive evidence was found to provide a mechanism with regard to gamma induced index change of the fiber using FBGs. Direct irradiation of germanosilicate fibers indicate structural transformation of glass structure (compaction/densification) and/or formation of permanent electric dipoles in the glass as a possible mechanism of index change in the fiber **[91]**. These studies proved that index modulation regimes are intrinsic to the glass matrix but no consensus seems to exist for the mechanism of index change.

Our systematic irradiation studies on LPFGs written in B/Ge doped fibers, procured from various sources, provide conclusive evidence of polarizability changes in the core network as a dominant mechanism for refractive index change (Section 5.4.3). The study also establishes that core compaction/density change (change in grating period) does not play any significant role in index change in B/Ge co-doped fiber **[90]**.

5.4 .1 Experimental details

To perform gamma-irradiation on LPFG, a 30 cm long part of the sensitive fiber with a 15 mm long non-recoated LPFG was placed on a metallic sample holder in a 280 μm wide tight fitting groove (the fiber cladding diameter is 245±12 μm). It was fixed under a slight tension at two points about 5 cm apart the grating with glass-ceramic epoxy Resbond 989 FS (Contronics, USA). The fiber with LPFG was connected to the OSA through splicing 4 m long patch cords made of pure silica core and fluorine doped cladding radiation resistant fiber for in situ transmission monitoring. The sample holder was placed in an irradiation chamber loaded with the Co^{60} source (BRIT, Gamma Chamber-900) delivering a dose rate of 1.3 kGy/h. The transmission measurements started 24 hours before gamma irradiation. The spectra were recorded at several doses like 2.5, 6.5, 30, 100 kGy and 1 MGy etc. The OSA was kept 'switched ON' during a full day time for recording and 'switched OFF' at night. It was stabilized for ½ h after every switch ON before data were recorded.

The temperature near LPFGs was 26±1°C throughout 60 days of measurements. With auto dip measuring and trace averaging option of the OSA, shifts in the resonance dip position were measured with an accuracy of ±0.2 nm. No mechanism for normalization of power fluctuation of the built-in broadband OSA source was applied.

5.4 .2 Results and discussion

The results of in-situ measurements of LPFG transmission spectra with doses up to 1.54 MGy are shown in Figs. 5.10, 5.11 and 5.12. The effects of radiation induced change on the transmission dips corresponding to different cladding modes including the TAP mode up to 102 kGy is shown in Fig. 5.10. The decrease of the separation between the dual dips of the TAP mode at 6.5 kGy signifies increase of the effective refractive index of the fiber. The dose measurements up to 100 kGy were repeated on three similar LPFGs and they all exhibited a similar response. The evolution of the TAP mode resonance at doses above 100 kGy is shown in Fig. 5.11. Already, at 102 kGy the two bands merge into one flat top broad dip. At 394 kGy, the dip narrows and thereafter the dip amplitude decreases without significant wavelength shift and finally at 1064 kGy, the mode completely goes out of resonance. Such behavior of the TAP mode is in agreement with dependence of

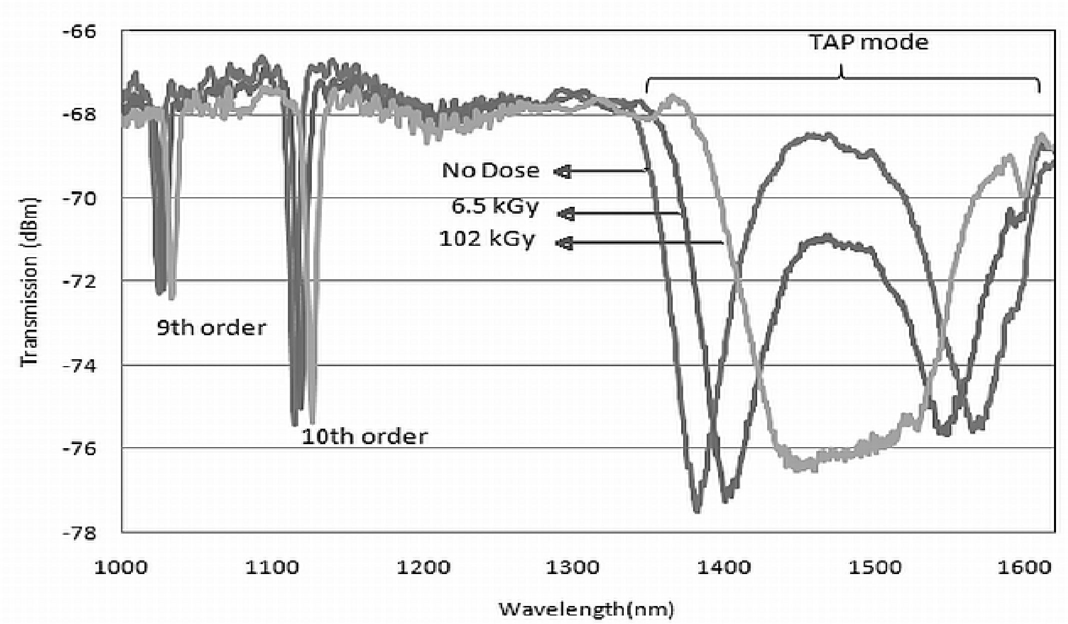

Fig. 5.10. In-situ transmission spectra of LPFG for doses up-to 102 kGy. Near TAP mode is shown for clear indication of increase of index change even for a dose of 6.5 kGy

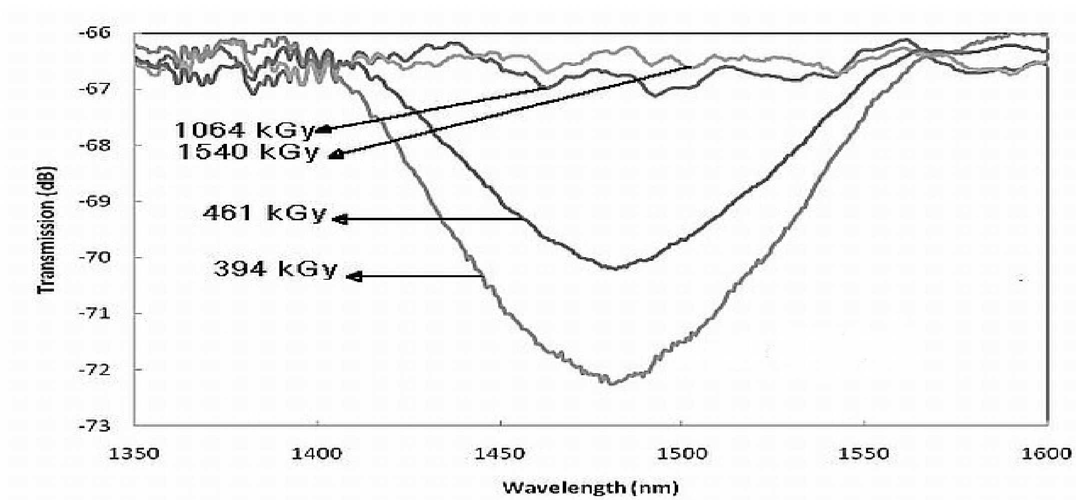

Fig. 5.11. Radiation induced changes corresponding to TAP mode in transmission spectrum of LPFG

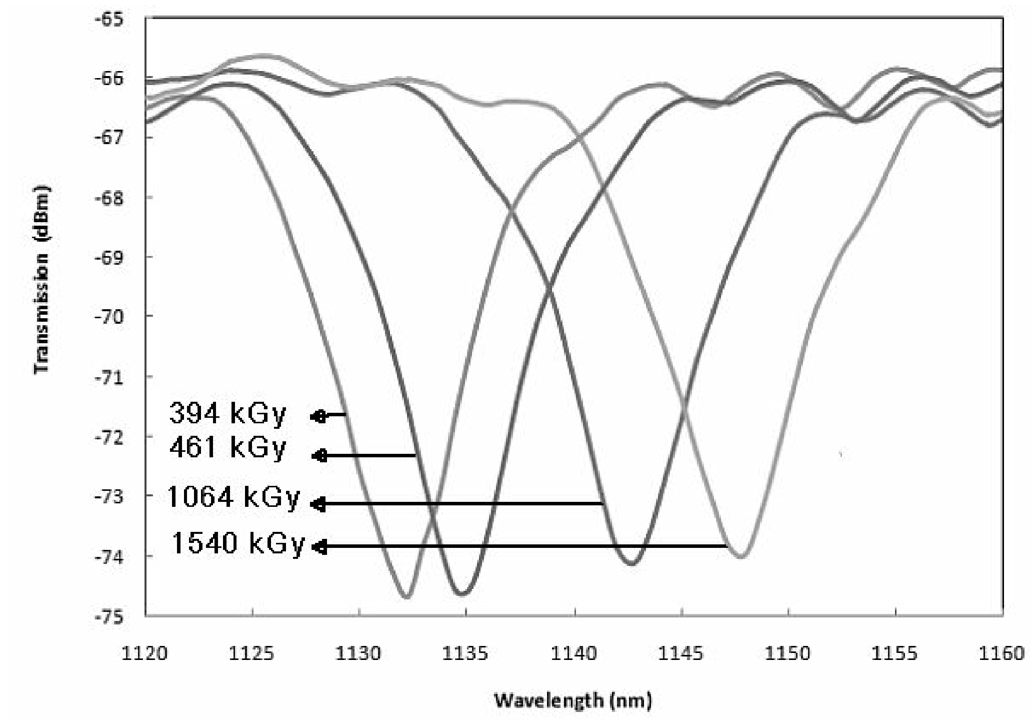

Fig. 5.12. In situ transmission spectra of 10th order cladding mode resonance of LPFG for high level dose

resonance wavelength on grating period and core-cladding RIs **[62]**. However, the absence of dip wavelength shift (DWS) makes it inconvenient for the analysis of RI changes at high doses. Therefore, the analysis was performed by observing the kinetics of the 10th order cladding mode resonance at 1115 nm as shown in Fig. 5.12. The induced wavelength shift is towards the red side (longer wavelength) and it increases monotonously without saturation up to a maximal accumulated dose of 1.54 MGy. A similar trend was observed for the 9th cladding mode resonance at 1024 nm (data not shown). Further, the strength of all resonance modes remains unchanged to an accuracy of about 5%.

5.4.3 RI calculation

The dip wavelength shift (DWS) $\Delta\lambda_D^i$ for i^{th} cladding mode is given by Eq. (5.2) and is reprinted for reference [39, 43, 86, and 90]

$$\Delta\lambda_D^i = \lambda_D^i \left(\frac{\Delta n_{co,eff} - \Delta n_{cl,eff}^i}{n_{co,eff} - n_{cl,eff}^i} + \frac{\Delta\Lambda}{\Lambda} \right) \qquad (5.3)$$

We first simulated the experimentally observed radiation induced shift of the 8th to 10th resonances assuming no refractive index (RI) changes. For all three resonances the observed shift could be explained by a grating period increase of ~2 μm at 100 kGy and of ~6.5 μm at 1.54 MGy. A small difference in the simulated period change for different resonances is within the peak shift estimation error. However, an elastic deformation corresponding to only a 0.3 μm period change requires the presence of stresses equivalent the silica breaking strength. The assumption of plastic deformation under gamma-radiation is not realistic because for the CO_2 laser written LPFGs the inscription mechanism is stress relaxation. This follows from the observation that the resonance dips shift to the blue during writing when the laser power is increased. We have also observed that if a CO_2 written grating is exposed with the broad beam CO_2 laser on the whole fiber grating zone the grating vanishes, which means that as all the fiber relaxes the index contrast reduces. Therefore, if the stress would be relaxed by ionizing radiation, the amplitudes of the resonances should also change, which wasn't the case.

Based on these simulation results, we can conclude that radiation-induced RI changes and not the grating period, should be the main reason for the observed shift of the resonances, at least at high radiation doses. This assumption is in agreement with **[43]**. The simulated effective index variations for different doses are given in Table III. It is well known that radiation hard fibers are made of pure silica and for doses up to MGy level such fibers show only small radiation-induced effects. Doping with P, Al, Ge, B, etc. significantly increases the radiation sensitivity even for sub-mol. % levels. The cladding of the presently used fiber is made of very pure low OH silica, while the core contains a significant amount of B and Ge. Such a cladding composition has been shown to be resistant to gamma up-to 1 MGy due to the absence of precursors of radiation induced color centers like NBOHC and E'-centers **[92]**. It is therefore reasonable to assume that the core RI changes are significantly higher than those in the cladding. This assumption allows an estimation of the core RI changes (Table 5.3, Δn_{co}). For these estimations, the phase matching curves are simulated with increased value of core refractive indices and the closest match to experimentally observed resonance wavelength is then taken as an estimation of the radiation modified fiber core RI. We calculated the Δn_{eff} in the B/Ge codoped fiber using Eq. (5.3) and the observed DWS for various dose values, neglecting the gamma-induced grating period changes. According to the Kramers-Kronig relation ionizing radiation induced RI changes are related with preferential absorption. Both for pure and doped silica the main contribution stems from deep UV absorption **[93]**. This means that the index is increasing in both cases. Therefore, neglecting the cladding index changes corresponds to an underestimation of the core index variation. The calculated effective RI change and the core RI change differ by 15-20% up to 100 kGy and for higher doses the difference slightly decreases. Such a behavior is in agreement with the assumption on the core index increase with no cladding index change, which results in a more power guided in the core. The maximal RI change in the range of 1.85×10^{-4} was obtained for the highest dose of 1.54 MGy. The values of 6×10^{-5} at 100 kGy and 1.7×10^{-4} at 1 MGy are consistent with reported values for B/Ge doped fiber for high fluence UV light and gamma-radiation [**44, 62, 93-95].**

In order to estimate the maximal possible core RI change under radiation, we applied the first order kinetic model **[93]** for the defect generation, which results in a saturating exponent dependence of the RI changes on the absorbed dose (Eq. 5.4). The net radiation induced modal refractive index change in the fiber *(*$\Delta n_{co,eff}$ - $\Delta n^{i}_{cl,eff}$ *)* is designated as Δ RI. The computation results are plotted in Fig. 5.13 and some representative values are tabulated in Table 5.3. Fig. 5.13 shows the fit of experimental data using Eq 5.4 and 5.4a.

$$\Delta RI = \sum_{k=1}^{N} a_k \left[1 - e^{\left(-\frac{D}{D_k} \right)} \right] \qquad (5.4)$$

$$\text{or,} \quad \Delta RI = b_N D + \sum_{k=1}^{N-1} a_k \left[1 - e^{\left(-\frac{D}{D_k} \right)} \right] \qquad (5.4a)$$

where $b_N = \dfrac{a_N}{D_N}$, N is the number of different channels, e.g. color centers, density variations etc. responsible for RI change, a_k and D_k are the maximal core RI change and the saturating dose for the k^{th} channel.

The experimental data (Table 5.3) on the induced core RI show no saturation with the dose increase. This means that at least one D_k is well above the maximal dose in the experiment. In this case, we can expand the exponent to get the simplified expression (Eq. 5.4a).

For the quasi-linear type of behavior observed in the experiment, fitting with Eq. 5.4 may be unstable because it depends on the ratio (a_N / D_N) of the two parameters and not on the parameters independently. With N = 2 (Eq. 5.4a), a good fit for high doses can be obtained as seen in inset of Fig. 5.13. The error of the retrieved refractive index change of ≈ 2×10^{-6} is due to the error in the RWS measurement accuracy of 0.2 nm. Adding one more exponent (N = 3) allows to improve the fit at low doses as shown in Fig. 5.13. Further increasing of N does not improve the fit, but makes it unstable. Comparison of the results for $N = 2$ and 3 shows that there is a mechanism which is important at low doses, but it saturates rather quickly (D_{sat} ~ 6.8 kGy). Another mechanism defines RI changes at 100 kGy range, and finally a third one, which govern the response at high doses.

TABLE 5.3 WAVELENGTH SHIFT INDUCED BY GAMMA RADIATION EXPOSURE OF NEAR TAP-LPFG WRITTEN BY CO_2 LASER IN B/GE CO DOPED FIBER

S.No.	Dose (kGy)	Experimentally Measured DWS (nm) of 10 th resonance mode	Measured RI change from DWS ($\Delta n_{eff,}$)	Calculated RI change through simulation of phase matching curve (**Physical RI: Δn_{co}**)
1.	6.5	3.8	1.7×10^{-5}	2.1×10^{-5}
2.	10.4	4.5	2×10^{-5}	2.5×10^{-5}
3.	102	11. 3	5×10^{-5}	6×10^{-4}
4.	1049	31.4	1.4×10^{-4}	1.6×10^{-4}
5.	1540	37.4	1.67×10^{-4}	1.85×10^{-4}

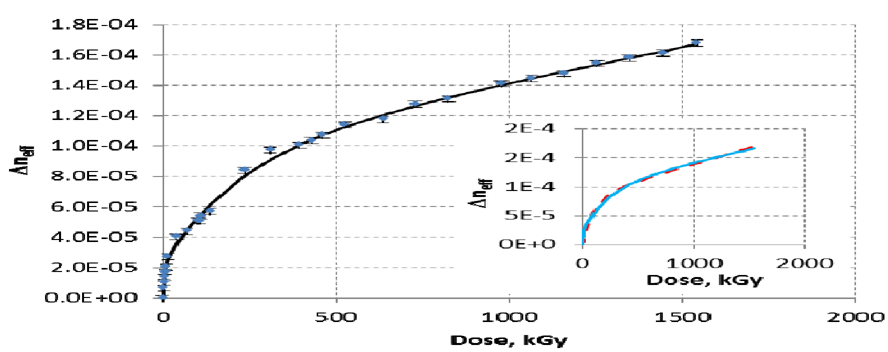

Fig. 5.13. Fit of the experimental data (triangles) using Eq.4 (a) with N=3. The inset compares fits with N =2 (solid line), N =3 (dash line) using Eq. 4

We can propose that the fast saturating term represents precursors or defects with a relatively low concentration present in the pristine fiber. Since we have neglected radiation induced densification (grating period changes) and still found a good agreement between modal and physical RI at high level dose, the origin of the non-saturating term can be attributed to the formation of permanent electric dipoles due to breakage of bonds as suggested by authors of **[91]**. This process is facilitated by high Boron content in the fiber core and the CO_2 laser based writing mechanism **[62]**. It also confirms our earlier claim that CO_2 laser written gratings do not interfere with gamma induced processes in B/ Ge doped fiber. Similar results were observed by us for LPFGs written by Arc-induced technique in B/Ge doped fiber procured from different manufacturers. Therefore, high gamma dose sensitivity in dose regime exceeding 100 kGy dose can be attributed to doping of Boron and does not depend on method of fabrication/draw induced defects of optical fiber [**44**].

5.5 Packaged device for dose sensing applications and its features

The LPFGs have been written in B/Ge co-doped fibers procured from various manufacturers such as Fiber Core, UK, INO-Canada and from CGCRI, Kolkata. The Boron Concentration (B_2O_3) in the core of the fiber varied from 3 wt % to 15 wt %. The gratings were written by CO_2 laser based scanning method or arc-induced point by point writing technique. LPFGs were also written in Germanosilicate fiber with zero concentration of Boron. In all cases, presence of Boron in the fiber provided high radiation senstivity.

It is known that due to involvement of cladding modes, the LPFGs are very sensitive to bend induced effects which necessitates proper mounting of grating sensor. Therefore various adhesives such as acrylates, epoxies, ceramics were studied in real time for their functional integrity. Though, cermaic based adhesive Resbond 954 was found excellent in performance, we developed a novel fixing method which eliminated the need for any adhesives. Five sensor devices having optimum dopant concnetrations were chosen and fully pacakged for long term monitoring. All devices functioned well up-to a dose of 1 MGy and measured the high level dose (>100 kGy) within an error of 10 %. Some devices are now under field trial at Indus-1 and Indus-2 synchrotron beam lines. The salient features of typical device are listed below:

5.5.1 Salient features of packaged gamma dose sensor (Wavelength encoded long period fiber grating dose sensor)

- Application: Integrated high level gamma dose monitoring
- The fiber Optic dose sensor probe is specially designed for monitoring high level integrated gamma dose in nuclear installations, accelerators and ITER like facilities. It can be used for long term real time or off-line integrated dose monitoring purposes.
- Packaged LPFG dose sensor specifications:
- Gamma dose range: a)1- 10 k Gy: with Resolution: 0.4 kGy
  and Sensitivity: 0.53 nm/ kGy
  b) 10-1000 kGy: Maximum error: ± 10 %
- Dimension: 100×50 mm^2
- Installation: Can be placed directly at any location with long pigtails.
- Operating temperature range: 25 – 80 ˚C

- Wavelength for measurement: Any wavelength between 1300-1650 nm (as per grating design)
- Option: With temperature compensation design.(i.e. built-in 2 LPFG inside, one for dose and another for temperature compensation)
- Measurement Procedure: Real time dose measurement upto 1MGy and offline measurements above 10 kGy. The dose is measured using supplied calibration curves.

5.5.2 Typical Spectrogram

Typical spectrograms are depicted in Fig. 5.14 and relevant calibration curves are depicted in Fig. 5.15 and 5.16. Fig. 5.17 presents the photograph of developed packaged gamma dose sensor.

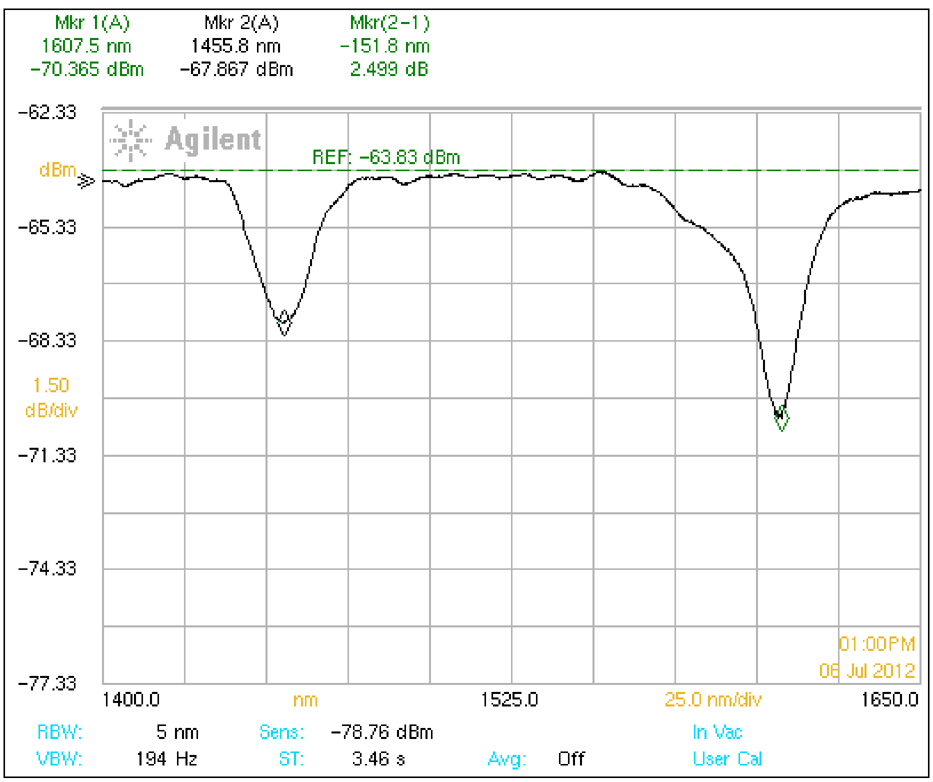

Fig. 5.14. Spectral transmission curve of LPFG

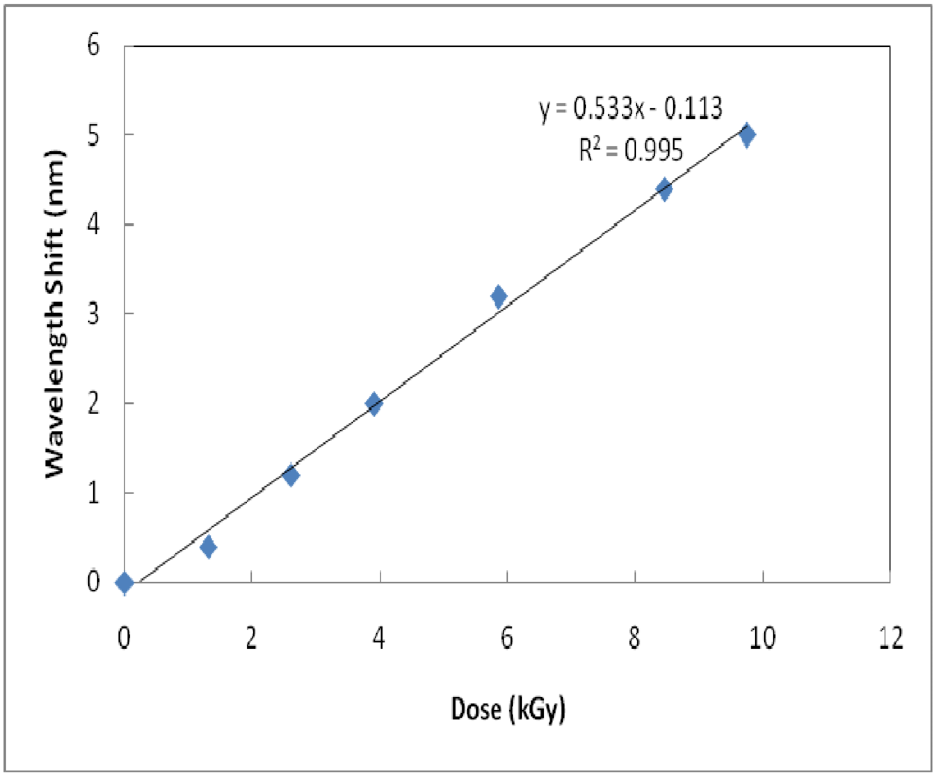

Fig. 5.15. Typical calibration curve (dose range 1 - 10 kGy)

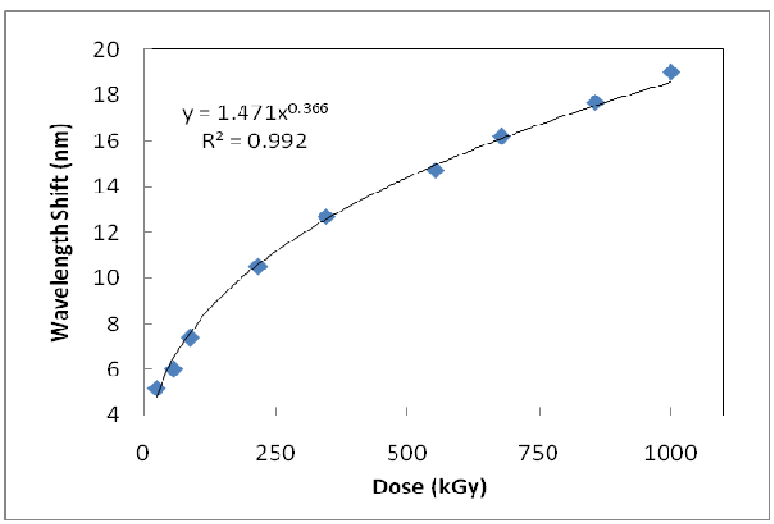

Fig. 5.16. Typical calibration curve (dose range 10 - 1000 kGy)

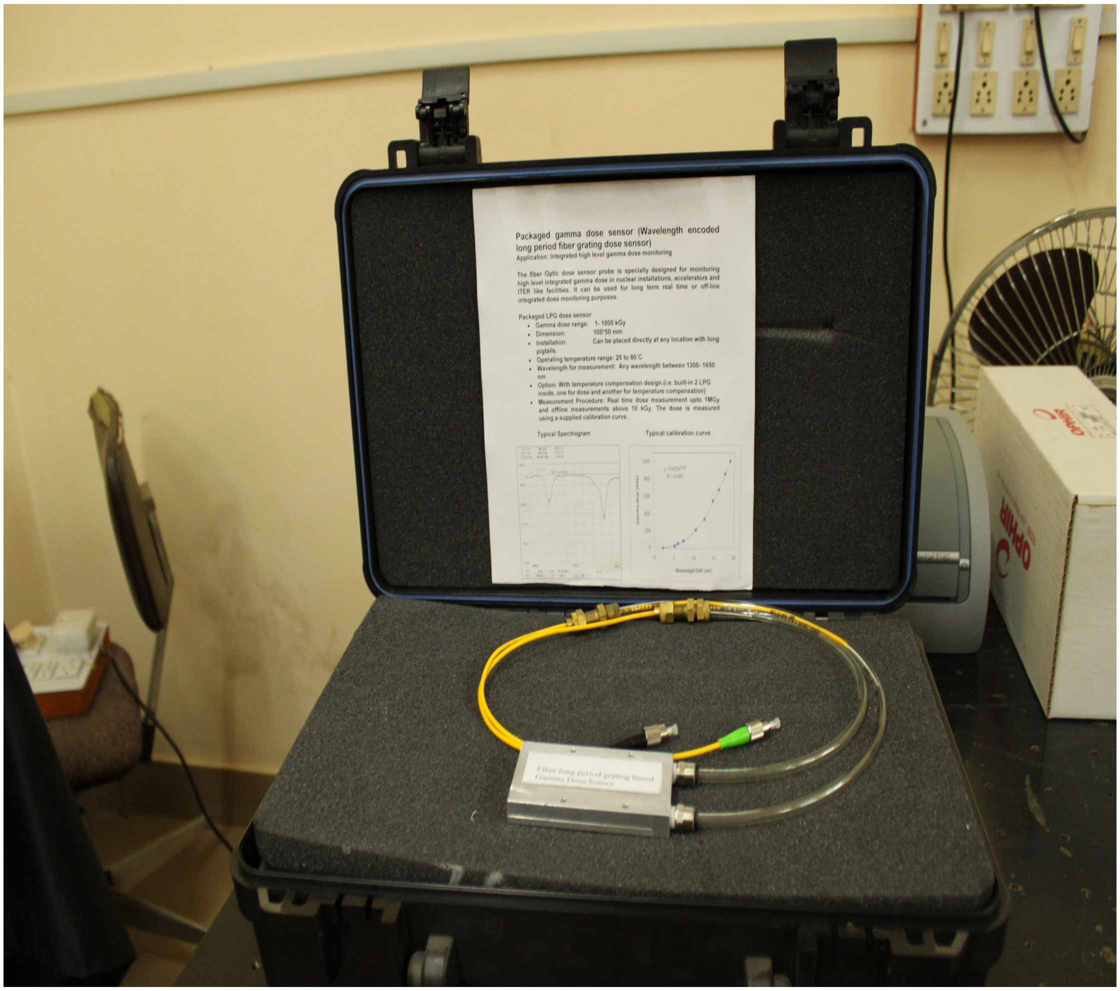

Fig. 5.17. Photograph of packaged gamma dose sensor

One such device has been under field trial at Septum magnet of Microtron source at RRCAT (see the picture shown in Fig. 5.18. The required accuracy for dose controls at the Undulator magnets of free electron lasers and accelerators is about 30-50 %. If the annealing is moderate or low, the peak shifts are independent of dose rate and so accuracy will be of the order of 10 %. Efforts are on to test these devices for such applications.

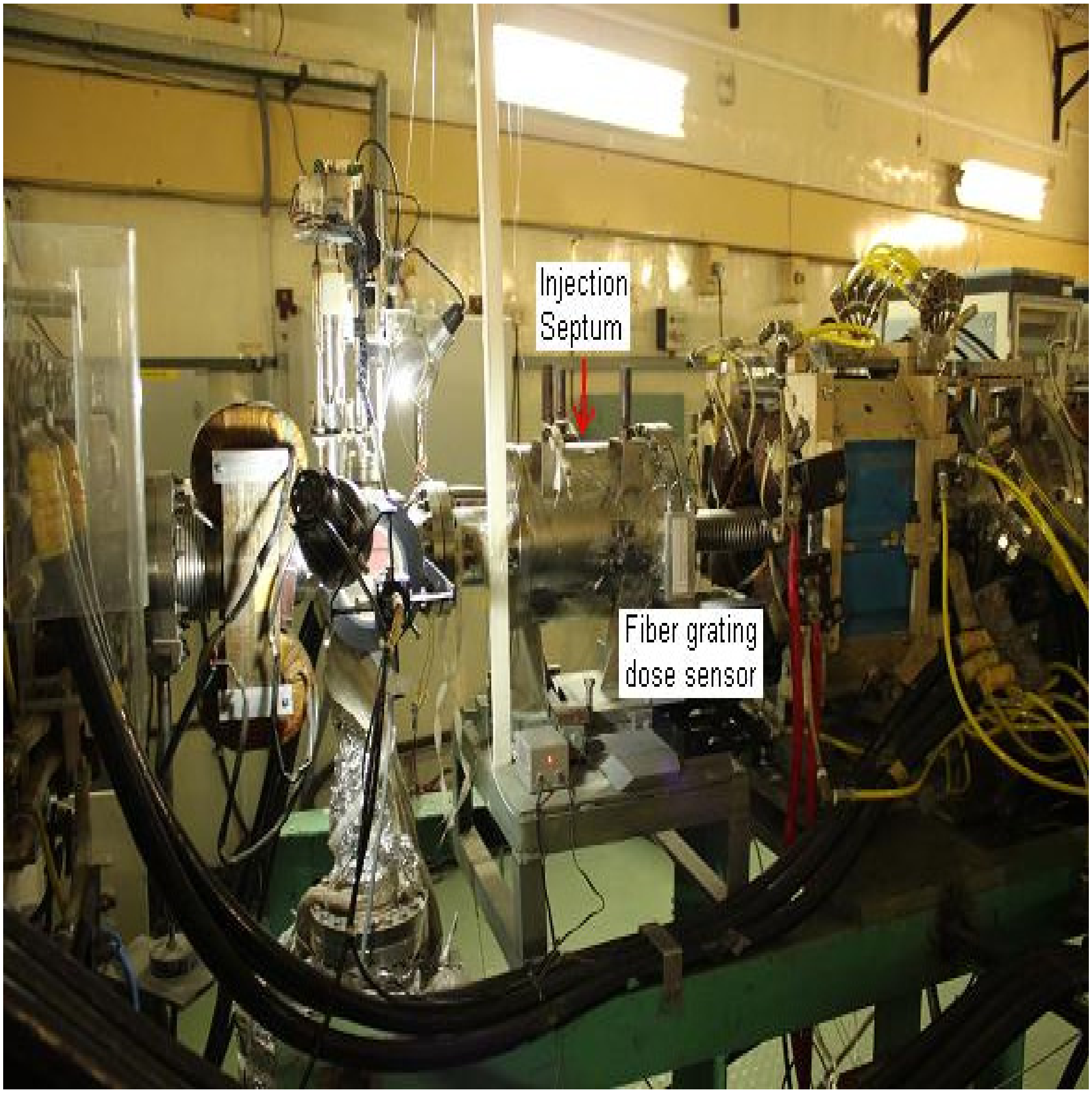

Fig. 5.18. Photograph of installed sensor at Microtron, RRCAT, Indore

Presently, typical LPFGs are sensitive for dose range above 1 kGy. However, specialty LPFG such as TAP-LPFG is sensitive above a few Gy dose. Devices are under fabrication to cover wide range of applications.

5.6 Conclusion

There exist many publications about irradiation tests of Fiber Bragg gratings (FBGs). Most reports show that FBGs are very insensitive to radiation and so well suited for temperature and strain sensing applications in nuclear reactors. Some recent reports suggest that radiation sensitivity of FBGs strongly depends on chemical fiber composition, history of fiber drawing conditions, grating inscription technique and post processing methods. Therefore, FBG based radiation dose sensors have not been reported yet.

We have systematically studied the effect of gamma dose on long period fiber gratings inscribed by CO_2 laser and Arc-induced technique. Real-time dose studies were conducted on LPFGs written in various commercially available single mode fibers such as B/Ge codoped fibers, High Ge doped fibers, standard communication fiber. The results clearly proved the active role of Boron for high radiation sensitivity. Radiation induced wavelength shifts of resonant modes in LPFGs written in B/Ge doped fibers did not saturate up to a dose of 1.5 MGy. It was also observed that the spectral shapes of resonances remain invariant. This study has established the foundation for development of first ever fully packaged, gamma dose sensor for high level dose up-to 1 MGy.

Understanding of refractive index (RI) changes in optical fibers induced by gamma radiation is of importance for design of sensors in applications such as fiber gyroscopes and diagnostic systems for thermonuclear reactors. Also some evidence suggests a link between photosensitivity and gamma sensitivity. We have suggested a novel approach to measure in-situ the gamma-induced RI changes in B/Ge doped fibers using LPFGs. Based on our experimental results, we have estimated index change of 1.85×10^{-4} at a dose of 1.54 MGy. The index changes are predicted to be due to polarizability changes facilitated by Boron doping and CO_2 based grating writing method.

CHAPTER 6

SUMMARY AND SCOPE FOR FUTURE WORK

The optical fiber grating technology has opened a new platform in sensor field. We have extensively investigated long period fiber gratings (LPFGs) written by X-Y scanning, high precision CO_2 laser and electrical arc discharges. These gratings were inscribed in photosensitive B/Ge doped fibers, high Ge doped fibers, Photonic Crystal fibers (PCFs) and other commercially available single mode fibers. Possible mechanisms of index modulations, e.g. residual stress relaxation, glass structure changes and physical deformation are analyzed.

The applications of LPFGs for temperature measurements up to 400 °C, temperature-insensitive axial strain measurements and leak detection have been demonstrated. The gratings in PCF fibers were shown to be gamma radiation resistant up to a dose of 100 kGy. The application of LPFG in PCF fibers for temperature-insensitive, strain sensing application has been demonstrated. The technology of writing specialty gratings, design criteria and mechanism of sensitivity enhancement in Turnaround point LPFGs (TAP-LPFGs) has been clearly established. These gratings were modeled, designed, fabricated and characterized.

It has been shown that both wavelengths encoded and/or true-amplitude modulated sensors can be developed by tailoring the LPFGs near TAP point. Further, we have presented CO_2 laser written exact TAP-LPFGs in B/Ge doped fibers for fuel adulteration detection. LPFGs offer the advantages of lower cost, tailorability and greater potential for fuel blending and fuel adulteration detection. The demonstrated grating sensitivity (1635 nm/RIU; RIU: refractive index unit) for surrounding refractive index (SRI) changes in the range 1.397 to 1.4372 is observed to be comparable to advanced surface plasmon resonance (SPR) based systems. Further, it has been shown that by utilizing the effect of SRI, these specialty gratings can be used for Photonic switching applications when switching time is not critical. The TAP-LPFGs show very high sensitivity of 0.96 nm/V % for adulteration of kerosene in petrol up to 10 % of adulteration. It is shown that these specialty gratings can easily detect the presence of 1 % of contamination of kerosene in petrol and can be employed for on-road measurements.

Extensive investigations were carried out to obtain fiber gratings with distinctly high gamma radiation sensitivity, and with as large a measurement as possible. In order to find the role of fiber material, the single mode fibers with different chemical composition were selected to write LPFGs with CO_2 laser based technique and Arc-induced method. The radiation induced effects on fiber gratings were studied both off line and in real time. Contrary to expectations, gratings in high Ge doped fibers (high defect concentration) are not found gamma radiation sensitive and showed resonance shift saturation effects above a dose of 100 kGy.

All gratings written in Boron doped fibers procured from different manufacturers displayed high radiation sensitivity during off line and online studies. These investigations led to the prediction of Boron as a sensitive core dopant for high radiation sensitivity. It is also observed that CO_2 laser based LPFG writing method and Arc-induced technique do not interfere with gamma-induced effects. Radiation induced attenuation and annealing effects up to 300 °C are studied for sensitive gratings. The radiation induced effects in B/Ge doped fibers are found to be near permanent after a dose exceeding 1 MGy.

The fiber optic wavelength encoded sensors of high nuclear radiation sensitivity and large measurement range have been designed, developed and fully packaged. Highest ever gamma dose sensitivity of 80 nm/65 kGy has been shown in TAP-LPFGs written by CO_2 laser. The evolution of changes in dip wavelength, grating modulation and dip widths have been studied in real time up to a dose of 1 MGy. It has been shown that the grating modulation (dip strength) and widths are negligibly affected in B/Ge doped fibers by high level gamma dose while the radiation induced shifts of resonant modes did not saturate up to the full dose. This study makes LPFGs in B/Ge codoped fibers as a strong candidate for high level gamma dose sensing applications.

We have proposed a novel approach to measure in-situ refractive index changes induced by gamma radiation in single mode fibers. These changes are derived from wavelength shifts of resonances of a CO_2 laser written LPFGs. We estimated the radiation induced index change in the core of the B/Ge co-doped fiber as 2×10^{-5} at 10 kGy dose and 1.8×10^{-4} at 1.54 MGy. The index changes are predicted to be due to glass polarizability changes facilitated by the presence of Boron in the fiber and the grating writing technique. It is for the first time that the kinetics of radiation induced RI changes in B/Ge doped fibers are seen up to 1.5 MGy dose levels. Based on the modeling results, we have predicted the saturated core RI change of 8.2×10^{-4} for doses above 15 MGy.

It will be interesting to extend this work and exploit the breakthroughs studies. I envisage following studies as listed below.

(1) Presently, LPFGs require both ends for sensing due to operation of transmission mode. If one end is coated with high reflectivity mirror, they will work like FBGs. Such devices can be more compact. Portable, in-expansive wavelength shift demodulation systems for LPFGs are not currently commercially available. This is partly related to their operation in transmission mode and broader bandwidth of resonances which requires high resolution system to minimize the measurement error. If these problems are solved, the systems based on LPFG sensors can be deployed for on-site road measurements and pumped micro fluidics.

(2) Our obtained results reveal the critical role of Boron as a dopant for increased gamma radiation sensitivity of long period fiber gratings. We intend to continue our investigations for optimizing Boron content and other fiber parameters. Scanning CO_2 laser based grating writing method is very flexible and reproducible. The mass production of these devices is therefore quite conceivable in the near future.

(3) There is a keen interest to study the kinetics of induced index changes in doped fibers due to evidences of a link between gamma radiation (ionizing radiation) and UV induced effects (photosensitivity). It is noteworthy to see that the Boron doped fibers show enhanced UV photosensitivity as well as high gamma radiation sensitivity. These effects in fiber Bragg gratings are known to be dependent upon fiber composition, impurity concentration and grating manufacturing parameters. Since efficient FBGs can only be made with high intensity UV light which strongly affect the fiber properties, it is not possible to predict the role of fiber composition on gamma-induced effects using FBGs.

Unlike FBGs, the efficient long period gratings can be made by CO_2 laser, Arc-induced method as well as by high intensity UV source. It is, therefore important to perform theoretical and experimental studies with long period fiber gratings to unravel the reasons for induced index changes by UV / ionizing radiation and their linkages. One can then predict the effects of one type of radiation while studying the other radiation.

REFERENCES

1. R. Kashyap, “Fiber Bragg Gratings,” Academic Press, New York, 1999A.
2. K. O. Hill, “Aperiodic distributed-parameter waveguides for integrated optics,” Appl. Opt., Vol. 13, pp. 1853-1856, 1974.
3. Ajoy Ghatak, “OPTICS”, Tata McGraw-Hill Publishing Company Ltd., 2009.
4. Alan D. Kersey, Michael A. et al., “Fiber grating sensors,” J. Lightw. Technol., Vol. 15, (8), pp. 1442-1462, August 1997.
5. L. Dong, “Photoinduced absorption change in germanosilicate preforms: evidence of the color center model of Photosensitivity,” Applied Optics, Vol. 34, no. 18, pp. 34-36, 1995.
6. J. Canning, K. Sommer, M. Englund, “Fiber gratings for high temperature sensor applications,” Meas. Sci. Technol. 12, pp. 824-828, 2001.
7. Martin J. O’Dwyer, Chen-Chun Ye, Stephen W. James, Ralph P Tatam, “Thermal dependence of the strain response of optical fiber Bragg gratings,” Meas. Sci. Technol., Vol. 15, pp. 1607-1613, 2004.
8. A.L.Huston, B.L. Justus et al., “Remote Optical fiber dosimetry” Nucl. Inst. and Methods in Phys. Research B, Vol. 184, pp. 55-67, 2001.
9. G.F. Fernando, A. Hammeed et al., “Structural integrity monitoring of concrete structures via optical fiber sensors: Sensor protection systems,” J. Structural Health Monitoring, Vol. 2(2), pp. 123-135, 2003.

10. F. Berghmans, A. Fernandez Fernanadez et al., "Radiation hardness of fiber optic sensors for monitoring and remote handling applications in nuclear environments," SPIE Proc. 3538, Photonic East, Boston, Nov. 2-5, 1998.

11. A. Faustov, P. Saffari, C. Koutsides et al., "Highly radiation sensitive type 1A FBGs for future dosimetry applications," IEEE Trans. Nucl. Sci., Vol. 59 (4), pp. 1180-1185, Aug. 2012.

12. A.I. Gusarov, F. Berghmans et al., "Behavior of fiber Bragg gratings under high total dose gamma radiation", IEEE Trans. Nucl. Sci., Vol. 47 (3), pp. 688-691, 2000.

13. A. I. Gusarov, D. Kinet et al, "Gamma radiation induced short-wavelength shift of Bragg peak in type I fiber gratings," IEEE Trans. Nucl. Sci., Vol. 57 (6), pp. 3775-3778, Dec. 2010.

14. A. Fernandez Fernandez, B. Brichard et al., "Real-time optical radiation dosimeters for nuclear environment monitoring around nuclear reactors," Fusion Engineering and Design, Vol. 83, pp. 50-59, 2008.

15. Katerina Krebber, H. Henschel, U. Weinand, "Fiber Bragg gratings as high dose radiation sensors," Meas. Sci. Technol., Vol. 17, pp. 1095-1102, 2006.

16. A. M. Vengsarkar, P.J. Lemaire et al., "Long-Period fiber gratings as band rejection filters," J. of Lightwave Technlogy, Vol. 14 (1), 1996, pp. 58-65.

17. A. M. Vengsarkar. J.R. Pedraazzani, J.B. Judkins, P.J. Lemaire, N. S. Bergano and C.R. Davidson, "Long-period fiber-gratings-based gain equalizers," Opt. Lett., Vol. 2, pp. 336-338, 1996.

18. D. D. Davis, T. K. Gaylord, E. N. Glytsis, S. C. Mettler, A. Vengsagar., Electronics Letters, Vol. 34 (302), 1998.

19. Yi-Ping Wang, “Review of long period fiber gratings written by CO_2 laser,” J. App. Phy., Vol. 108 (8), pp. 1-37, 2008.

20. B. H. Kim, Y. Park et al., “Residual stress relaxation in the core of optical fiber by CO_2 laser irradiation,” Optics Lett., Vol. 26 (21), 2001, pp. 1657-1659.

21. G. Rego, P.V.S. Marques, J.L. Santos, H.M. Salgado, “Arc-Induced Long-Period Gratings”, Fiber and Integrated Optics, Vol. 24 (3 & 4), pp. 245-259, 2005.

22. Sanjay Kher, Smita Chaubey, Jai Kishore, SDVSJ Raju, S. M.Oak, “Fiber Optic Temperature-insensitive strain sensor for nuclear applications”, Int. J. App. Engineering and Tech., Vol. 1(1), pp. 61-67, Oct. –Dec 2011.

23. Stephen W James, R.P. Tatam,”Optical fiber LPG sensors: Characteristics and Application,” Meas. Sci. Technol., Vol. 14, 2003, pp. 49-61.

24. Khaliq S., James S.W. Tatam R.P., “ Enhanced sensitivity fiber optic long period grating temperature sensor,” Meas. Sci. Technol., Vol. 13, 2002, pp. 792-795.

25. Yinian Zhu, Ping Shum, J. Hao et al., “Strain-insenstive and high-temperature long period gratings inscribed in Photonic crystal fiber,” Optics Lett., Vol. 30 (4), Feb. 5, 2005.

26. Frazao O, Ferreira L.A., et al., “Applications of fiber optic grating technology to multiparamter measurement,” Fiber Integr. Opt., Vol. 24, pp. 227-244, 2005.

27. Vikram Bhatia, “Applications of long-period gratings to single and multi-parameter sensing,” Optics Express, Vol. 4 (11), 1999, pp. 457-462.

28. Xinwei Lan, Qun Han et al., “TAP-LPFGS fabricated by CO_2 laser point by point irradiations,” IEEE- Photon. Technol. Lett., Vol. 23 (22), 2011, pp. 1664-1666.

29. Sanjay Kher, Smita Chaubey, Jai Kishore, S.M.Oak., "Detection of fuel adulteration with high sensitivity using turnaround point long period fiber gratings in B/Ge doped fiber" IEEE Sensors Journal, Vol. 13, No. 11, pp. 4482-4486, 2013.

30. H. Xuan, W. Jin, M. Zhang, "CO_2 laser induced long period gratings in optical microfibers" Optics Express, Vol. 17, No. 24, 21882-21890, 2009.

31. Cheung, S. M. Topliss et al., "Response of fiber optic long period gratings operating near the phase matching turning point to the deposition of nano structured coatings, " J. OSA B 25 (6), 2008, pp. 897-902.

32. Ruchi Garg, S. Tripathi, K. Thyagarajan, W. J. Bock, "Long period fiber grating based temperature compensated high performance sensor for bio-chemical sensing applications," Sensors and Actuators B, 176, 2013, pp. 1121-1127.

33. Xianfeng Chen, K. Zhou, L. Zhang, I. Bennion, "Dual-peak LPGs with enhanced RI sensitivity by finely tailored mode dispersion that uses the light cladding etching technique," Appl. Optics, Vol. 46 (4), 2007, pp. 451-457.

34. Bharat R. Acharya, T. Krupenkin, S. Ramchandran et al., "Tunable optical fiber devices based on broadband long-period gratings and pumped microfluidics," Appl. Phy. Lett. Vol. 83 (24), 15 Dec. 2003.

35. E.J. Friebele, P.C. Schultz, M.E. Gingerich, "Compositional effects on the radiation response of Ge-doped silica-core optical fiber waveguides," Appl. Opt., Vol. 19, No. 17, pp. 2910-2916,1980.

36. D. L. Gribson, "Nature of defects and defect generation in optical glasses," in SPIE Proc., 1985, Vol. 541, pp. 38-59.

37. M.C. Paul, R. Sen, D. Bohra et al., "Gamma ray radiation induced absorption in Ti

doped single mode fibers at low dose levels," Optical Materials, Vol. 29, 2007, pp. 738-745.

38. S. A. Vasilev, E. M.Dianov et al., "Performance of Bragg and LPGs written in N- and Ge-doped silica fibers under gamma-radiation," IEEE Trans. Nucl. Sci., Vol. 45 (3), 1998, pp. 1580-1583.

39. G. Rego, A. Fernandez Fernandez et al., "Effect of ionizing radiation on the properties of arc-induced long-period fiber gratings," Appl. Opt., Vol. 44, no. 29, Oct. 2005.

40. Henning Henschel, Stefan K. Hoeffgen, Jochen Kuhnhenn, Udo Weinand, "High radiation sensitivity of Chiral long period gratings", IEEE Trans. on Nucl. Sci, vol. 57, No.5, pp. 2915 – 2922, Oct. 2010.

41. P. Kniazewski, M. Kujawinska etal., "Application of the microinterferometric Tomography setup to the reliability tests of fiber sensors exposed to cumulative gamma radiation," Nano- and Micro-metrology, Munich, SPIE Proc. 5858, 2005, pp. 88-91.

42. A. F. Fernandez, B. Brichard and F. Bergmans, "In situ measurement of refractive index changes induced by gamma radiation in germanosilicate fibers," IEEE-Photon. Technol. Lett., vol. 15, no. 10, pp. 1428-1430, 2003.

43. Sanjay Kher, Smita Chaubey, Raman Kashyap, S. M. Oak, "Turnaround-Point long period fiber gratings (TAP-LPFG) as high radiation dose sensors", IEEE- Photonics Technol. Lett., Vol. 24, (9), pp. 742-744, 2012.

44. Sanjay Kher, Smita Chaubey, S. M. Oak, A. Gusarov, “Measurement of gamma-radiation induced refractive index changes in B/Ge doped fiber using LPGs,” IEEE-Photon. Technol. Lett., Vol. 25, No. 21, pp. 2070-2073, Nov. 1, 2013.

45. K.O. Hill, G. Meltz., “Fiber Bragg grating technology fundamentals and overview,” J. Lightw. Technol., Vol. 15, No. 8, pp. 1263-168, August 1997.

46. E. M. Dianov, D. S. Stardubov et al., “Refractive –index gratings written by near-ultraviolet radiation,” Optics Letters, Vol. 22, no. 4, pp. 221-223, 1997.

47. Y. Kondo, K. Nouchi et al., “Fabrication of long-period fiber gratings by focused irradiation of infrared femtosecond laser pulses,” Optics Letters, Vol. 24, No. 10, pp. 646-648, May, 1999.

48. G. Rego, O. Okhotnikov et al., “High temperature stability of long period fiber gratings using an electric arc,” JLT, Vol. 19, no. 10, pp. 1574-1579, 2001.

49. M. Fujumaki., Y. Ohki et al., “Fabrication of long-period fiber gratings by use of ion implantation,” Optics Letters, Vol. 25, pp. 88-90, 2000.

50. I. K. Hwang, S. H. Yun, B.Y. Kim, “Long-period fiber grating based upon periodic microbends,” Optics Letters, Vol. 24, pp. 1263-1265, 1999.

51. S. Chaubey, Sanjay Kher, S. M. Oak, “Radiation and taper tuning of long period grating for high sensitivity strain measurement”, IEEE proceedings of WFOPC-2011, ISSN: 1927-5056, pp 1-4, Dec. 2011.

52. Abdelrafik Malki, G. Humbert et al., “Investigation of the writing mechanism of electric-arc-induced long-period fiber gratings,” Applied Optics, Vol. 42, no. 19, pp. 3776-3779, 2003.

53. Smita Chaubey, P. Joshi, Sanjay Kher, “Design and development of long-period grating

sensors for temperature monitoring," Sadhana, Vol. 32, part 5, pp. 513-519, Oct. 2007.

54. Yunqi Liu, Ho Wai Lee et al., "Glass structure changes in CO2-laser writing of long-period fiber rgatings in Boron-doped single mode fibers," JLT, Vol. 27, no. 7, pp. 857-863, April 1,2009.

55. H.W. Lee, K.S. Chiang, "CO_2 laser writing of long-period fiber gratings in photonic crystal fiber under tension," Optics Express, vol. 17, no. 6, pp. 4533-4539, 2009.

56. G. Kakarantzas, T. Birks, P. Russel, "Structural long-period gratings in photonic crystal fibers," Optics letters, Vol. 27, pp. 1013-1015, 2002.

57. C.S. Kim, Y. Han et al., "Induction of refractive index changes in B-Doped optical fibers through relaxation of the mechanical stress," Optics Commun., Vol. 185, pp. 337-342, Nov. 2000.

58. X. Shu, Lin Zhang, I. Bennion, "Sensitivity characteristics of long-period fiber gratings," JLT, Vol. 20, No. 2, Feb. 2002.

59. Sanjay Kher, Smita Chaubey, S.M.Oak, "Long period fiber grating based nuclear radiation sensors for high level dose applications", J. Instrumentation Science & Technology, Vol. 41, issue 2, 2013.

60. See Yenn Chong, Jung-Ryul Lee et al., "Design of copper/carbon coated fiber Bragg grating acoustic sensor net for integrated health monitoring of nuclear power plant," Nuclear Engineering and Design, Vol. 241, pp. 1889-1898, 2011.

61. Zhiyong Wang and S. Ramchandran, "Ultrasensitive long-period fiber gratings for broadband modulators and sensors," Optics Letters, Vol. 28, no. 24, pp. 2458-2460, 2003.

62. X. Shu, Lin Zhang, I. Bennion, “Sensitivity characteristics of long-period fiber gratings,” JLT, Vol. 20, no. 2, pp. 255-266, 2002.

63. Haiyun Chen, Zhengtian Gu, “Design optimization of an intensity-interrogated long period fiber grating film sensor operating near the phase-matching turning point,” Meas. Sci. Technol., Vol. 23, pp. 035105-035112, 2012.

64. V. Bhatia, A. M. Vengasarkar, “Optical fiber long period grating sensors,” Optics Letters, Vol. 21, no. 9, pp. 692-694, 1996.

65. M. Smietana, W. J. Bock et al., “Increasing sensitivity of arc induced long-period fiber gratings-pushing the fabrication technique towards its limit,” Meas. Sci. Technol., Vol. 22, pp. 015201-206, 2011.

66. Bhatia V., Campbell D. K. et al., “Temperature-insensitive and strain insensitive long period grating sensors for smart structures,” Opt. Engg., Vol. 36, pp. 1872, 1997.

67. Byounggho Lee, S. Roh, J. Park, Current status of micro and nano-structured optical fiber sensors, Optical Fiber Technol, 15 ,209-221, 2009.

68. Sukhdev Roy, “Fiber optic sensor for determining adulteration of petrol and diesel by Kerosene,” Sensors and Acturators – B, Vol. 55, pp. 212-216, 1999.

69. V. P. Bhatnagar, “An ultrasonic method to find liquid fuel adulteration,” J. Acoust. Soc. India, Vol. 9, pp. 19-23, 1981.

70. M. Shahru Bahari, W. J. Criddle, JDR Thomas, “Determination of the adulteration of petrol with kerosene using rapid phase titration procedure,” Analyst, vol. 115, pp. 417-419, 1990.

71. Minh Chau phan Huy, G. Laffont et al., “Three-hole microstructured optical fiber for efficient fiber Bragg grating refractometer,” Optics Letters, vol. 32, no. 16, pp.2390-

2392, 2007.

72. H. Homola, “Surface plasma resonance based sensors,” Springer series on Chemical Sensors and Biosensors, Springer, 2006.

73. N.Shivesen, R. Horvath et al., “Deep probe metal-clad waveguide biosensors,” Biosensors and Bioelectronics, Vol. 22, No. 7, pp. 1282-1288, 2007.

74. Vandana Mishra, Subhash Jain et al., “Fuel adulteration detection using long period fiber grating sensor technology,” Indian J. of Pure and App. Phy., Vol. 46, pp. 106-110, 2008.

75. U. S. Raikar, A.S. Lalasangi et al., “Concentration and refractive index sensor for methaol using short period grating fiber,” Optik, Vol. 122, pp. 89-91, 2011.

76. S.A.Vasilev, E. M.Dianov et al., “Postfabrication resoance peak positioning of long-period cladding mode coupling graitngs,” Optics Letters, Vol. 21, pp. 1830-1832, 1996.

77. Agostino ladicicicco, S. Campopiano et al., “Spectral behavior in thinned long period gratings: effects of fiber diameter on refractive index sensitivity,” Applied Optics, vol. 46, no. 28, pp. 6945-6952, 2007.

78. Qing-Li Jin, Wen-Jing Gu et al., “Optimal design of temperature-insensitive long period fiber gratings for athermal refractive index sensor,” Optik, Vol. 122, pp. 2147-2150., 2011.

79. G.R. Possetti, L.C. Cocco et al., “Application of long period fiber grating-based transducer in the fuel industry,” Meas. Sci. Technol., Vol. 20, pp. 034012-034021, 2009.

80. J. Linesh, T.M. Libish et al., “Periodically tapered LPG for ethanol concentration detection in Ethanol-gasoline blend,” Sensor & Trasducers Journal, Vol. 125, no. 2, pp. 205-212, 2011.

81. J. R. Sambles, G. W. Bradbery and Fuzi Yang, "Optical excitation of surface plasmons: an introduction," Contemporary Physics, Vol. 32, no. 3, pp. 173-183, 1991.

82. Raman Kashyap and Galina Nemova, "Surface plasmon resonance based fiber and planar waveguide sensors: review article," Sensors, pp. 645162, 2009.

83. Guy Cheymol, Herve Long et al., "High level gamma and Neutron irradiation of silica optical fibers in CEA OSIRIS nuclear reactor," IEEE Trans. Nucl. Sci., Vol. 55, no. 4, pp. 2252-2258, 2008.

84. A. L. Huston, B. L. Justus, T. L. Johnson, " Fiber-optic-coupled, laser heated thermoluminiscence dosimeter for remote radiation sensing," Applied Physics Letters, Vol. 68, no. 24, pp. 3377-3379, 1996.

85. J.C. Polf, E.G. Yukihara et al., "Real time luminescence from Al2 O3 fiber dosimters," Radiation Measurements, 38, pp. 227- 240, 2004.

86. Vedda A., Chiodini N. et al., "Doped fibers for remote radiation dosimetry," Appl. Phys. Lett., Vol. 85, No. 26, 2004, pp. 6356-6358.

87. A. Fernandez Fernandez, B. Brichard et al., "Real-time fiber optic radiation dosimeters for nuclear environment monitoring around thermonuclear reactors," Fusion Engineering and Design, Vol. 83, pp. 50-59, 2008.

88. Robert R. J.Maier, W. N. MacPherson et al., "Fiber Bragg gratings of type I in smf-28 and B/Ge fiber and type IIA B/Ge fiber under gamma radiation up to 0.54 MGy," Proceedings of SPIE , Vol. 5855, SPIE, Bellingham, WA 2005.

89. A. Gusarov, D. Kinet et al., "Gamma radiation induced short-wavelength shift of the Bragg peak in Type I fiber gratings," IEEE Trans. Nucl. Sci., Vol. 57, no. 6, pp.3775-3778, 2010.

90. Sanjay Kher, Smita Chaubey, S.M.Oak, "Long period fiber grating based nuclear radiation sensors for high level dose applications", J. Instrumentation Science & Technol., Vol. 41, issue 2, 2013.

91. D. P. Hand and P. St. J. Russell , "Photoinduced refractive-index changes in germanosilicate fibers", Opt. Lett., Vol. 15, No. 2, January 15, pp. 102-104, 1990.

92. A. L. Tomashuk, and M.O. Zabezhailov, "Formation mechanism of precursors of radiation induced color centers during fabrication of silica optical fiber preform," J. of Applied Physics, 109, pp. 083101-083104, 2011.

93. D. L. Griscom, M. E. Gingerich, and E. J. Friebele, "Model for the dose, dose-rate and temperature dependence of radiation-induced loss in optical fibers," IEEE Trans. Nucl. Sci., vol. 41, no. 3, pp. 523-527, Jun 1994.

94. D.L.Williams, B. J. Ainslie, J. R. Armitage, R. Kashyap, R. Campbell, "Enhanced UV Photosensitivity in Boron co doped Germanosilicate fibers", Electronics Letters, Vol. 29, No. 1, pp. 45-47, 1993.

95. S. Girard, J. Kuhnhenn, A. Gusarov, B. Brichard, M. V. Uffelen, Y. Ouerdane, and A. Boukenter, "Radiation effects on silica-based optical fibers: recent advances and future challenges," IEEE Trans. Nucl. Sci., Vol. 60, no. 3, pp. 2015-2037, 2013.

96. Eric Linder, John canning et al., "Post-hydrogen –loaded draw tower fiber bragg gratings and their thermal regeneration", App. Opt., vol. 50, no. 17, pp. 2519-2522, 10 June 2011.

97. Dong L.,Archamaut, J.L., Payne, D.N., "Single pulse Bragg grating written during fiber drawing," Electron Lett. 29 (17), 1577-1578, 1993.

98. B. Lee, S. Roh, J. Park, "Current status of micro and nano structured optical fiber sensors", Optical Fiber Technol. 15, pp. 209-221, 2009.

99. B. L. Justus, A. L. Huston et al., “UV dosimetry using thermoluminiscence of semiconductor doped Vycor glass,” App; Phys. Lett., Vol. 6719, No. 28, pp. 1179-1181, Aug, 1995.

100. K. Gill, R. Grabit et al., “Gamma and neutron radiation damage studies of optical fibers,” J. Non-crystalline Solids, 216, pp. 129-134, 1997.

101. R. F. Cregan, B. J. Mangan, T. A. Birks et al.,“Single-mode photonic bandgap guidance of light in air,” Science, 285, pp. 1537-1539, 1999.